EXPERIMENTAL INVESTIGATION OF TWO DIMENSIONAL WAKES BEHIND FLAT PLATES

BY

PK. MD. OMAR FARUQUE

A THESIS

SUBMITTED TO THE DEPARTMENT OF MECHANICAL ENGINEERING
BANGLADESH UNIVERSITY OF ENGINEERING & TECHNOLOGY, DHAKA
IN PARTIAL FULFILMENT OF THE REQUIREMENTS FOR THE DEGREE
OF MASTER OF SCIENCE IN ENGINEERING(MECHANICAL)

BANGLADESH UNIVERSITY OF ENGINEERING & TECHNOLOGY, DHAKA
NOVEMBER, 1983

EXPERIMENTAL INVESTIGATION OF TWO DIMENSIONAL WAKES BEHIND FLAT PLATES

ACCEPTED AS SATISFACTORY FOR PARTIAL FULFILMENT OF THE REQUIREMENTS FOR THE DEGREE OF MASTER OF SCIENCE IN ENGINEERING (MECHANICAL), BUET, DHAKA

EXAMINERS

1.	DR. S. M. NAZRUL ISLAM 23/11/83	CHAIRMAN (SUPERVISOR)
2.	DR. ABU MOHAMMAD AZIZ-UL-HUQ 23/11/83	MEMBER
3.	DR. DIPAK KANTI DAS 23/11/83	MEMBER
4.	DR. M. A. TAHER ALI 23/11/83	MEMBER
5.	DR. M. ABDUL HALIM 23.11.83	MEMBER

ABSTRACT

The present experimental investigation was on the mean flow parameters of the wakes, identifying the initial conditions. The experiment was done in a subsonic wind-tunnel of test section size ; 45.72 cm x 45.72cm x3.25cm. Two different plates of thickness, 1.905cm and 0.159 cm respectively at the trailing edge, were used to generate the wakes. The aspect retios (width of the wind tunnel/ plate thickness at the trailing edge) at the trailing edge of the plates were 24 and 288 respectively. Experiments were carried out for Reynolds number, $R_{ed} = 5.48 \times 10^5, 4.17 \times 10^5, 3.01 \times 10^5$ and 2.312×10^5 for which the flow in a duct may be assumed to be turbulent. Mean properties of the flow at the trailing edge and in the wake, downstream from the trailing edge, were determined experimentally.

Pitot-static tube was used to measure the veolcity and static pressure heads. The wind tunnel was calibrated for four different flow parameters. There were negligible pressure and velocity gradients in the axial direction within the test-section.

Within the wake, near the trailing edge of the plate the transverse velocity gradient was high. The velocity gradient decreases with increse of axial distance.

DEDICATION

TO

HAZRAT MOHAMMAD
(PEACE BE UPON HIM)

ACKNOWLEDGEMENT

The author is highly grateful to his supervisor Dr. S.M. Nazrul Islam, Associate Professor, Department of Mechanical Engineering, Bangladesh University of Engineering & Technology, Dhaka without whose guidance, encouragement and invaluable suggestions, this work would not have been possible. The author also expresses his deep gratitude to Dr. Abu Mohammad Aziz-ul Huq, Prof. and Head Department of Mechanical Engineering, BUET, who assisted him in various ways at every phase of the work.

He is also indepted to Dr. Dipak Kanti Das, Dr.M.A. Taher Ali and Dr. M. Abdul Halim for their constructive criticism and invaluable suggestions which have definitely raised the quality of the work. The author is indebted to Dr. J. R. Chowdhury, the Director of the Computer Centre for permission to use the Computter.

Many thanks are to the staff members of the various workshops of BUET for their assistance in fabricating the experimental set-up.

Finally, the author wishes to thank Mr. M.A. Gaffur for typing the thesis and Mr. Md. A. Salam for drawing the figures with patience and care.

The Author

TABLE OF CONTENTS

LIST OF FIGURES

Figures

Figures

LIST OF TABLES

LIST OF APPENDICES

NOMENCLATURE

A, A_1	Constants
a, a_2	Constants in empirical equations
B, B_1	Constants
b	Width of the mixing zone
c, c_1	Constants
C_{dm}	Drag co-efficient, equation (3.2.6)
C_d	Drag co-efficient, equation (3.2.10)
D	Plate thickness
D_1	Drag per unit depth
d	Width of the wind tunnel
d_1	diameter of the cylinder
f	a function of η
f'	first defferentiation of f
g	acceleration due to gravity
H	Shape factor
h'	Velocity/pressure head
k_2, k_3	constants
L	Characteristic body dimension
ℓ	Prandtl's mixing length
ℓ_1	length scale

M	momentum defect per unit time and depth
m	exponent
n, n_1	constants
P	Mean Static pressure
P_1	Pressure due to velocity head
q	constant
R	gas constant
r_o	radius of the wire
R_{ed}	Reynolds Number based on the width of the wind tunnel and the average velocity
$Re_{\theta e}$	Reynolds Number based on the momentum thickness and the average velocity.
s	Specific gravity
T	absolute temperature
U	free-stream velocity
u	axial velocity
u*	Shear velocity
u_1	Velocity Scale.
v	transverse mean velocity
u', v'	fluctuating velocity in X & Y direction
$Y_{\frac{1}{2}}$	half width of the wake
X, Y	co-ordinate system

α_1 , α_2	constants
β	mixing angle
β_1	a function of axial distance along the duct
δ	boundary layer thickness
δ^*	displacement thickness
θ	momentum thickness
ϕ	angle
δ_t	turbulent or eddy diffusivity
ν	Kinematic viscosity
η	self-preserving variable
ρ	density
ε_1	constant
χ	constant used to define Prandtl's new formula
τ	shear stress

subscripts

a	air
c	center line
i	axial direction
ℓ	liquid
max	maximum
rms	root mean square

re	relative
u	uncertainty
w	wall
av	average
o	trailing edge
reu	uncertainty of relative quantity.

CHAPTER - I

INTRODUCTION

1.1 General

A wake is formed behind a solid body which is being draged through a fluid at rest or behind a solid body which has been immersed in a stream of a fluid. The velocities in a wake are smaller than those in the main stream , and the loss in the velocity within the wake is amount to a loss of momentum which causes drag in the wake. The difference of momentum within the wake and the free stream causes an exchange of momentum between them, and the wake spreads in the axial direction. Consequently the difference between the mean velocity in the wake and that in the main stream becomes smaller.

The wake behaves like free shear flows if it is not obstructed by the surrounding fixed boundaries. The characteristic features of this flow is important for many practical cases, so, it is getting attention of many research groups.

1.2 Formation and Degeneration of wakes

When a fluid in motion separates from a surface and shears with another fluid having lower velocity forms two layers of different momentum. Such difference causes an exchange of momentum to form a shear layer. The flow in the shear layer may be in presence of pressure gradient or in its absence. The shear layer is said to be free shear layer if it is not obstructed by boundaries. After

separating from the surface the fluid in contact with the outer boundary of the wake folds back into its surroundings. This folding engulfs the surrounding fluid and forms a ring vortex core which rolls downstream. After one or two revolutions, the vortices interact strongly and break down into turbulent eddies [1]* if they originate from turbulent boundary layers. The interactions of turbulent eddies causes large scale vortical motions; small scale vortical motions also evolve through breakdown of the large eddies.

The general picture of the turbulent wake is depicted in Fig. 1.1 with a dip in the velocity profile. The width of the wake increases with distances from the body, and the dip in the velocity profile gradually levels off.

1.3. Self preservation of wakes

A large scale vortical motion is formed in the near region and a small scale vortical motion is evolved through breakdown of the large eddies at the far region of the wake. The small eddies contain less energy and they are invariant to mean and turbulent stresses in the field. From the physical view point the flow is said to be self-preserving when the eddies are invariant.

---

* Number in the parentheses indicate reference.

For self-preserving flow, velocity and length scales, for two-dimensional wake may be expressed as follows[2];

$$U-U_c = A_1 X^{-\frac{1}{2}} \; ; \quad \ell_1 = B X^{\frac{1}{2}} \qquad 1.1$$

where A_1 and B_1 are the constants.

According to the self-preservation hypothesis, the velocity defect and the Reynolds stress become invariant with respect to axial distance if they are expressed in terms of the local length and velocity scales.

An analytical solution of the governing equation may be obtained by using self-preserving laws. The results may not guarantee the occurrence of self-preservation in practice. But it is identified by many authors[2, 3] that the mean quantities achieve self-preservation earlier than turbulent quantities. Experimental results of Keffer [3] shows that all measured turbulent and mean quantities within wakes are fully self-preserving beyond X/d=500.

1.4 Application of wakes

The flow near the trailing edge of an airfoil is of considerable interest from the view point of its application, and the wake of a flat plate is a limiting case of an airfoil. The study of wake will be useful for the design of airfoils. The wake is generated behind any kind of structures, such as buildings, towers, bridges etc.

for any wind velocity. For high wind velocity the wake strength becomes high to damage the structure. Wakes generated behind the moving cars and ships cause a loss of energy. The characteristics of the wakes are useful for designing structures, cars and ships to minimize the energy losses associated with wakes. A maneuvering aircraft or submarine, which is accelerating or decelerating leaves behind it a momentum defect in the form of a jet or wake when it changes speed. To determine the power loss required for such operation, the characteristics of the wakes should be known.

Longitudinal pressure gradients can occur quite often, specially in combustors, interactions between shock waves and shear layers, and separated flow. Very little is presently known, either experimentally or theoretically, concerning the influence of longitudinal pressure gradients on turbulent free mixing. Detailed data are necessary in this case for designing combustor and so forth.

CHAPTER - II

LITERATURE SURVEY

2.1 General

The term wake is commonly applied to the region of non-zero vorticity on the down-stream side of a body immersed in a flow. In the turbulent wake the effects of the molecular viscosity is negligible, and it is turbulent from the starting if it is generated by turbulent boundary layer at the beginning of the wake. The study of the wake is not new but its physical importance in the sense of shear layer parameters induces the researchers to investigate wake in more detail. The researchers investigated the wake both experimentally and theoretically to make its use more conveniently. Some investigations of wakes by various authors are presented in this chapter with their findings and conclusions.

2.2 Experimental Investigation

Chevray and Kovasznay [4] investigated two dimensional wake behind a thin flat plate mounted in the low speed wind tunnel. Measurements were taken with a single channel constant temperature hot-wire anemometer both for mean velocity and for turbulence. Reynolds number based on boundary layer thickness, δ, was $\frac{\delta U}{\nu} = 1.5 \times 10^4$ for all investigations. The boundary layer thickness and momentum thickness at the exit were 5.5 cm & 0.58cm respectively. Using the experimental values of mean velocities the author calculated

the corresponding momentum thickness and the width of the wake. The flow in the wake was found approximately similar except close to the trailing edge. It is shown that the flow achieved approximate self-preserving at a distance $\frac{X}{\theta_o} = 300$, and exact self-preservation may occur at a distance where the shape factor, H, would achieve unity. It is to be noted here that the trailing edge turbulence level was not mentioned.

Hiroshi and Kuriki [5] experimentally studied the mechanism of transition in the wake of three thin flat plates of different dimensions. The plates were placed parallel to a uniform flow at subsonic speeds. The maximum thickness of the three plates were 0.3 and 3mm respectively and the Reynolds number based on length of the plates ranged from 6×10^4 to 4×10^5. For the measurement of the mean velocity distribution, both fine pitot-tube and hot-wire anemometer were used. At the trailing edge of the plate the boundary layer was laminar. Other trailing edge conditions such as boundary layer thickness, displacement thickness and shape factor were not mentioned by the authors [5]. They classified the transition region into three subregions viz linear, non-linear and three dimensional. In the two-dimensional(linear and no-linear)region the center-line velocity was found to vary exponentially.

In the three dimensional region it was approximately linear. From the velocity distribution curves the authors showed that until X = 30 to 40 mm, the distribution varied slowly, while a sharp increase of central velocity was found from X= 40 to 60 mm. The experimental values of the mean velocities were found to fit to an empirical equation given below:

$$\frac{U}{U_o} = 1 - \frac{U_o - U_c}{U_o} \exp\left(a\left(Y/Y_{\frac{1}{2}}\right)^2\right) \qquad (2.2.1)$$

where, a = 0.69315

The theoretical distribution for a fully developed laminar wake of the above form and the experimental data were in good agreement with each other. However, they did not mention variation of the momentum thickness and the width of the wake in the axial direction. As the exit condition is laminar the development of the wake is not similar to that of the result obtained by Chevray and Kovasznay[4].

Gartshore [6] investigated the two dimensional wake of a square ($\frac{1}{4}$ inch) rod at adverse pressure gradients and at the pressure gradient for exact self-preservation. The velocity ratio $(U-u_c)/U$ was maintained approximately constant after $x/d_1 = 50$. The flow through wakes having Reynolds numbers, 6300 and 7300 , based on trailing edge thickness, were studied without identifying the characteristics of the trailing edge.

Mean velocities were measured with a round pitot tube having round tips together with static taps located in one of the side walls. A DISA constant temperature hot-wire anemometer was also used to obtain measurements of the turbulent quantities. The experimental values of mean velocities showed approximate self-preserving after $x/d_1=50$, where the half width, $Y_{\frac{1}{2}}$, and the external velocity parameter, U^{-m},(m = 3.16 and 3.2 for Reynolds number 6300 and 7300 respectively) behaved linear with axial distances. But in the near region of the wake the half-width, $Y_{\frac{1}{2}}$, and external velocity parameters were non-linear. The experimental values of the mean velocities were found to fit to an empirical equation given below:

$$\frac{U - u}{U - u_c} = \exp\left(-a\,(Y/Y_{\frac{1}{2}})^2\right) \qquad (2.2.1)$$

where, a = ln2.

Similar equation was also obtained by Hiroshi and Kuriki [5] for two-dimensional wakes for flat plates.

Keffer [3] investigated the wake of the two-dimensional cylinders of sizes $\frac{1}{2}$ inch, 5/16 inch and 3/16 inch with straining the flow. The tunnel speed was held constant at 18 ft/sec so that the corresponding Reynolds number based on cylinder diameters were 4630, 2890 and 1740 for cylinder diameters $\frac{1}{2}$, 5/16 and 3/16 inch respectively. The mean quantities were measured with a pitot static tube. Keffer [3]

plotted the wake growth and the decay of the center-line velocity defect against X. The author found that the wake width increase exponentially with distance downstream. The mean velocity distribution of the wake profiles were in no way self-preserving. The relationships for the scales which the author derived are given below:

$$u_1 \sim \beta_1^{\frac{1}{2}}, \quad \ell_1 \sim \beta_1^{\frac{1}{2}} \tag{2.2.3}$$

where u_1 and ℓ_1 are characteristic velocity and length scales for the flow and β_1 is the total strain which has been applied to the wake. However, for a more complete description, measurements of the turbulent quantities would be required. It is not clear what kind of mechanism is most important in the entrainment of external fluid at the wake edge, a gradient type of diffusion, or the large laterally directed mixing jets which are significant in an unstrained wake.

Schlichting's [7] work, which is mentioned in this section is devoted to an experimental investigation of the flow in the wake of a two-dimensional body. The experiments were conducted within a wind tunnel at a speed of about 50m/sec. Reynolds number based on the diameter(d_1=10mm) was $Re = \frac{U d_1}{\nu} = 2.38 \times 10^4$. He found that the half-width of the wake was varied parabolically and the center-line velocity defect was varied exponentially. Experimental values of mean velocities were found to fit to an empirical equation given below:

$$\frac{U - u}{U - u_c} \cdot (1 - \eta^{3/2})^2 \tag{2.2.4}$$

Where $\eta = \frac{Y}{b}$, b is the width of the wake and Y is the vertical distance from the wake center line. Schlichting's experimental results did not indicate the intitial boundary layer parameters. These results agree satisfactorily with wake generated by a very thin boundary layer at the beginning, but it may deviate from the results with thick boundary layer at the beginning. Hall and Hislop[8]investigated the velocity and temperature distributions in the turbulent wake behind a heated body of revolution. They also found that the experimental values of the mean velocities fitted satisfactorily with the empirical equation given by Schlichting [7]in eqn. (2.2.4). Swain [9]also obtained in a similar manner such an expression for the velocity profile in an axially symmetrical wake. The dimensionless profile of velocity defect was obtained experimentally by Rehichardt [10] in the wake behind a heated wire at a distance of $X=100r_o$ (r_o is the radius of the wire) from it. Similar experiments were also done by Fage and Falkner [11]in the wake behind a heated prismatic rod at a distance of $X = 72\ r_o$ from it. The attempt of Goldstein [12] and other students of Taylor to apply the vorticity transfer theory for determining the velocity profile in an axially symmetric wake did not lead to results which agree with experimental data. The experimental results for wakes behind two dimensional

cylinder shows close agreement with the results of two-dimensional wakes behind flat plates. Demetriades and Anthony[13] investigated the supersonic axisymmetric wake. The plot of $(1-u_c/U_o)^{-3/2}$ against X/D, which the authors plotted, shows a good agreement with the theoretical results obtain by prediction method. The predicted axial variation of Reynolds number is considerably different from that shown by Demetriades [13]. He showed Reynolds number to be nearly constant for X/D greater than about 30.

2.3 Theoretical study

To find the form of the velocity profile in a two-dimensional wake Schlichting[7] used momentum equation of the form given below:

$$uv + \frac{\delta}{\delta X}\int_{\alpha}^{Y} u^2 dy + \ell^2\left(\frac{\delta u}{\delta Y}\right)^2 = 0 \qquad (2.2.5)$$

in which the expression for turbulent shear stress is taken from Prandtl's old theory of turbulence $(\tau/\rho = \ell^2\left|\frac{\delta u}{\delta Y}\right|\frac{\delta u}{\delta Y})$ and pressure gradient is neglected. The Prandtl's mixing length, ℓ, was defined in terms of the width of flow,

$$\ell = cb \qquad (2.2.6)$$

The author defined the velocity profile in a conventional functional form $U-u = (U-u_c)\, f(\eta)$, where $\eta = Y/b$. To determine the profile, Schlichting[7] used

$$b = K_2\sqrt{X} \qquad (2.2.7a)$$

and $$U-u_c = \frac{n}{\sqrt{X}}\, U \qquad (2.2.7b)$$

Using the expression for ℓ and u_c in the momentum equation (2.2.5) an ordinary differential equation was derived in the following form:

$$\eta f = \eta f'^2 \qquad (2.2.8a)$$

where, $\lambda_1 = 2c^2 n/K_2$ (2.2.8b)

Equation (2.2.8a) is subjected to the following boundary conditions:

1. At the edge of the wake $(\eta = \frac{Y}{b} = 1)$

$U-u = 0$ and $\frac{\delta(U-u)}{\delta Y} = 0$, i.e. $f = f' = 0$ (2.2.9)

2. On the axis of the wake $(\eta = \frac{Y}{b} = 0)$

$U-u = U-u_c$, $\frac{\delta(U-u)}{\delta Y} = 0$, i.e. $f = 1, f' = 0$ (2.2.10)

The solution of the equation (2.2.8a) with boundary conditions given in equations (2.2.9) and (2.2.10) is;

$$\frac{U-u}{U-u_c} = f(\eta) = (1-\eta^{3/2})^2 \qquad (2.2.11)$$

The constant, c, involved in the Prandtl's mixing length expression was determined to be 0.18 ($\ell/b = 0.18$). The values of the constant, K_2, and n, in equation (2.2.7a) and (2.2.7b) can be determined by using Schlichting's [7] equations in the form, $n = 1.4\sqrt{a_2 L}$ and $K_2 = 0.8\sqrt{a_2 L}$ where a_2 is an empirical constant. For wake behind a two dimensional cylinder, Schlichting [7] obtained experimentally the value of a_2 as 1.23.

To find the form of the velocity profile in an axially symmetric wake Taylor [14] uaed momentum equation of

the form given below:

$$\frac{1}{Y}\frac{\delta}{\delta X}\int_{\alpha}^{Y}(U-u)\,UY\,dY + l^2\left(\frac{\delta u}{\delta Y}\right)^2 = 0 \qquad (2.2.12)$$

Here the expression for shear stress is taken in accordance with Prandlt's old theory . The Prandtl's mixing length, l was defined in terms of the width(wake radius) of the wake, $l=cb$. The author used the conventional functional form of velocity profile given below:

$$b = K_3^3\sqrt[3]{X} \qquad (2.2.13a)$$

and $$U-u_c = n_1 UX^{-2/3} \qquad (2.2.13b)$$

After transformation he obtained for an axially symmetric wake, the same differential equation as for a two-dimensional wake.

$$\eta f = \alpha_2^2 f'^2 \qquad (2.2.14)$$

where, $\alpha_2 = 3n_1c^2$ (2.2.15)

With the same boundary conditions given in equation (2.2.9) and (2.2.10), equation (2.2.14) may be integrated to give the same velocity profile as in a two-dimensional wake:

$$\frac{U-u}{U-u_c} = f(\eta) = (1-\eta^{3/2})^2 \qquad (2.2.16)$$

Reichardt[10] used momentum integral equation to find the form of the velocity profile in a two-dimensional wake. The author used Prandtl's new formula for shear stress

$$\frac{\tau}{\rho} = \nu_t \frac{\delta u}{\delta Y}$$

where, $\nu_t = \chi b(U-u_c)$

If Prandtl's new formula for shear is used, the momentum

equation for a two-dimensional wake takes the following form under constant pressure gradient:

$$2\frac{d}{dx}\int_{\infty}^{Y} U(U-u)dY - \nu_t \frac{\partial u}{\partial Y} = 0 \qquad (2.2.17)$$

The velocity profile in the cross-section of a two-dimensional turbulent wake according to Prandtl's new theory of turbulence and Reichardt's theory [10] is ;

$$\frac{U-u}{U-u_c} = \exp\left(\frac{1}{2\varepsilon_1 x} Y^2\right) \qquad (2.2.18)$$

The constant ε_1 for a two dimensional wake was determined from the experimental results of Schlichting [7] and Reichardt [10]. They also obtained the following form of the velocity profile in an axially symmetric wake far from the body,

$$\frac{U-u}{U-u_c} = \exp\left(\frac{Y^2}{2\varepsilon_1 x}^{2/3}\right) \qquad (2.2.19)$$

2.4 Recent Approach

The shear layers are recently investigated from the view point of its structure and eddy sizes. Such flow is identified to be irregular type with its structure in the coherent form. A coherent structure is a connected, large-scale turbulent fluid mass with a phase-correlated vorticity over its spatial extent [15]. This specially phase-correlated vorticity is called the coherent vorticity. Vortex, rings, rolls, spirals, etc. are example of coherent structures. The presence of large-scale organized motions in the turbulent shear flows, though apparent for a long time and implied by

the mixing length hypothesis was suggested first by Townsend [16] and investigated in detail by Meller and others [17, 18]. Near field coherent structure in wake was observed by flow visualization by the authors [19,20]. A coherent structure is responsible for transports of significant mass, heat and momentum without necessarily being highly energetic itself. Sophesticated experimentation has been developed to investigate the coherent structure.

Differential methods of calculation is also an useful tool for predicting the turbulent flows in shear layers. The turbulent model of semi-empirical equations developed by Launder , et. al [21] and others [22, 23] are very powerful method for predicting shear flow.

2.5 Mean Static Pressure

Mean static pressure in wakes behind the body depends upon the size of the body. When the thickness of the body is small there is negligible pressure gradient in the axial direction. If the thickness of the body is large the pressure gradient can not be ignored. Such pressure gradient within the wake plays an important role for its development. Gartshore[6] was the first who investigate the influence of the pressure on the wake development. Gartshore[6] measured the lateral turbulence intensity distribution for three kinds of wakes viz:

i) wake at adverse pressure gradient

ii) wake at pressure gradient, required for self-preservation

iii) wake at zero pressure gradient

The results of wakes at three pressure gradients studied by Gartshore [6] showed a considerable variation of flow parameters in the near region for varying pressure gradient. Hiroshi and Kuriki [5] used alluminium plates for the side wall of the test section. The plates were adjusted in order to keep the stream-wise static pressure distribution constant. The experimental results of Hiroshi and Kuriki [5] show a significant deviation from the results obtained by Gartshore [6]. Such a deviation is due to the increase of pressure gradient. No pressure measurements were made by Chevray and Kovasznay [4] because the static pressure within the wake was quite low(P= 1mm H_2O) and the wakes generated behind a very thin plate(thickness = 0.16 cm).

2.6 Problem and objectives

The flow development identifying the initial condition has not been done much, except lately by Chevray and Kovasznay [4] and others. The present experimental investigation is to be done identifying the initial conditions. The flow both at the trailing edge of the plate and at the downstream from the plate will be studied experimentally. Wakes produced by two different plates having different velocity profiles

at the trailing edge will be investigated. The exit Reynolds number based on the average velocity and the momentum thickness at the trailing edge will be varied in order to investigate the effect of exit Reynolds number on the wake development.

The mean velocity and pressure within the wake are to be measured for different initial conditions at various locations from the trailing edge of the plate. The experimental results will be compared with the existing theoretical and experimental results. The wake geometry is to be determined for various Reynolds numbers. The variation of drag co-efficient for different Reynolds number is also to be calculated.

CHAPTER - III

GOVERNING EQUATIONS

3.1 General

Turbulent motion is governed by the Navier-Stokes differential equations. The general solution of the non-linear Navier-Stokes equations is not available. In order to apply Navier-Stokes equations to practical cases, hypothesis and empirical assumptions have to be introduced to obtain a closed set of equations with time average dependent variables. Here the conventional order of magnitude principle is applied to the general momentumm equation to obtain the equation in a simpler form. Later these equations are used for evaluating the wake properties.

3.2 Fundamental equation for two-dimensional wakes

Applying the order of magnitude principle and using continuity equation, the momentum equation may be written in the following form [24]:

$$\frac{\partial}{\partial X}u(u-U) + \frac{\partial}{\partial Y}v(u-U) + \frac{\partial}{\partial Y}\overline{u'v'} = 0 \qquad (3.2.1)$$

The pressure gradient and the effect of molecular viscosity are neglected in the above equation.

In wakes, u-U vanishes at sufficiently large values of Y, and it does so for $\overline{u'v'}$. After integrating the equation (3.2.1) with respect to Y over the entire flow. The result is,

$$\frac{\partial}{\partial X}\int_{-\infty}^{\infty} u(u-U)\,\delta Y = 0 \qquad (3.2.2)$$

The total momentum defect in a wake is constant, so,

$$\rho \int_{-\infty}^{\infty} u(u-U)\,\delta Y = M \qquad (3.2.3)$$

The momentum integral equation(3.2.3) can be used to define a length scale for turbulent wakes. Imagining that the flow past an obstacle produce a completely separated, stagnant region of width 2θ . Then $2\rho U^2\theta$ represents the net momentum defect per unit time and depth.

Thus, $-2\rho U^2\theta = M$ (3.2.4)

Equating equation(3.2.3) and (3.2.4) , we have

$$-2\rho U^2\theta = \rho \int_{-\infty}^{\infty} u(u-U)\,\delta Y$$

$$\text{or, } \theta = \int_0^{\infty} \frac{u}{U}\left(1-\frac{u}{U}\right)\delta Y \qquad (3.2.5)$$

where, θ is called the momentum thickness of the wake. The momentum thickness is related to the drag coefficient of the obstacle that produces the wake. The drag coefficient, C_{dm}, is defined by,

$$D_1 = -\tfrac{1}{2} C_{dm}\,\rho U^2 L \qquad (3.2.6)$$

where, D_1 is the drag per unit depth and L is the characteristic height of the obstacle. The drag , D_1, produces the momentum flux,M. So, equating equations (3.2.4) and (3.2.6),

$$2\rho U^2\theta = \tfrac{1}{2} C_{dm}\,\rho U^2 L \text{ or } C_{dm} = \frac{4\theta}{L} \qquad (3.2.7)$$

The momentum integral equation for drag on the obstacle having pressure gradient is given by

$$D_1 = L\left\{\int_{-\infty}^{\infty}(P_o + \rho U_o^2)\,\delta Y - \int_{-\infty}^{\infty}(p+\rho u^2)\,\delta Y\right\} \qquad (3.2.8)$$

But according to the definition of drag coefficient

$$D_1 = \tfrac{1}{2} C_d \rho U_o^2 L \qquad (3.2.9)$$

Equating equations(3.2.8) and (3.2.9) , we have,

$$\tfrac{1}{2} C_d \rho U_o^2 L = L\left\{\int_{-\infty}^{\infty}(P_o + \rho U_o^2)\,\delta Y - \int_{-\infty}^{\infty}(p+\rho u^2)\,\delta Y\right\}$$

$$C_d = \frac{1}{\frac{1}{2}\rho U_o^2}\int_{-\infty}^{\infty}(P_o - P)\,\delta Y + 2\int_{-\infty}^{\infty}\left(1 - \frac{u^2}{U_o^2}\right)\delta Y \qquad (3.2.10)$$

3.3 Empirical Equations

The mean velocity distribution for self-preserving wake is given by the following semi-empirical equation ;

$$\frac{U-u}{U-u_c} = \exp\left(-a\left(\frac{Y}{Y_{\frac{1}{2}}}\right)^2\right) \qquad (3.2.11)$$

where, $a = \ln 2$ (3.2.12)

A semi-empirical relation for half width of the wake, follows from the measurements of Schlichting and Reichardt [10]

$$Y_{\frac{1}{2}} = 0.35\sqrt{X}\sqrt{C_{dm}L} \qquad (3.2.13)$$

CHAPTER - IV

EXPERIMENTAL SET-UP AND EXPERIMENTS

4.1 General

Many experimental investigations on wake flows have been published, but only a few have identified the exit conditions at the trailing edge of the plate. The main objective of this investigation is to study the effect of initial conditions on wakes which involves;

(i) Measurement of mean velocity and pressure distribution

(ii) Determination of self-preserving characteristics of velocity within the wakes.

(iii) Study of wake properties useful in practice.

All these properties are measured experimentally and compared with the existing theoretical and experimental results.

4.2 Experimental facilities

To accomplish the objective described in the previous section flat plates were chosen to generate wakes. Two flat plates of different thicknesses were used to form the wakes. The thickness of the plate-I is taken about 10 times the thickness of plate-II in order to examine the effect of thickness on wake. These two thicknesses are considered to be the extream cases for assuming the flow to be two-dimentional.

The length and span of both plates were 91.5 cm and 45.7 cm respectively. Plate-I was made of wood having its leading edge in the form of a symmetrical wedge upto 15.0 cm of the plate and the remaining part maintained to be the same thickness, 1.905 cm. until the trailing edge. The surface of the plate was polished to make it smooth. Plate-II was made of wood of thickness, 1.27 cm having its leading edge in the form of a symmetrical wedge upto 15.0 cm of the plate and the trailing edge tapered linearly down to 0.159 cm over a length of 10 cm. Fine mesh G.I. screens(6 holes/cm) were inserted at 10 cm up-stream from the trailing edge of the plates. The plates were made in such a way that it fits tightly at the mid-height of the working section. A schematic diagram with pertinent dimensions are shown in Fig. 4.1.

Fig. 4.2 is a diagram of a straight subsonic wind tunnel of suction type which was used for this experiment. The air was sucked by a fan(38 in. dia) of capacity 30,000 cfm situated at the downstream side of the working section. The tunnel illustrated above has a working section of size (45.7 cm x 45.7 cm x 3.25m) . The wind tunnel was originally designed and constructed by Islam [25] and installed by Khalil [26]. The mesh G. I. screens were inserted at the inlet of a large contraction ratio converging duct. Following the converging duct there were four consecutive square cross - sectional ducts as shown in

Fig. 4.2. The first duct(45.7 cmx45.7 cmx 96.5 cm) was made of wood and the plates were placed at the mid-height of the cross-section within this duct . The second and third ducts(45.7 cm x 45.7 cm x 76.2 cm) were made of perspex sheet while the fourth one(45.7 cm x 45.7 cm x 76.2 cm) was made of wood. Adequate holes were provided at the bottom of the perspex ducts along the central line for inserting the pitot-static tube. There was also one hole at a distance of 15 cm from the inlet of the second duct, at the mid-height of the side wall for inserting the pitot-static tube inside the duct.

4.3 Measuring equipment

Pitot-Static tube was used to measure the mean velocity of flow. The pitot-static tube was traversed vertically up and down by rack and pinion arrangement over a vertical stand with a vernier scale to read upto 0.01 inch(0.0254 cm). The outer diameter at the end of the pitot-tube was one sixteenth of an inch (0.159 cm) . The pitot-static tube was connected to an inclined draft gauge. The scale of the draft gauge was graduated to a precision of 0.02 inch(0.05 cm).The draft gauge was set horizontal with the help of a spirit level. The liquid used in the manometer was kerosene oil of specific gravity 0.81. In order to prevent the vibration of the sensor the pitot-static tube was supported by a 0.635 cm diameter brass rod. The sensing point was 10 cm above the top of the rod. This was done to avoid the disturbance in the flow

due to the presence of the brass rod. For inserting the pitot-tube into the duct 12 holes were provided along the central line of the bottom of the duct. Static pressure was measured by means of static tube. A schematic diagram of the experimental set-up is shown in Fig. 4.3. This experimental technique was also used by Khalil [26] for investigating turbulent shear layers.

4.4 Calibration of the wind tunnel

For the calibration of the wind tunnel, the velocity and the pressure in the test section were measured. The purpose of calibration was to examine the uniformity of velocity and pressure within the test section without using the wake generating plate in the upstream.

In order to determine the velocity and pressure heads in the test section the pitot-static tube was traversed up and down by rack and pinion arrangement over a stand. From the draft-gauge the velocity heads and the pressure heads were recorded and the velocity and pressure at different points across the cross-section were calculated. The velocity heads and the pressure heads were recorded at two stations, viz X= 5, 122 cm where X is the distance measured from the inlet of the test section. It is seen that the velocity profiles are similar at the two sections, and the experimental points for the two sections collapse on a single curve and hence there

exists no velocity gradient in the axial direction. The velocity distribution is also symmetrical about the center-line as shown in Fig. 4.4. The velocity profile is flat across the test section except for a small boundary layer at the top and bottom walls of the test section. The area under the velocity profile was computed and therefrom the average velocity across the test section was determined. Reynolds number of the flow was calculated on the basis of the average velocity and the width of the test section, such calibrations were performed for flows with Reynolds numbers used in this investigation.

The boundary layer thickness was obtained by measuring the distance, Y, from the wall for which u/U=0.99. The wall momentum thickness was calculated by using eqn. (3.2.5) . The computed values of different flow parameters for the test-section are given below in Table 4.1.

TABLE 4.1

CHARACTERISTICS OF THE VELOCITY PROFILE IN THE TEST SECTION CALIBRATIONS

Average Velocity U_{av} (m/sec)	Reynold No. Red	Wall momentum thickness θ_w (cm)	Boundary Layer thickness (cm)
17.83	5.4844×10^5	0.128	1.65
13.56	4.1695×10^5	0.139	1.90
9.79	3.0102×10^5	0.144	2.03
7.52	2.3124×10^5	0.161	2.54

Fig. 4.5 shows the pressure distribution in the test section at the axial distance, X = 5, 122 cm. The two sets of experimental points show negligible difference as shown in Fig.4.5. This implies that there exists negligible pressure gradient in the axial direction within the test-section.

4.5 Experimental procedure

After the calibration, the duct made of G.I. sheets was replaced by the wooden duct mounted with the wake generating flat plate at the mid-height. A schematic diagram of the experimental set-up is shown in Fig. 4.3.

The thin wake was allowed to grow in the downward direction through the perspex duct. In order to investigate the wake along the axial direction, the mean velocity and the static pressure were recorded at various distances(viz X=5, 7.6, 11.4, 30.5, 45.7, 61, 91.5, 106.7, 122, 137 cm) from the trailing edge of the flat plate. The manometer reading was quite stable except over a narrow range near the wall where it fluctuated. However, in this region average of five observations was taken for a reading at a point.

Similarly readings were taken at the trailing edge of the plate, and in the wake for different Reynolds number.

The room temperature and the pressure were taken at the beginning and at the end of each experiment. The average of the two was taken as the recorded data for the experiment.

4.6 Uncertainty statement

The uncertainty of the measurements of the mean velocity and pressure are influenced by the variation of specific gravity of liquid (in draft gauge) which is associated with the variation of the ambient temperature and pressure, the accuracy of the angle of inclination of the pitot static tube to the mean flow direction and the accuracy of the measurements of the draft gauge reading. Uncertainties presented here were calculated by using the procedure given in Appendix - I. The uncertainty of mean velocity, u_U/U was estimated to be less than $\pm 1.4\%$. The uncertainty of pressure P_{reu}/P_{re} was estimated to be less than $\pm$ 0.6%. The uncertainty in measuring the linear distance was negligible. Temperature and pressure(atmospheric) variation during the experiments were $1.5^{o}F$ and 0.05 (inch of Hg) respectively.

CHAPTER - V

RESULTS AND DISCUSSION

5.1 General

Mean properties of the flow at the trailing edge**, and in the wake at the downstream of the trailing edge were determined experimentally. The experiments were performed by varying initial conditions at the trailing edge. All these experimental data have been analysed to obtain some informations regarding the wake development. This chapter presents comparisons of experimental and theoretical results of mean flow properties in wakes. All computations and data analysis were performed by using a desk calculator and on IBM 370-115/2 computer. The computer programs are given in Appendix - III.

5.2 Trailing edge conditions

The increase of velocity with transverse distance, Y, from the plate surface indicates relative movement of the particles in the boundary layer. As the boundary layer is thin, the velocity gradient in the transverse direction is high. Fig. 5.1a shows the velocity distributions at the trailing edge of the plate-I (D = 0.75 inch) 1.905 cm thick and plate - II (D= 0.063 inch) 0.159 cm thick. The figure shows that the veolcity profiles, at the trailing edge, contain boundary layers which are important for the development of the wakes. The boundary layer velocity profile is shown in Figure 5. 1b. in a magnified scale. Momentum thickness of the velocity profiles are calculated graphically at the trailing edge

---

**Trailing edge measurement was at $X = -1$mm from the end of the plate

of both the plates, by using equation (3.2.5). which is found to decrease with the increase of free stream velocity. This momentum thickness and the free stream average velocity are used to define the Reynolds number. The characteristics of the turbulent boundary layer at the trailing edge(X= -1mm)of the plates for different flow parameters are shown in Table 5.1. The experimental values of velocity within the boundary layer are fitted to the universal turbulent velocity profile near the wall in the coordinate system u^+ vs y^+ . The universal profile near the wall is,

$$u^+ = B \log y^+ + A \qquad (5.2.1)$$

where, $u^+ = u/u^*$, $y^+ = \frac{u^* y}{\nu}$, and B & A are constants. The three constants u^+, A & B are optimised on the basis of the least rms errors between experimental values and equation (5.2.1) which did not exceed, 1.744224, for any case. The method of optimisation is given in detail in Appendix - II. The constants A & B for different initial conditions were found close to each other, and the values are given in Table 5.1. The constants A & B were determined experimentally by many authors including Lugwieg. [27], Klebanoff [28] & Schultz [29]. The values of the constants should very within the range 4.0 to 7.15 for A, and 5.0 to 6.7 for B as reported in ref. [30]. The optimum values of A & B determined by fitting the present experimental results with equation (5.2.1) are within the range already

specified by Duncan [30]. Fig. 5.2shows the plotting of the universal velocity profile given by equation (5.2.1) for the five initial conditions already mentioned. The values of constants A and B , and the nature of curves in Fig. 5.2 are typical representation of turbulent boundary layer on the wall. If the profiles in Fig. 5.2 are plotted on the plane with same axes all the experimental points for different boundary layers at the trailing edge will collapse on a same line, hence it is a typical representation of fully developed turbulent boundary layer. In addition, the values of Reynolds numbers based on momentum thickness and average velocity given in Table 5.1 are high in comparison to the typical values necessary for the assumption of turbulent boundary layer.

TABLE 5.1

CHARACTERISTICS OF THE VELOCITY PROFILE AT THE TRAILING EDGE OF THE PLATES

Plate	Average free-stream velocity U_{av} (m/sec)	Momentum thickness θ (cm)	Reynolds Number Re_θ	Boundary layer thickness δ (cm)	Friction velocity u* cm/Sec)	Constant B	Constant A
I	18.10	0.0894	2.18×10^3	0.762	0.832	5.79	6.04
I	13.49	0.1107	2.01×10^3	0.885	0.683	5.73	4.72
I	9.99	0.1422	1.90×10^3	1.016	0.509	5.42	5.34
I	7.65	0.1651	1.70×10^3	1.270	0.418	5.22	4.96
II	23.81	0.0552	1.77×10^3	1.270	1.199	5.82	6.10

It is to be noted here that the initial conditions play an important role for the development of wakes. But many authors [6, 3] did not identify the initial conditions for the study of wakes. This was probably due to the fact that boundary layer for their cases were very thin. Islam [1] has already identified that the initial conditions have a big influence on the development of shear layer for jets. As the development of wake is similar to that of jet flows, the effect of initial conditions is worthy to note down for wake flows.

5.3 Free Stream Flow

The free stream velocity, U, represents the uniform flat part of the velocity profile outside the wake and it is parallel to the X-axis. The free stream velocity drops instantaneously when the boundary layer separates from the plate to form the wake. Such drop is observed for thick plate-I upto the axial distance, $X/\theta = 50$, after which it achieves a uniform and constant value. Fig. 5.3 shows that the drop of the free stream velocity upto $X/\theta = 50$, is not more than 4% for the plate - I. Such a drop of free-stream velocity was not identified in the case of a thin plate-II. From the consideration of potential flow theory, there exists adverse axial pressure gradient at the beginning of the wake and it achieves zero axial

pressure gradient after $X/\theta = 50$. The drop of the uniform free-stream velocity is due to the increase of flow area as the profile separates from the plate-I . But for the Plate-II, the increase in flow area at the beginning of the wake is not much to decrease the free-stream velocity significantly. The free stream velocity does not vary with the Reynolds number, $Re_{\theta e}$, except close to the plate-I . But it is independent of Reynolds number for thin plate as in the case of plate-II. Similar conclusion was also drawn by Chevray and Kovasznay [4] and they considered flat free-stream velocity profile without considering pressure gradient.

5.4 Tunnel wall characteristics

The wake studied here is a two dimensional one and submersed in an approximately uniform free stream velocity in the test section of a wind tunnel. The free stream flow pattern has a boundary layer on the wall of the test section. Though the free stream velocity is approximately constant, the boundary layer on the wall of the test section is presented to examine its variation in the axial direction.

Fig. 5.4a, 5.4b, 5.4c and 5.4d show the velocity profile with their megnified boundary layer in Figs.5.4e ,f,g and h on the wall for different Reynolds numbers. The experimental points are fitted to the universal velocity pro-

file on the wall in the form given by equation (5.2.1). The constant A, B and u* are optimised (APPENDIX-III) for the least value of the rms errors between the experimental values and the values from equation(5.2.1)at each section.The optimum values of A & B determined here are found to fall within the range given by many authors including Duncan [30]. For the purpose of fitting, the value of u* was varied in a step of 0.01 to get the optimum values of A and B for a minimum rms error. The values of rms error did not exceed 0.89 for any case for the values of A and B reported here in table 5.2. For turbulent boundary layers values of A and B determined by the authors [27, 28, 29] are within a range 4.0 to 7.15 for A and 5.0 to 6.7 for B. The universal velocity profile on the wall at different axial stations are shown in Fig. 5.5. From this plot it is evident that the boundary layer on the wall is turbulent. Wall momentum thickness of the velocity profiles are calculated by using equation (2.2.5) and given in Table 5.2. The wall momentum thickness in Table 5.2 shows an increase with the decrease of Reynolds number. For a Reynolds number the momentum thickness maintain its constant value with the increase of axial distance. This indicates that the boundary layer on the wall is developed. The wake generated here is not strong enough to influence the mean parameters in the wall boundary layer within the axial distance

TABLE 5.2

CHARATERISTICS OF THE VELOCITY PROFILE
AT THE WALL OF THE EXPERIMENTAL DUCT

R_{D_e} \ X/D	2.66	4.00	6.00	16.00	24.00	32.00	48.00	56.00	64.00	72.00	
2.18×10^3	0.816	0.810	0.709	0.786	[illegible]	0.771	0.760	0.762	0.747	0.744	U^* m/s
	5.880	5.870	5.850	5.850	[illegible]	5.730	5.810	5.790	5.760	5.750	B
	4.410	4.490	4.950	4.540	[illegible]	5.300	4.709	4.840	5.220	5.250	A
	1.650	1.650	1.650	1.650	[illegible]	1.650	1.650	1.650	1.650	1.650	δ(cm)
	0.128	0.128	0.128	0.128	[illegible]	0.128	0.128	0.128	0.128	0.128	a(cm)
2.01×10^3	0.658	0.655	0.654	0.646	[illegible]	0.643	0.637	0.637	0.630	0.629	U*m/s
	5.660	5.760	5.740	5.730	[illegible]	5.730	5.730	5.710	5.700	5.700	B
	5.560	4.470	4.640	4.510	[illegible]	4.540	4.650	4.700	4.870	4.880	A
	1.905	1.905	1.905	1.905	[illegible]	1.905	1.905	1.905	1.905	1.905	δ(cm)
	0.140	0.140	0.140	0.140	[illegible]	0.140	0.140	0.140	0.140	0.140	a(cm)
1.9×10^3	0.511	0.510	0.510	0.506	[illegible]	0.502	0.502	0.499	0.498	[illegible]	U^* m/s
	5.530	5.540	5.520	5.710	[illegible]	5.500	5.51	5.50	5.50	[illegible]	B
	4.350	4.180	4.130	4.700	[illegible]	4.270	4.300	4.330	4.330	4.370	A
	2.083	2.083	2.083	2.083	[illegible]	2.083	2.083	2.083	2.083	2.083	δ(cm)
	0.145	0.145	0.145	0.145	[illegible]	0.145	0.145	0.145	0.145	0.145	a(cm)
1.7×10^3	0.415	0.414	0.414	0.414	[illegible]	0.414	0.414	0.414	0.414	0.414	U^* m/s
	5.310	5.310	5.310	5.320	[illegible]	5.320	5.310	5.310	5.320	[illegible]	B
	4.040	4.040	4.000	4.000	[illegible]	4.000	4.000	[illegible]	[illegible]	[illegible]	A
	2.410	2.410	2.410	2.410	[illegible]	2.410	2.410	2.410	2.410	2.410	δ(cm)
	0.157	0.157	0.157	0.157	[illegible]	0.157	0.157	[illegible]	[illegible]	0.157	a(cm)

covered in the experiments. Fig. 5.6 shows the variation of friction velocity on the wall with axial distances. Friction velocities are also approximately constant with axial distances from the trailing edge except very close to the trailing edge. The friction velocities determine by the curve fitting principle of the universal velocity profile equation (5.2.1) and the experimental values show a small deviation from its constant value in the near region. The momentum thickness already mentioned remain constant with axial distances. Here it is to be noted that for each $Re_{\theta e}$ = 2.18×10^3, 2.01×10^3, 1.9×10^3 and 1.7×10^3, the friction velocities at various axial distance are approximately constant as shown in Fig.5.6.

5.5 Wake development

5.5.1 Velocity and shape factor

Fig. 5.7 a, b, c &d show the variation of mean velocity distribution in wakes for $Re_{\theta e}$ = 2.18×10^3, 2.01×10^3, 1.9×10^3 and 1.7×10^3 respectively. The velocity distribution in the wake is likely to be complicated in the neighbourhood of the flat plate because of high velocity gradient. The vortex shading from the surface of the plate is being convected into the stream direction, and diffused by viscosity. It follows that ultimately convection is more important than

streamwise diffusion and that streamwise gradient is small compared with that in the lateral plane at the downstream plane. As the velocity gradient with the axial distance gradually decreases, the flow tends to become self-preserving with the increase of axial distance Figs. 5.7a, b, c and d show the development of the wakes with increasing the widths. Such a spread of the wake is logical, from the view point of energy transfer to the wake from the surrounding. The geometrical parameters of the wakes will be discussed later.

The momentum thickness within the wake was calculated from the experimental data by using equation (3.2.5) at different axial distancesin the down stream of the wake. The values of momentum thickness for different $Re_{\theta e}$, are shown in Fig. 5.8. The wake momentum thickness increases with the increase of Reynolds number, $Re_{\theta e}$. But the momentum thickness in the wake for a fixed $Re_{\theta e}$ is found to be independent of the axial distance from the trailing edge. Chevray and Kavasznay [4] also determined the momentum thickness to be constant within the wake. This fact can also be interpreted from the momentum equation neglecting pressure gradient given by equation (3.2.5) . The momentum thickness within the wake increases with the increase of Reynolds Number, $Re_{\theta e}$, for the same plate. The momentum thickness will also depend upon the

plate thickness. For the plate II, which is very thin, the value of momentum thickness was calculated to be 0.065 cm, for, $Re_{\theta e} = 1.77 \times 10^3$.

The Shape factor, $H = \delta^*/\theta$, is plotted in Fig. 5.9 as a function of axial distance. The slope of the curve for any Reynolds number decreases at a higher rate in the region close to the trailing edge and it decreases at a slower rate with the increase of axial distance. This trend of the shape factor curve in Fig. 5.9 shows an indication of self-preservation of flow. The flow will be absolutely self-preserving when the shape factor tends to be unity. The shape factor vary with Reynolds number, $Re_{\theta e}$, as shown in Fig. 5.9. A comparison with the results of Chevray and Kovasznay[4] is also presented to show a satisfactory agreement of the present results.

5.5.2 Half width and center-line velocity

The half width is an important geometrical dimension for length scale, generally used for explaining the self-preserving flow. Dimensionless half width($2y_{\frac{1}{2}}/C_{dm}L$) of the wakes are plotted against axial distances, which are shown in Fig. 5.10. Half width of the wake which are calculated from the semi-empirical equation (3.2.13) given by Schlichting [7] for two-dimensiotnal wakes are also plotted in the same Fig. 5.10 to compare with that of

experimental results for plate - 1 and plate-II. The axial variation of half width of the wake near the trailing edge of the plate deviate from that of semi-empirical results,but it agrees with empirical results after X/C_{dm} L=50. The development of wake depend upon the initial conditions which are already mentioned. Schlichting's[7] results are valid for a very thin boundary layer at the beginning. Fig. 5.10a also present the fact that with the decrease of intial boundary layer for higher Reynolds number the experimental results approach towards Schlichting's equation (3.2.13). It is also to be noted that the effect of the initial condition exists only upto a certain axial distance and then the flow forgets its state of origin. Similar case is also explained by Islam [1] and Hussain and Zedan[31] for jets. This is probably due to the nature of energy transfer from large scale to small scale eddies which depends on vortex pairing. The spread parameter for the wake is shown in Fig. 5.10b which achieves approximately a constant value , δ= 0.675 at X/θ=200 for the Reynolds numbers studied.

Dimensionless center-line velocity defect is plotted in Fig. 5.11 against the dimensionless axial distance, $X/C_{dm}L$. For the four different Reynolds number, the experimental value fall on a same line except close to the trailing edge. The plot in Fig. 5.11 also shows a comparison with the results of Schlichting's experiments . Near the trailing edge of the plate-I velocity defect is less than that of Schlichting's experimental results. But after $X/C_{dm}L > 40$

the experimental velocity defect is greater than that of Schlichting's experimental results. For the thin plate-II with thin boundary layer at the beginning the present results come closer to the Schlichting's values. The center -line velocity is also plotted in a coordinate system $(1-\frac{U_c}{U_o})^{-2}$ vs. X/θ in Fig. 5.12, which is a conventional plotting given by many authors [21, 22, 32]. Theoretical results of Korst & Chow [22] and the experimental results of Chevray and Kovasznay [4] are also shown in the same Fig. 5.12 to compare the present experimental results. Near the trailing edge of the plate- I the velocity increment at the centre-line of the wake is greater than that of Chevray and Kovasznay [4] and Korst and Chow [22]. After X/θ = 120, the present results lie between Korst and Chow's [22] theoretical results and Chevray and Kovasznay's [4] experimental results. Korst and Chow [22] calculated the differential momentum and continuity equation using Prandtl's model of shear stress. For all calculations Korst and Chow [22] used a flat velocity profile at the beginning of the wake. In the near region Korst and Chow's [22] results agree satisfactorily with Chevray and Kovasznay's [4] results and it does not agree in the region after X/θ = 100. This is an indication that the Prandtl's model of shear stress is not applicable in the region after X/θ = 100. The present results with considerable boundary layer thickness at the beginning shows a deviation from both Korst & Chow's [22] and Chevray and Kovasznay's [4]

results. It is already mentioned that the flow forget its initial condition with the increase of axial distance due to its transformation to small scale motion. So, at further downstream region the present wake will agree with Chevray and Kovasznay's [4] wake.

5.5.3 Self preservation

Dimensionless velocity distribution for the wakes are shown in Fig. 5.13a, 5.13b, 5.13c, 5.13d and 5.13e corresponding to the Reynolds number 2.18×10^3, 2.01×10^3, 1.90×10^3, 1.70×10^3 and 1.77×10^3 respectively to examine their self-preservation. The half width, $Y_{\frac{1}{2}}$, is used as length scale in the self-preservation plot. The velocity distribution in Fig. 5.13a-e do not show self-preservation, but it may become similar only at large distance downstream from the trailing edge of the flat plate. No similarity of mean velocity is observed near to the trailing edge of the plate. The semi-empirical equation (3.2.11) derived by Gartshore [6] and Keffer [3] for similarity profile are also shown in Fig. 5.13a, 5.13b, 5.13c, 5.13d and 5.13e for comparison. Deviation of the experimental results from the semi-empirical equation (3.2.11) may be expressed in rms error. This rms error was calculated and found to decrease gradually with the axial distance as shown in Table 5.3. The rms errors for the plate-II (0.159 cm thick) were calculated to be 0.079 at X/D=16 and 0.057 at X/D = 56. The least rms error is an

TABLE 5.3

rms ERRORS AT VARIOUS DISTANCE FROM THE TRAILING EDGE OF THE PLATE-I

$X/D \rightarrow$ / $Re\theta_e \downarrow$	16	24	32	48	56
2.18×10^3	0.077	0.074	0.069	0.062	0.058
2.01×10^3	0.0795	0.078	0.072	0.064	0.060
1.90×10^3	0.0830	0.081	0.076	0.071	0.068
1.70×10^3	0.1190	0.110	0.099	0.098	0.096

an indication of self-preservation. Examining the rms error in Table 5.3 it can be concluded that the flow achieves self-preservation earlier with the higher Reynolds number, $R_{e\theta_e}$. From a comparison of Fig. 5.13a and Fig. 5.13d it is clear that the flow is nearer to self-preservation in Fig. 5.13a for $R_{e\theta_e} = 2.18\times10^3$ than that in Fig. 5.13d for $R_{e\theta_e} = 1.7\times10^3$ at $X/D = 56$. The values of rms errors for various Reynolds number, $R_{e\theta_e}$, are plotted in Fig.5.14 to show that the rms error is less for higher Reynolds number at an axial distance. So, the wake velocity profile becomes similar(self-preserving) earlier for higher Reynolds number. The flow is not self-preserving in the range of axial distance covered in this investigation as the least rms error is of the order of 0.058, which is considered to be high for self-preservation. The semi-empirical self-preserving velocity profile can also be expressed as :

$$\frac{U-u}{U-u_c} = \exp\left(-\sigma\left(Y/Y_{\frac{1}{2}}\right)^2\right) \qquad (5.5.1)$$

where the spreading parameter, σ, replaces 'a' of the equation(2.22). The spreading parameter, σ, is already shown to be constant after $X/\theta = 200$ for all Reynolds numbers studied here. Using the constant value of σ in equation(5.5.1)it is plotted in Figs. 5.13 a,b,c &-d to show a comprison with Gartshore's[6] equation (2.22).

5.5.4 Wake drag

Drag co-efficient due to the wake is calculated from the momentum thickness equation (3.2.7) obtained by neglecting pressure is plotted in Fig. 5.15 against Reynolds numbers. Fig. 5.15 shows that the drag co-efficient increases with the Reynolds number. Drag co-efficient is also calculated by applying equation (3.2.10) near the trailing edge of the plate considering the effect of pressure. The result is plotted in Fig. 5.15 to show a comparison. Drag co-efficient calculated by the above two methods are in agreement at each point. This indicates that the effect of pressure is negligible.

5.5.5 Pressure in wake

Fig. 5.16 shows the variation of pressure in wakes for the Reynolds number 2.18×10^3, 2.01×10^3, 1.9×10^3 and 1.7×10^3. In Fig. 5.16 the pressure at the free stream region is nearly constant, and it varies only near the trailing edge of the plate-I and within a very small region about the center-line of the wake. Drop of pressure is higher for higher Reynolds number as shown in Fig. 5.16. Pressure drop in vicinity of the trailing edge is also high for thick plate. There is no pressure gradient in the transverse direction near the trailing edge of the plate, if the plate thickness is very small as shown in Fig. 5.17. The same case was also reported by Chevray and Kovasznay [4].

CHAPTER - VI

C O N C L U S I O N

The present investigation is on the two-dimensional turbulent wakes formed behind flat plates in a wind tunnel. Two flat plates of different thicknesses were used for generating the wakes at four different exit Reynolds numbers, i.e. $Re_{\theta e} = 2.18 \times 10^3$, 2.01×10^3, 1.9×10^3 and 1.7×10^3. The boundary layers were turbulent at the trailing edge of the plate, and the wakes formed with these boundary layer were assumed to be turbulent from the exit. The initial boundary layer is identified to be turbulent on the basis of the experimental values of velocities, which fit to the universal velocity profile of turbulent boundary layer. The uniform flow that surrounds the wake is confined by the wall of the test section. The boundary layer on the test-section wall is also identified to be turbulent. The wall momentum thickness decreases with the increase of Reynolds number, but remains approximately constant with the increase of axial distance. This indicates that the development of the wake at the mid of the test section does not influence the mean parameter in the wall boundary layer within the axial distance covered in the experiment.

For the same Reynolds numer the wake momentum thickness is found to be constant with the axial distances, but it increases with the increase of Reynolds number and plate thickness. The shape factor of the wake decreases with the increase of Reynolds number and with the axial distance from the trailing edge but it decreases with decrease of plate thickness. The decrease of the shape factor to unity is an indication of self-preservation of flow. The velocity distribution in the neighbourhood of the flat plate is unstable due to the presence of high velocity gradient in the axial direction and it decreases gradually to make the flow self-preserving. The flow is not found to be self-preserving in the range of investigation upto $X/D = 56$. The axial variation of half width of the wake is approximately linear except close to the trailing edge. But it is determined to be a linear function of axial distance by many authors, starting from the trailing edge considering flat velocity profile at the beginning. The present results agree with the existing results after a certain axial distance $X/C_{dm}L = 50$, where the effect of initial conditions are insignificant. The rate of increase of the central-line velocity is rapid in the near region of the wake & it becomes slow with the increase of axial distance. For thinner wake

generating plate, the central line velocity increase at a higher rate with the axial distance. The flow within the wake does not show complete self-preserving within the axial distance covered in the investigation. But for higher Reynolds number it tends to become self-preserving earlier for the same plate thickness at the beginning. If the wake generating body is thinner it also tends to become self-preserving earlier. It is observed a small pressure gradient in transverse direction near the trailing edge of the thick plate, but it is not observed for thin plate.

REFERENCES

R E F E R E N C E S

1. Islam, S.M.N., Prediction and Measurement of Turbulence in the Developing Region of Axisymmetric Isothermal free Jets, Ph.D. Thesis, Deptt. of Mech.Engg., University of Windsor, Windsor, OWT, Canada, 1979

2. Keffer, J.F., "The uniform distribution of a turbulent wake", J. Fluid Mech., Vol. 22; Part-I, 1965, P.135.

3. Keffer, J.F., "A note on the expansion of Turbulent Wakes", J. Fluid mech., vol. 28, Part-1, 1966, P. 183.

4. Chevray, R. and Kovasznay, L.S.G., "Turbulence Measurements in the wake of a thin flat plate", AIAA Journal, vol. 7, No.8, August, 1969, P.1641.

5. Hiroshi, S. and Kuriki, K., " The mechanism of Transition in the Wake of a Thin Flat Plate placed parallel to a uniform Flow", J. Fluid mech., vol. 11, 1961, P.321.

6. Gartshore, I.S., "Two-dimensional Turbulent Wake", J. Fluid mech., vol. 30, Part-3, 1967, P. 547.

7. Schlichting, H., "Uber das ebene Winds Chatten Problem", Thesis Gottingen, Ingr. Arch. 5, 1930, P. 533.

8. Hall, A.A. and Hislop, G.S., "Velocity and Temperature distribution in the Turbulent Wake Behind a Heated Body of Revolution", Prac. Cambridge Phi. Soc. 34, 1938, P.345.

9. Swain, L.M., "On the Turbulent Wake Behind a Body of Revolution", Proc. Roy. Soc.(London), A, 135, 799, 1929, P.647.

10. Reichardt, H., "Gesetzmassigkeiten der freien turbulenz", VDI- Forschungsh, 1951, P. 414.

11. Fage, A. and Falkner, V.M., "The Transport of Vorticity and Heat Through Fluids in turbulent Motion", Proc. Roy. Soc., (London), A, 135, Appendix, 1932.

12. Goldstein, S., "Note on the Velocity and Temperature Distribution in the Turbulent Wake Benind a Heated Body of Revolution", Proc. Cambridge Phil. Soc. 34, 1938, P.351.

13. Demetriades, A., "Mean Flow Measurements in an Axisymmetric Compressible Turbulent Wakes", AIAA Journal, vol. 6, No.3, 1958 , P. 482.

14. Taylor, G.I., "The Transport or Vorticity and Head Through Fluid in Turbulent Motion", Proc. Roy. Sec., (London), A. 135, 828, 1932, p. 828.

15. Hussain, A.K.M.F., " Coherent Structures", Aerodynamics and Turbulence Laboratory, July, 1921, P.6.

16. Townsend, A.A., The Structure of Turbulent Shear Flow, Cambridge U. Press(1956).

17. Meller, G.L. and Herring, B.J., "Two methods of Calculating Turbulent Boundary Layer Behavior Based on Numerical Solution of the Equation of Motion", D.J. Cockrell, eds stanford University C.1969, P.331.

18. Payne, F.R. & Lumley J.L., Phys Fluid Suppl. , 10, 5194(1967).

19. Brown, G.B. , Physical Sec. 47, 1935, P.703.

20. Anderson, A.B.C., J. Acous. Sec. Amer, 26, 1954, P. 21.

21. Launder,B.E., Morse,A., Rodi W. and Spalding B.B., "A comparison of the performance of six turbulence models", Proc. Hypersenic Aircraft Fluid Mechanics Branch, NASA Langley Research Center, Mampton, Virgine, 1924-1972.

22. Korst, H.H. and Chow,W.L.," On the Correlation of Analytical and Experimental Free Shear Layer Similarity Profiles by Spread Rate Parameters", Trans. ASME, Ser D. J. Basic Engg., Vol.93, No.3, Sept. 1971, P. 377.

23. Schetz, Joseph,A.,"Some Studies of the Turbulent Wake Problem", Astronant. Acta, Vol. 16, No.2,Feb. 1971, P. 107.

24. Abramovich,G.N., The theory of turbulent jets, The M.I.T. Press, Massachusetts Institute of Technology. Cambridge, Massachusetts

25. Islam, S.M.N. , Design & Construction of Closed Circuit Wind Tunnel, M.Sc. Engg. Thesis, Department of Mechanical Engg. BUET, Dhaka, 1975.

26. Khalil,G.M., The initial region of plane turbulent mixing layer, Ph.D. Thesis, Department of Mech. Engg. BUET, Dhaka, 1982.

27. Lugwieg, H. and Tillmann,W., Ingn.Arch,17,1949,P.288.

28. Klebanoff, P.S. and Diehl, Natl advisory comm Aeronaut. Tech.,Notes No. 2475, 1951.

29. Schultz-Grunow, F., Luftfahrt Forsch,17, 1940,P.239.

30. Duncan,W.J. , Thom A.S. and Young,A.D.,An Elementary Treatise on the Mechanics of Fluids, The English Language book Society and Edward Annold Ltd. F.L. B.S. Ed.1967, P. 307.

31. Hussain, A.K.M.F. and Zedan, M.E.," Effect of the Initial Condition on the Axisymmetric Free Shear Layer", Physics of Fluids, Vol. 21, No.9,Sept.1978, P.1475.

32. Thomas,M.,Torda,T.P. and Bradshaw,P., "Turbulent Kinetic Energy equation and Free Mixing" Proc. Hypersonic Air-Craft Fluid Mechanics Branch, NASA Langley Research Center, Hampton, Virgina, 1924-1972.

FIGURES

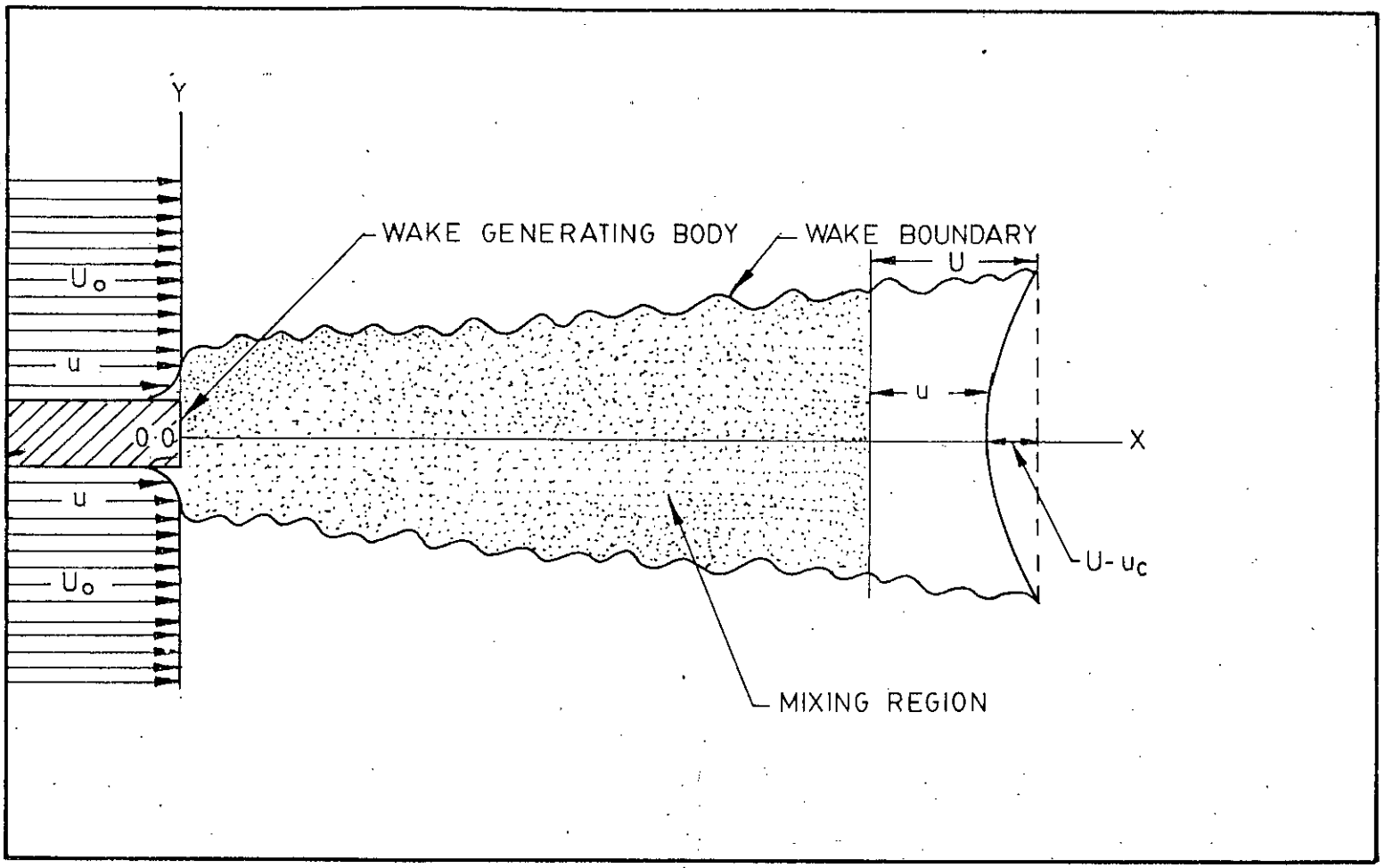

FIG 1.1 WAKE GEOMETRY AND NOMENCLATURE

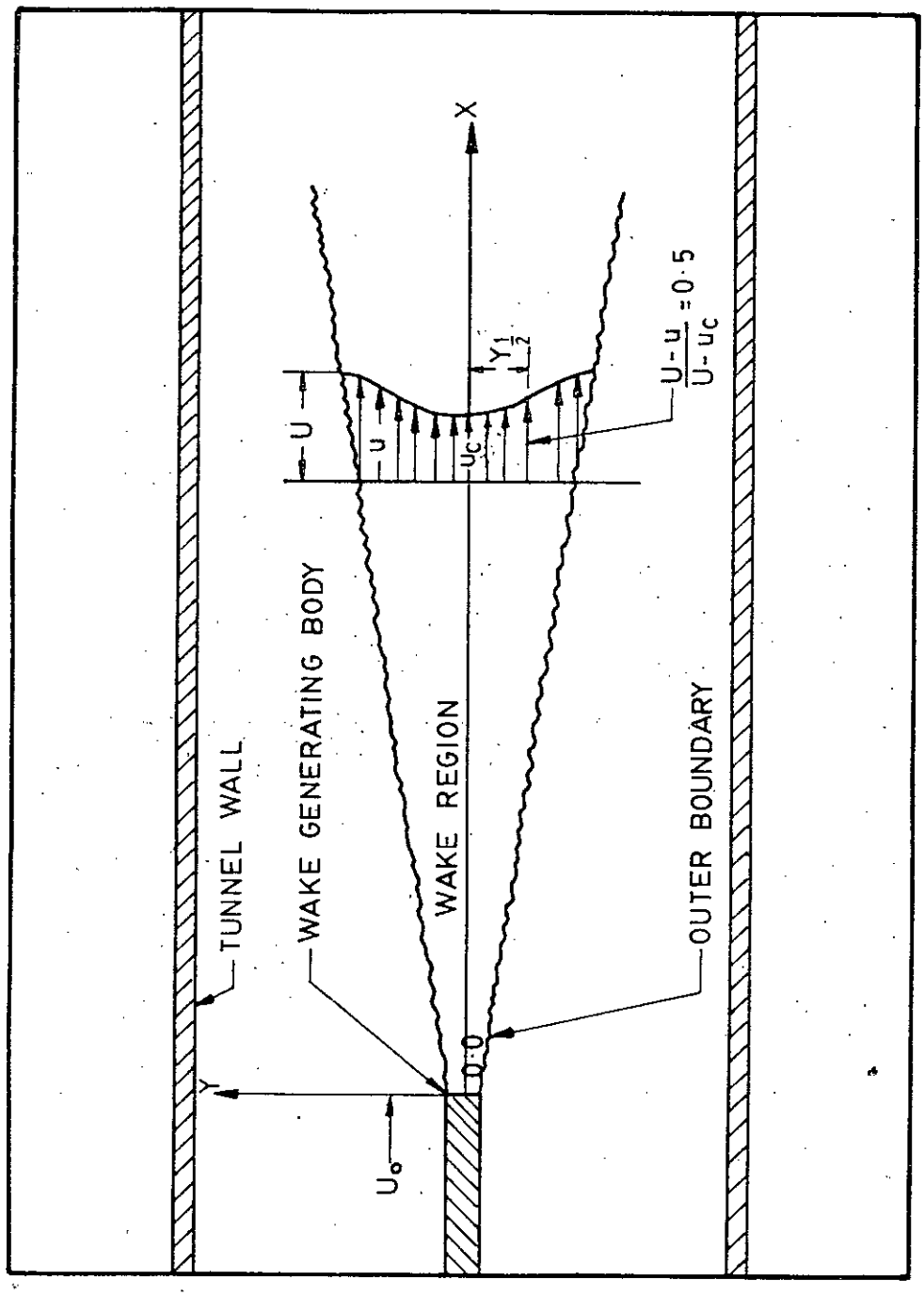

FIG. 3·1 CO-ORDINATE SYSTEM OF WAKE

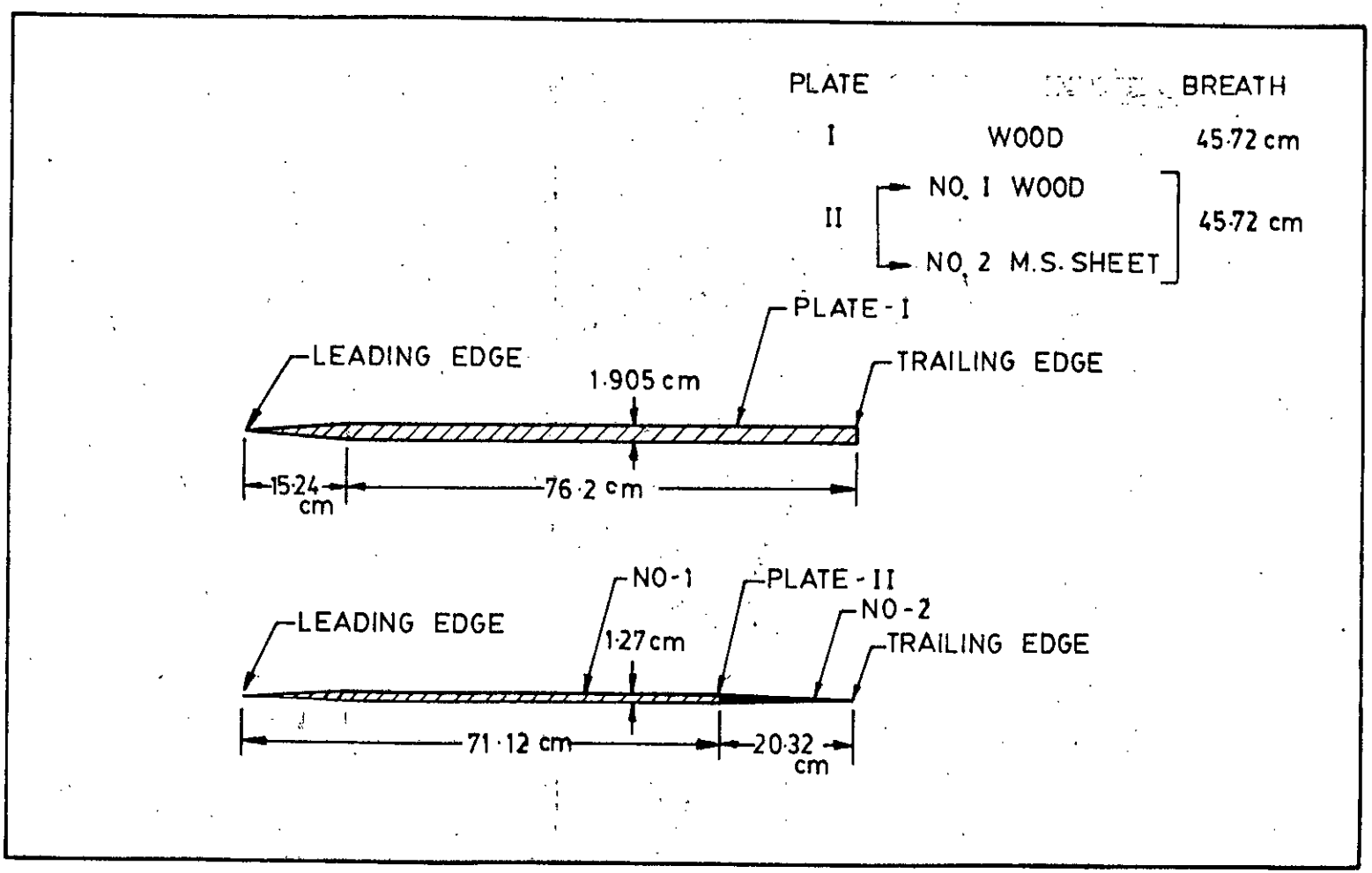

FIG.4.1 SCHEMATIC DIAGRAM OF THE WAKE GENERATING PLATES

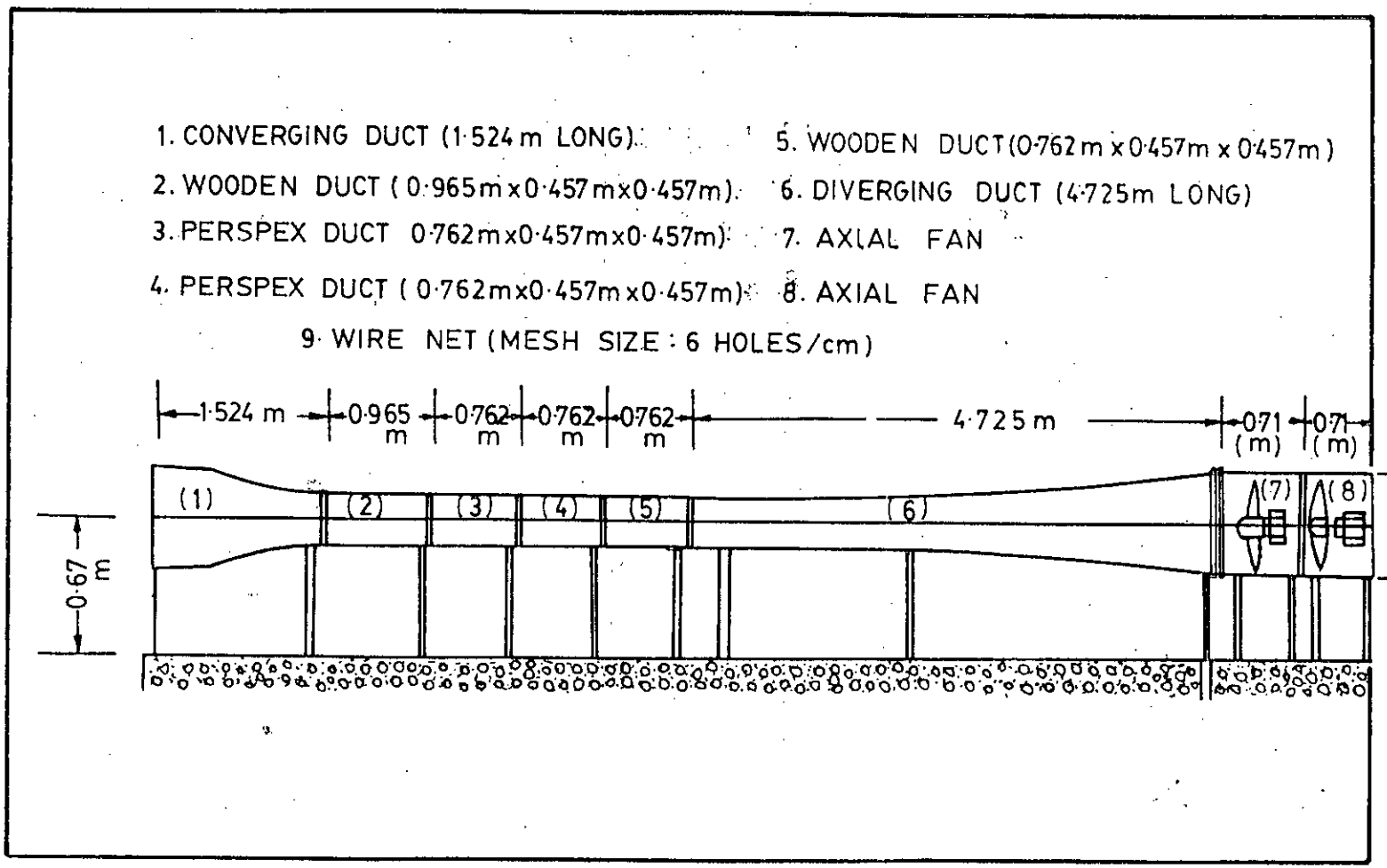

FIG.4.2 SCHEMATIC DIAGRAM OF THE WIND TUNNEL

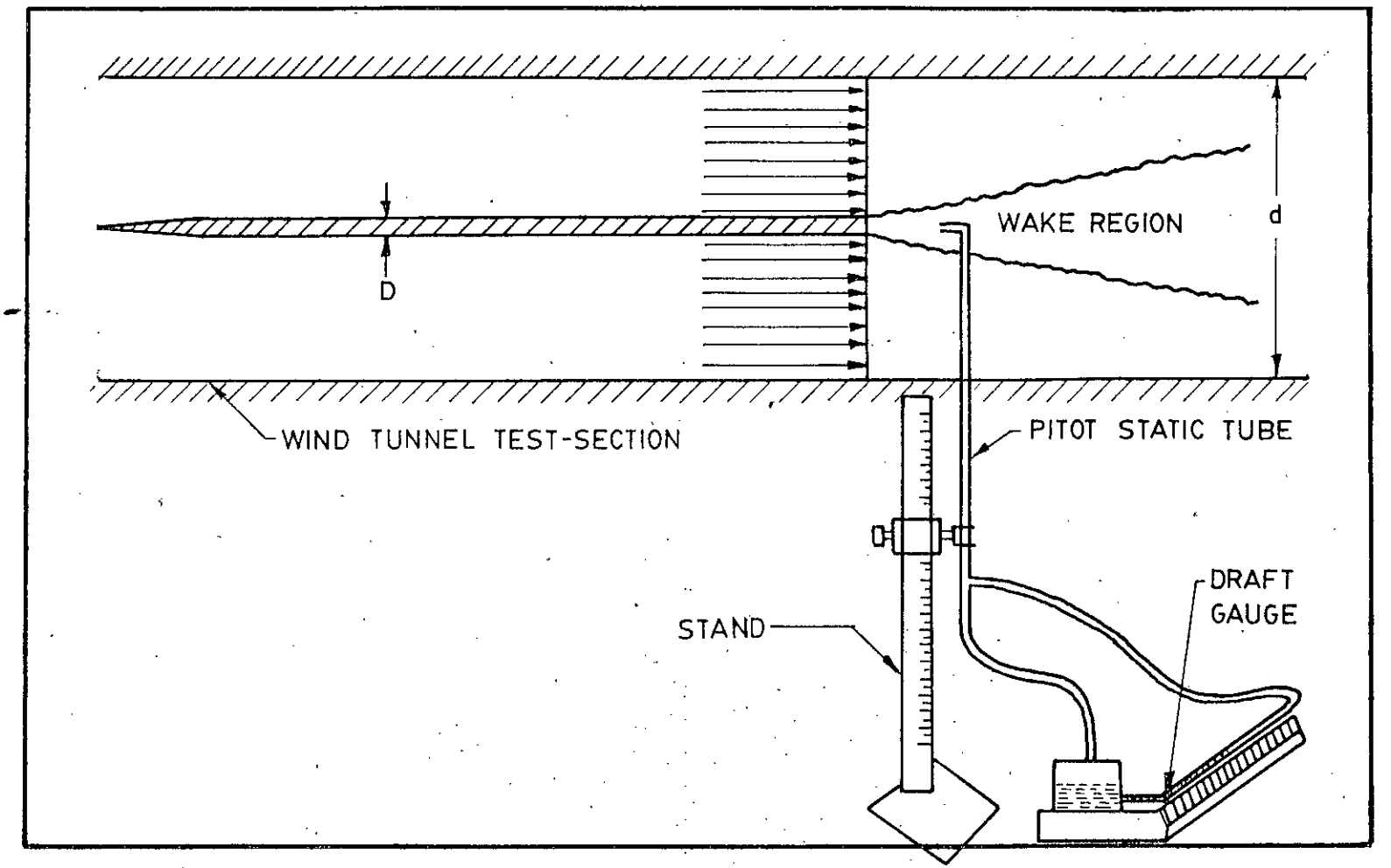

FIG. 4.3 SCHEMATIC DIAGRAM OF THE EXPERIMENTAL SET-UP

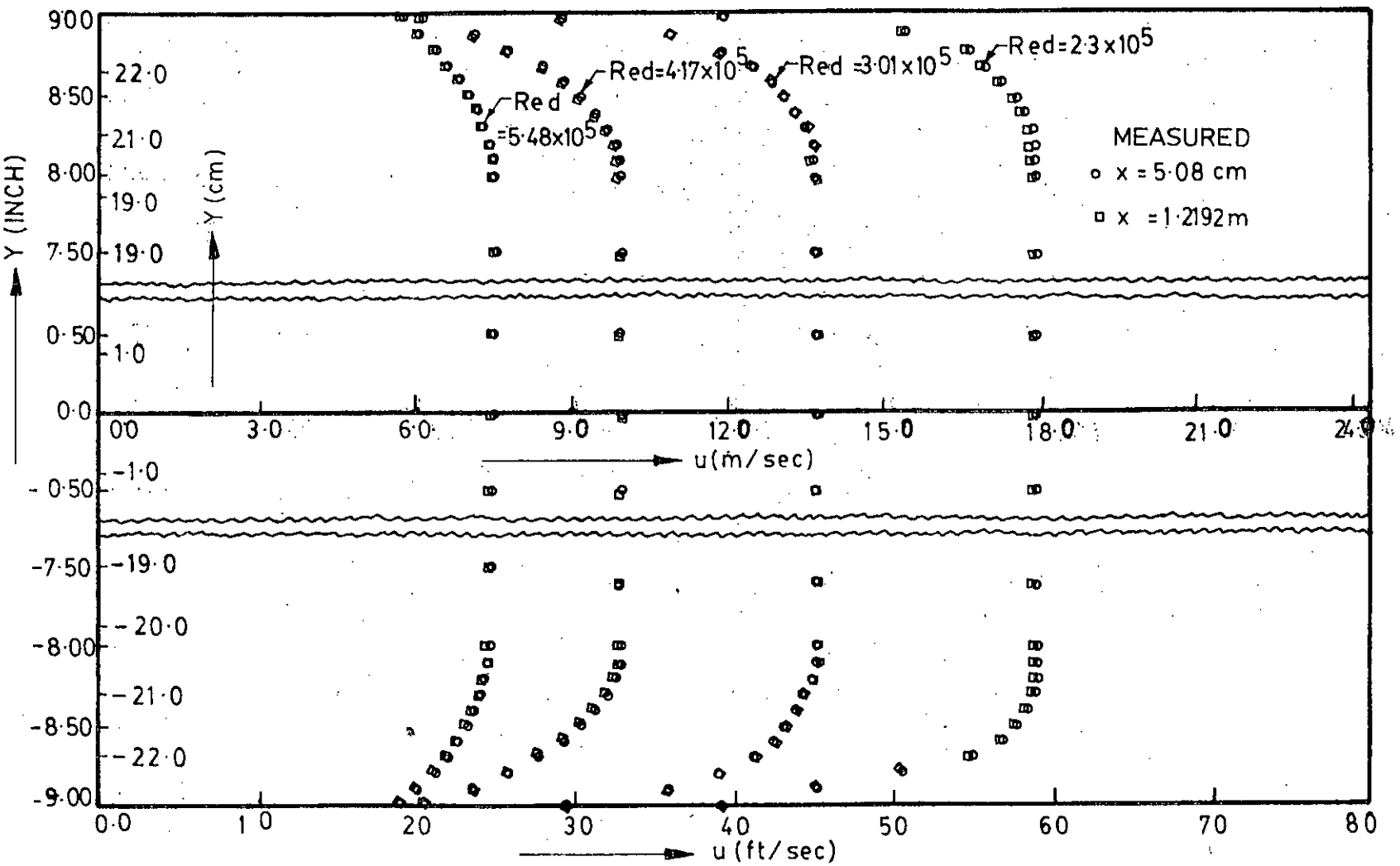

FIG 4·4 VELOCITY DISTRIBUTION IN TUNNEL TEST SECTION FOR CALIBRATION

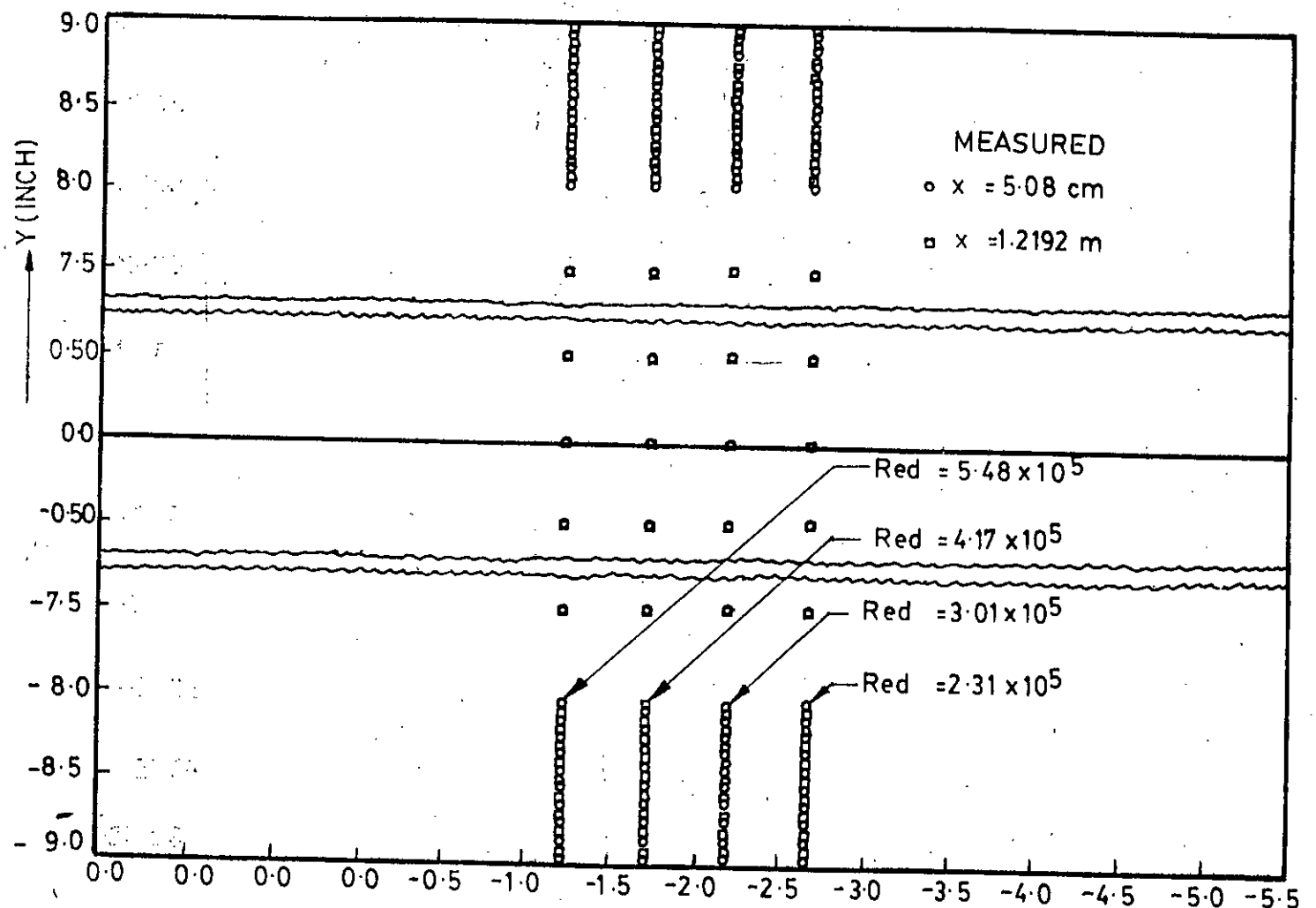

FIG. 4·5 PRESSURE DISTRIBUTION IN THE TUNNEL TEST SECTION FOR CALIBRATION

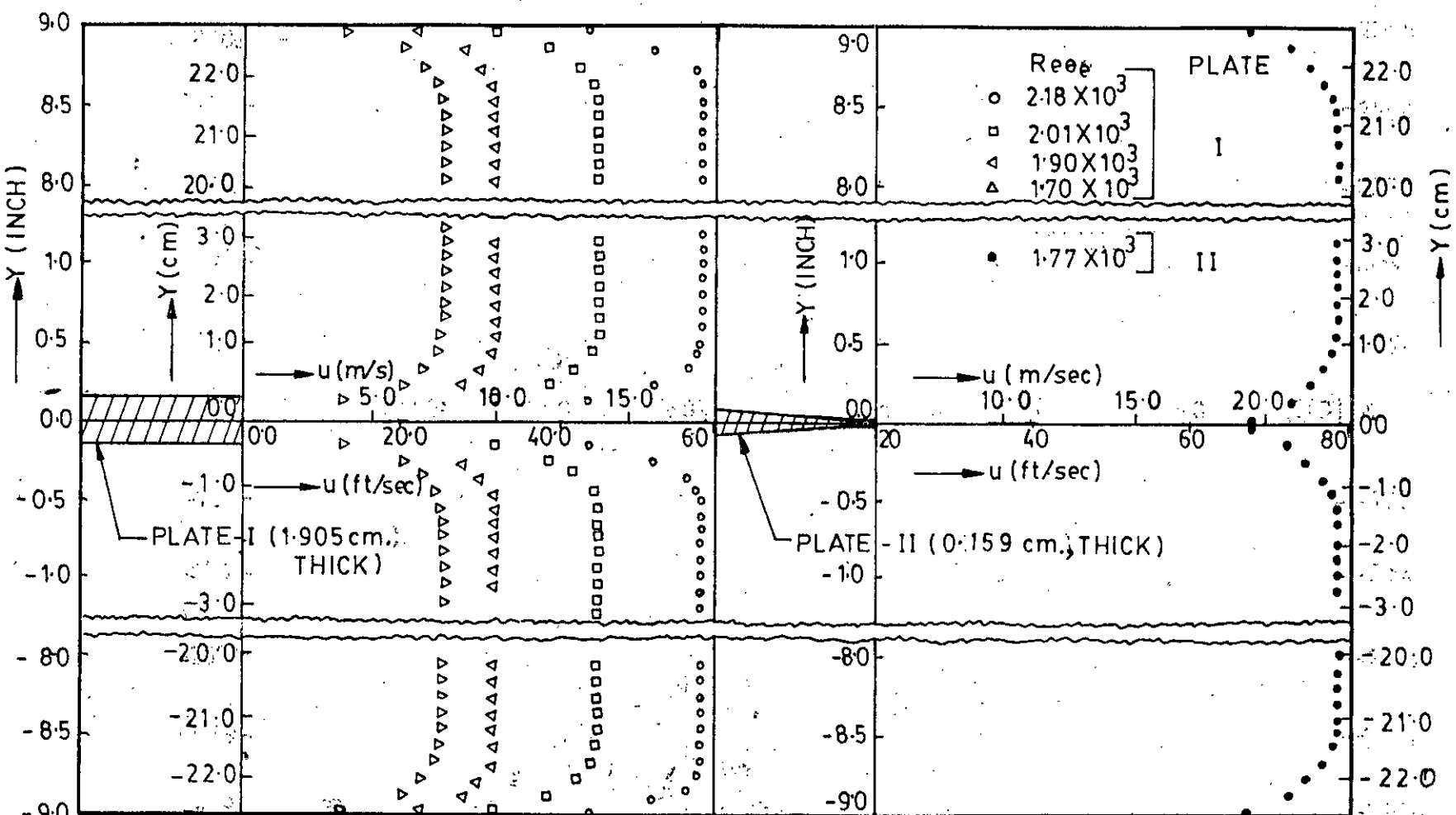

FIG. 5.1 VELOCITY DISTRIBUTION AT THE TRAILING EDGE OF THE PLATES

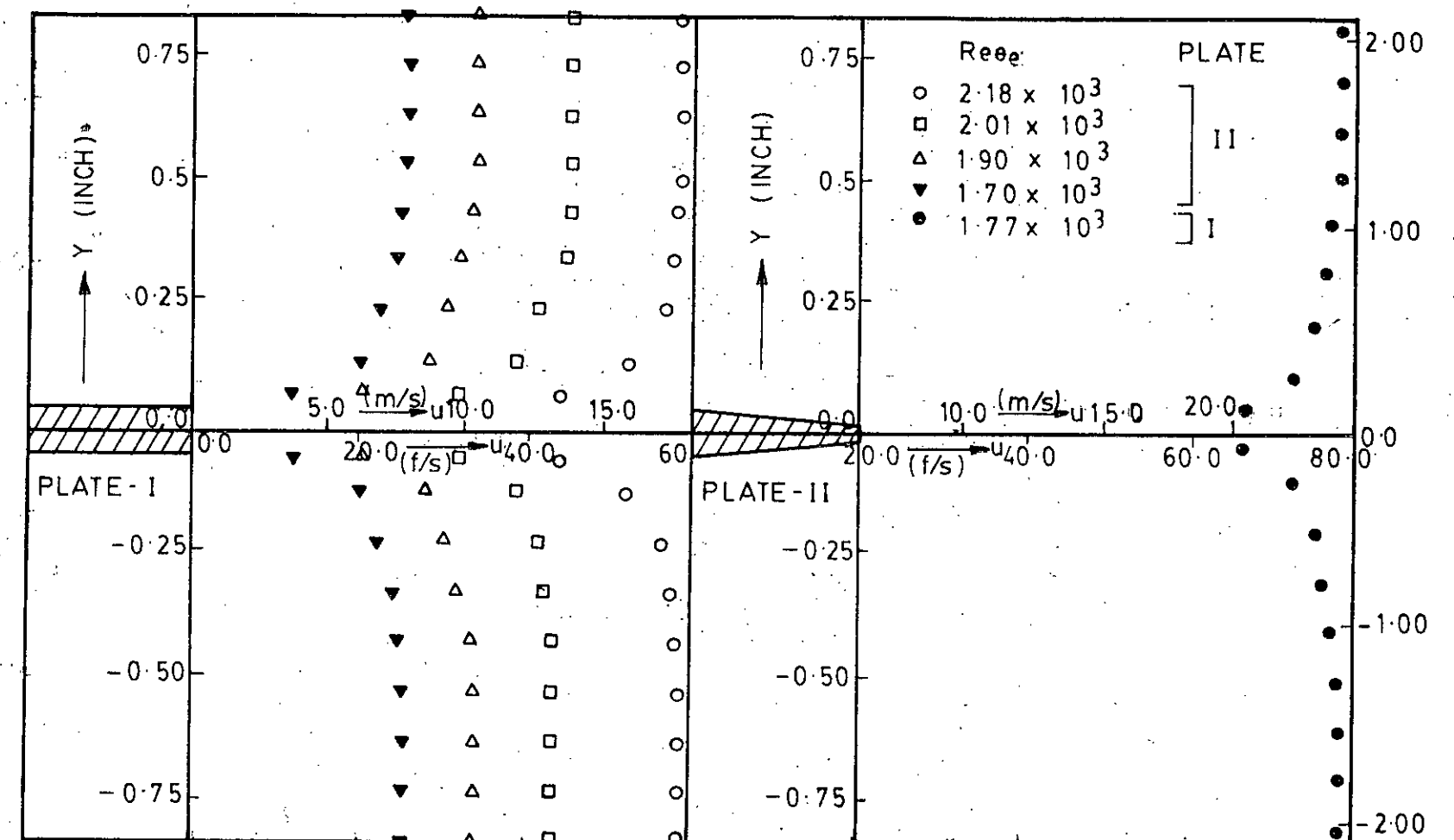

FIG. 5·1·b MAGNIFIED BOUNDARY LAYER VELOCITY PROFILE AT THE TRAILING EDGE OF THE PLATES

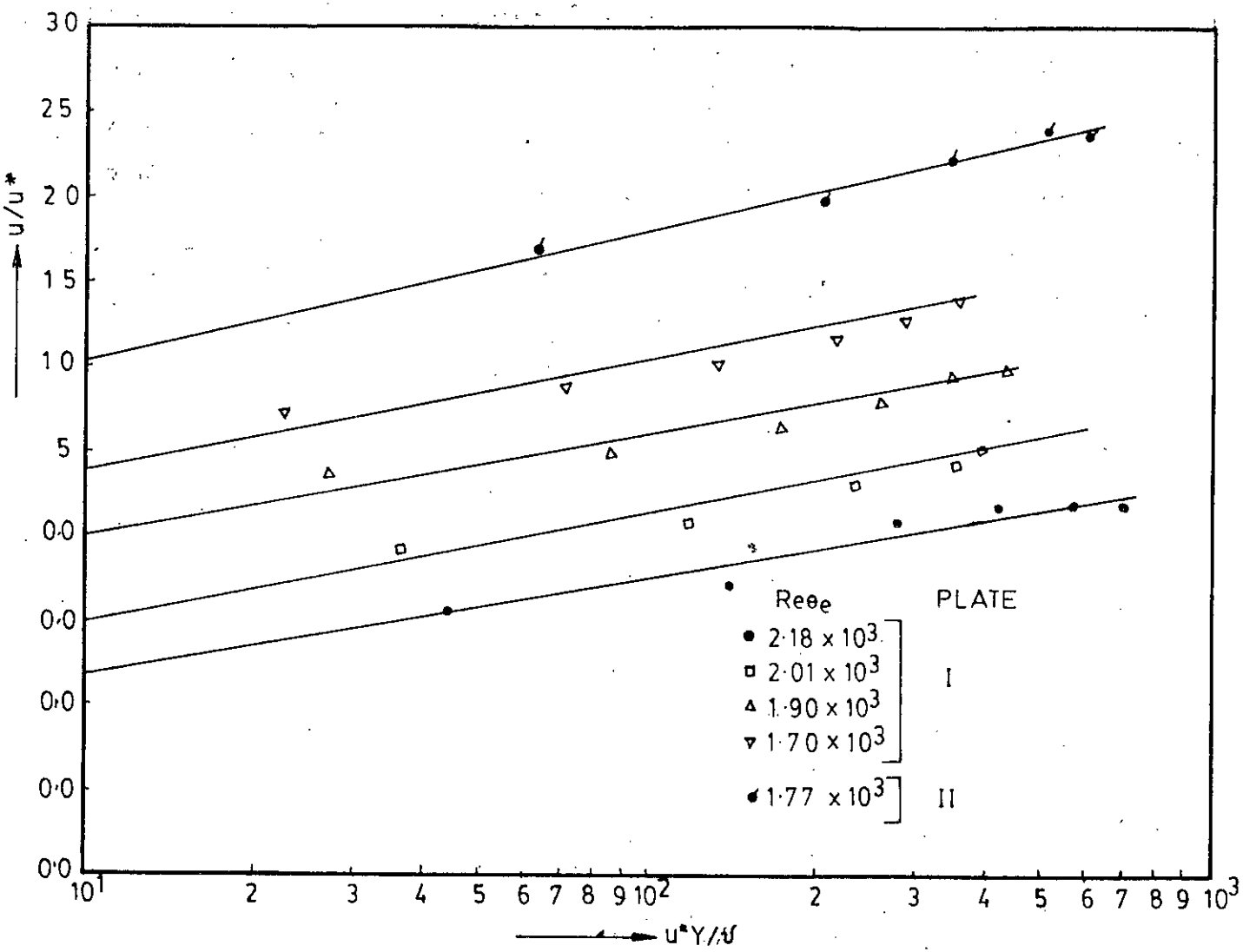

FIG.5.2. UNIVERSAL VELOCITY PROFILES AT THE TRAILING EDGE OF THE PLATES

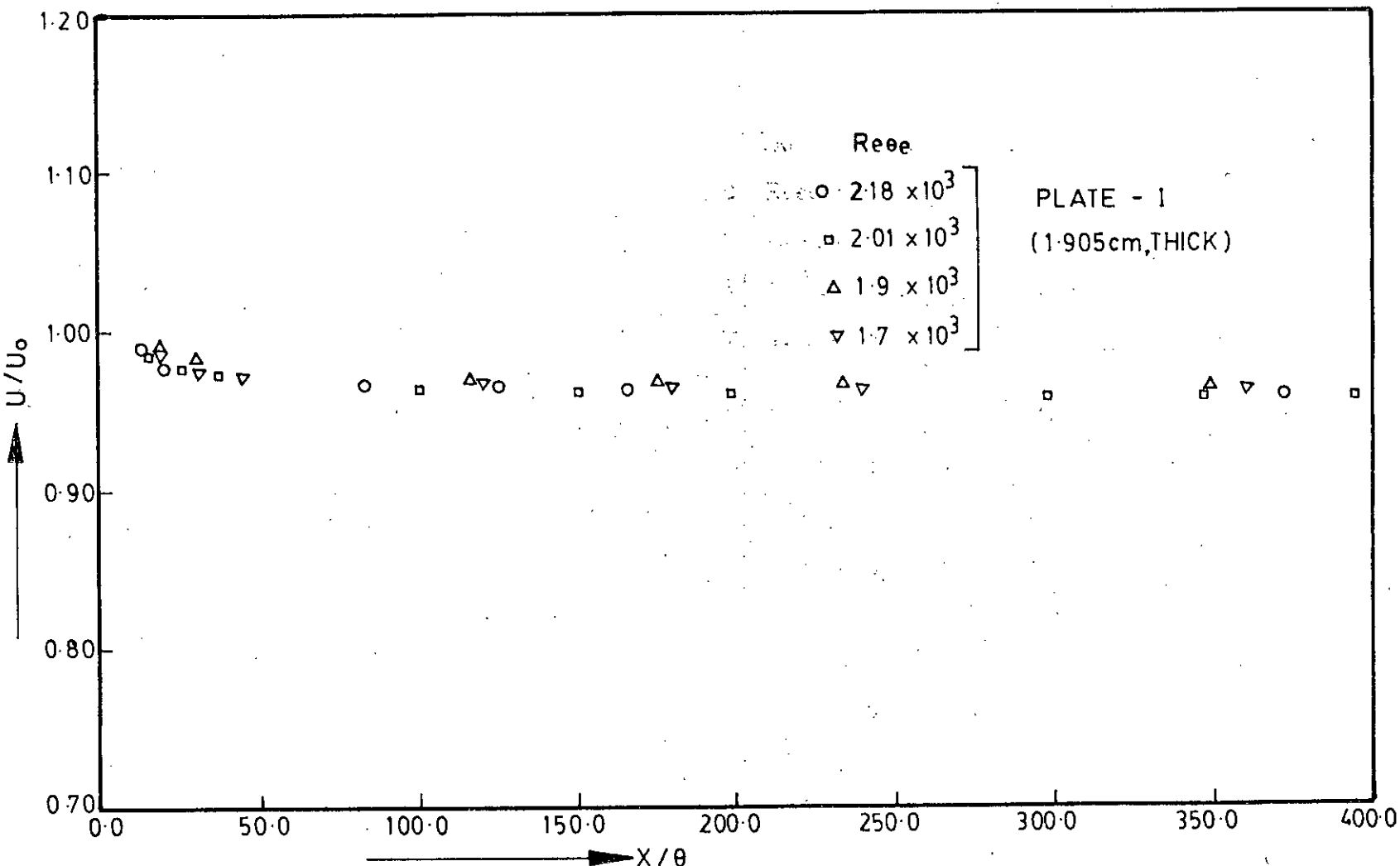

FIG.5.3 DIMENSIONLESS FREE-STREAM VELOCITY AT VARIOUS DISTANCES FROM THE PLATE

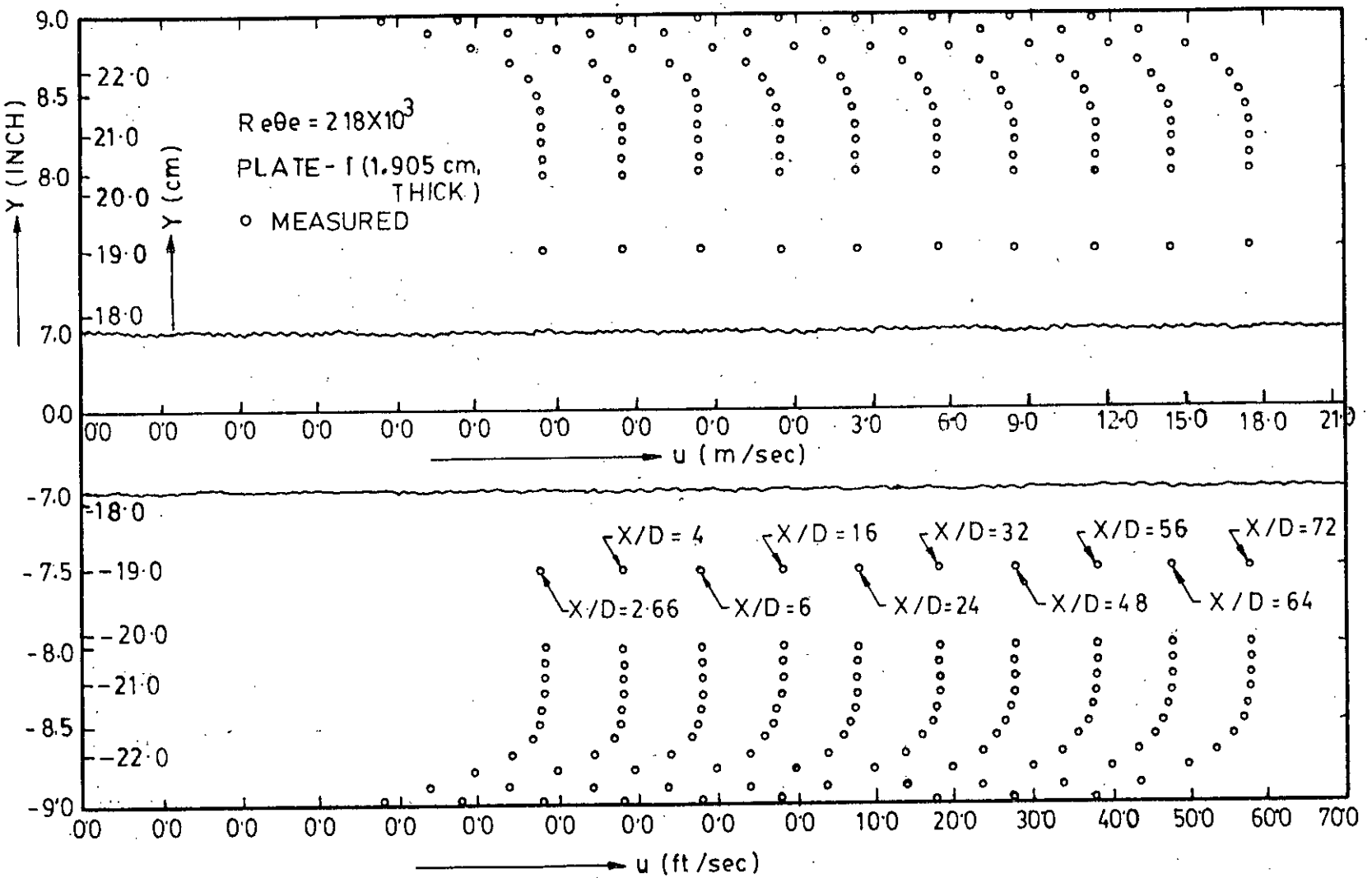

FIG.5.4a. VELOCITY DISTRIBUTION AT THE WALL OF THE TEST SECTION

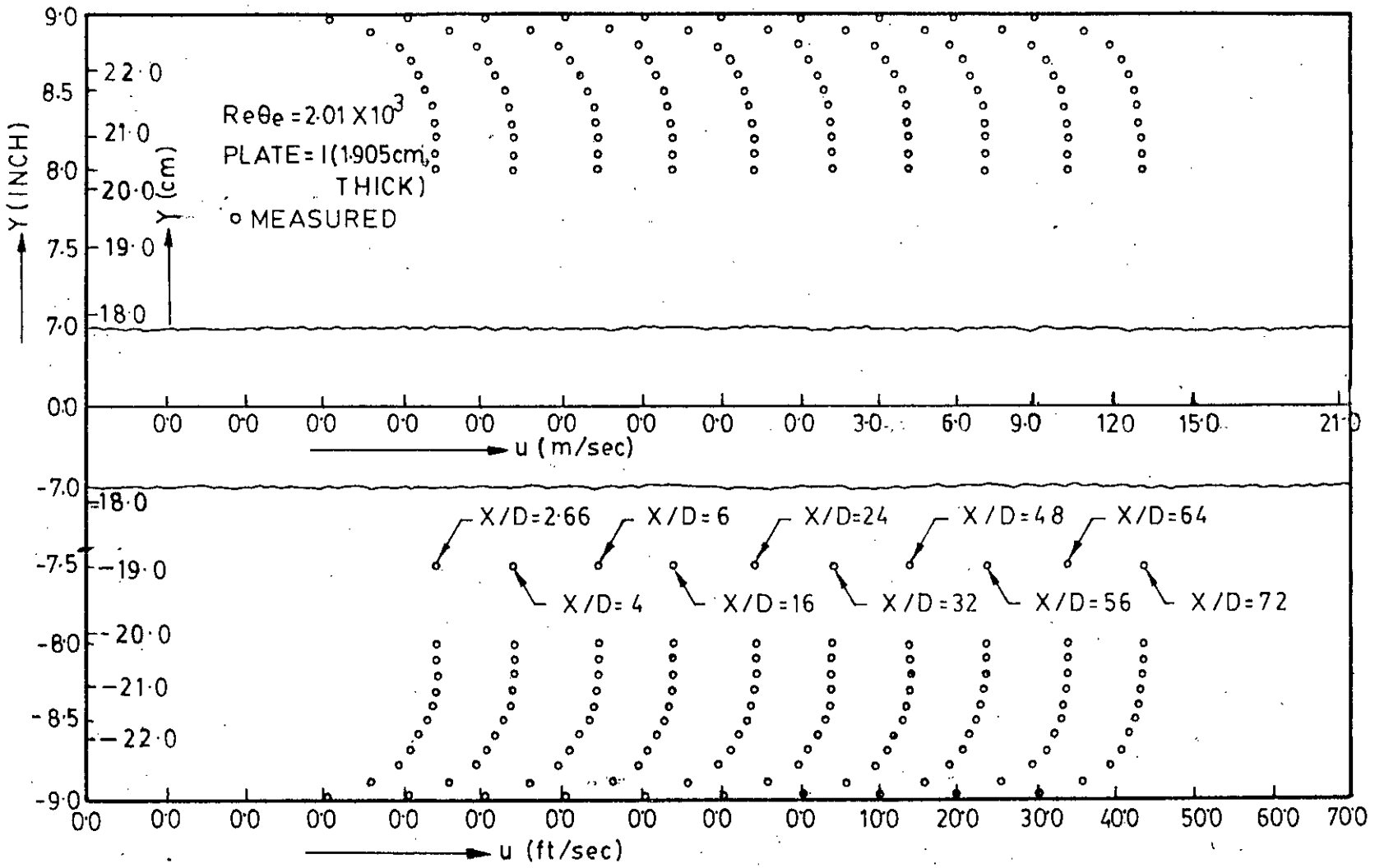

FIG.5.4b. VELOCITY DISTRIBUTION AT THE WALL OF THE TEST SECTION

55937

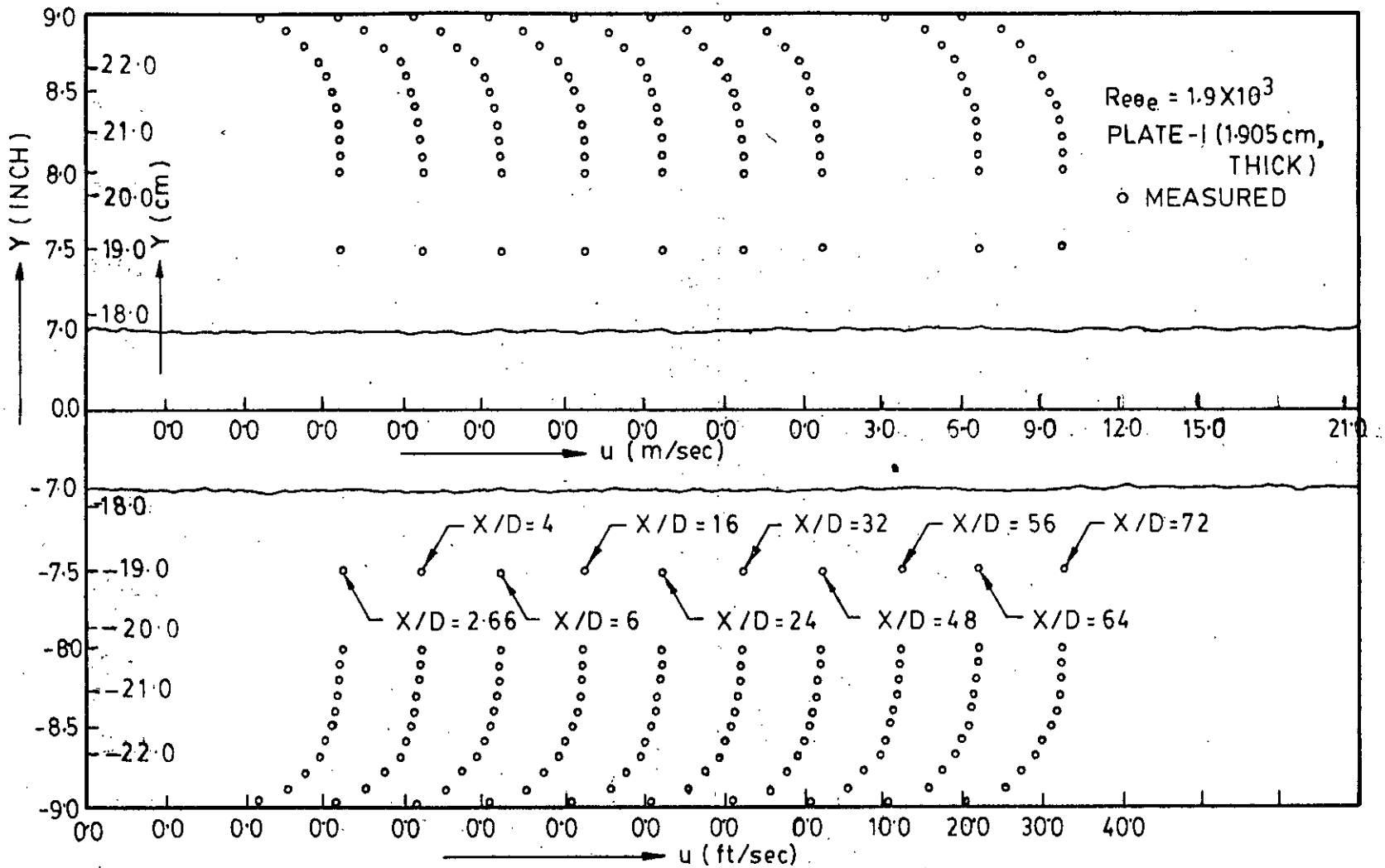

FIG.5.4c. VELOCITY DISTRIBUTION AT THE WALL OF THE TEST SECTION

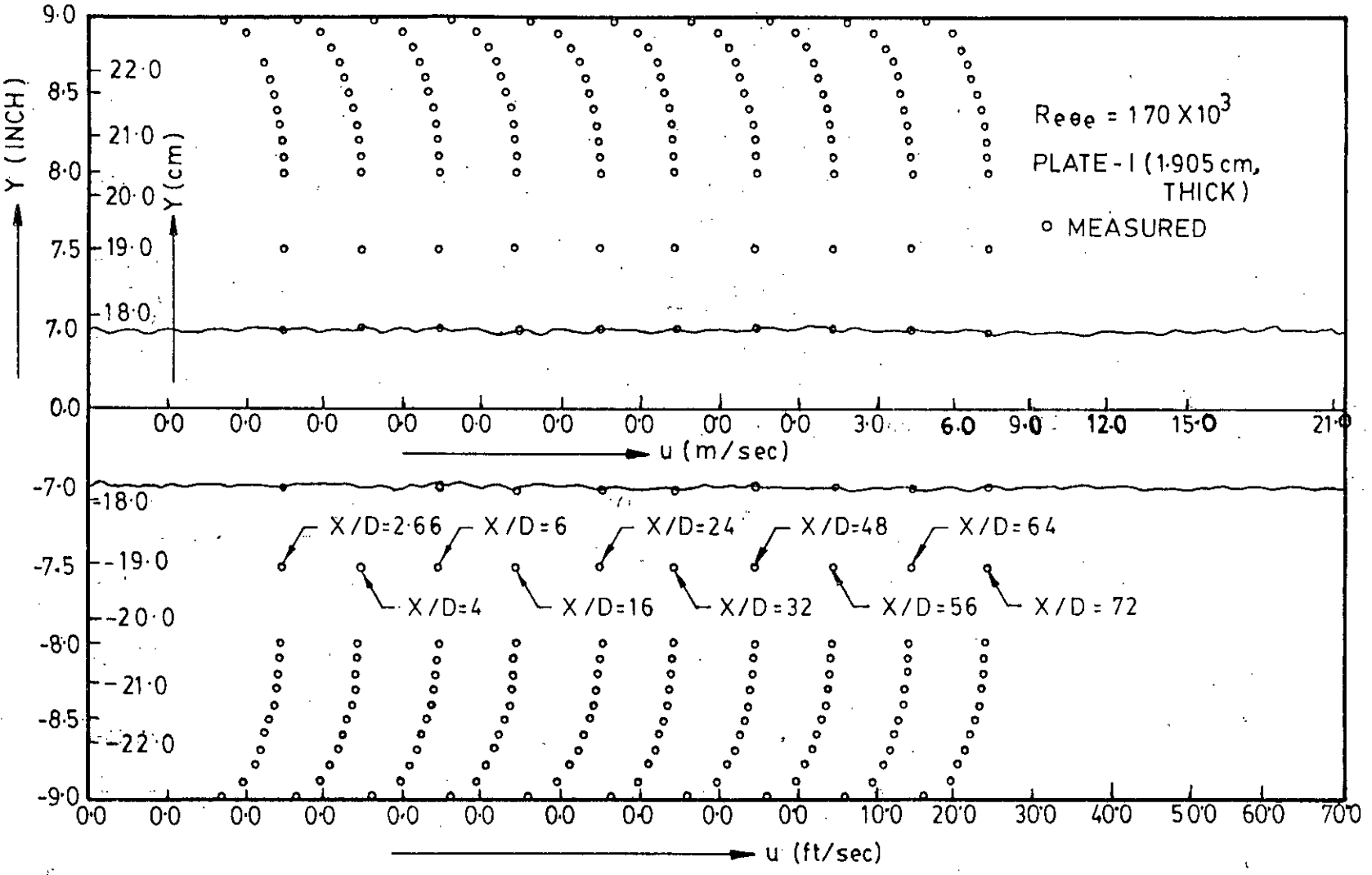

FIG.5.4d. VELOCITY DISTRIBUTION AT THE WALL OF THE TEST SECTION

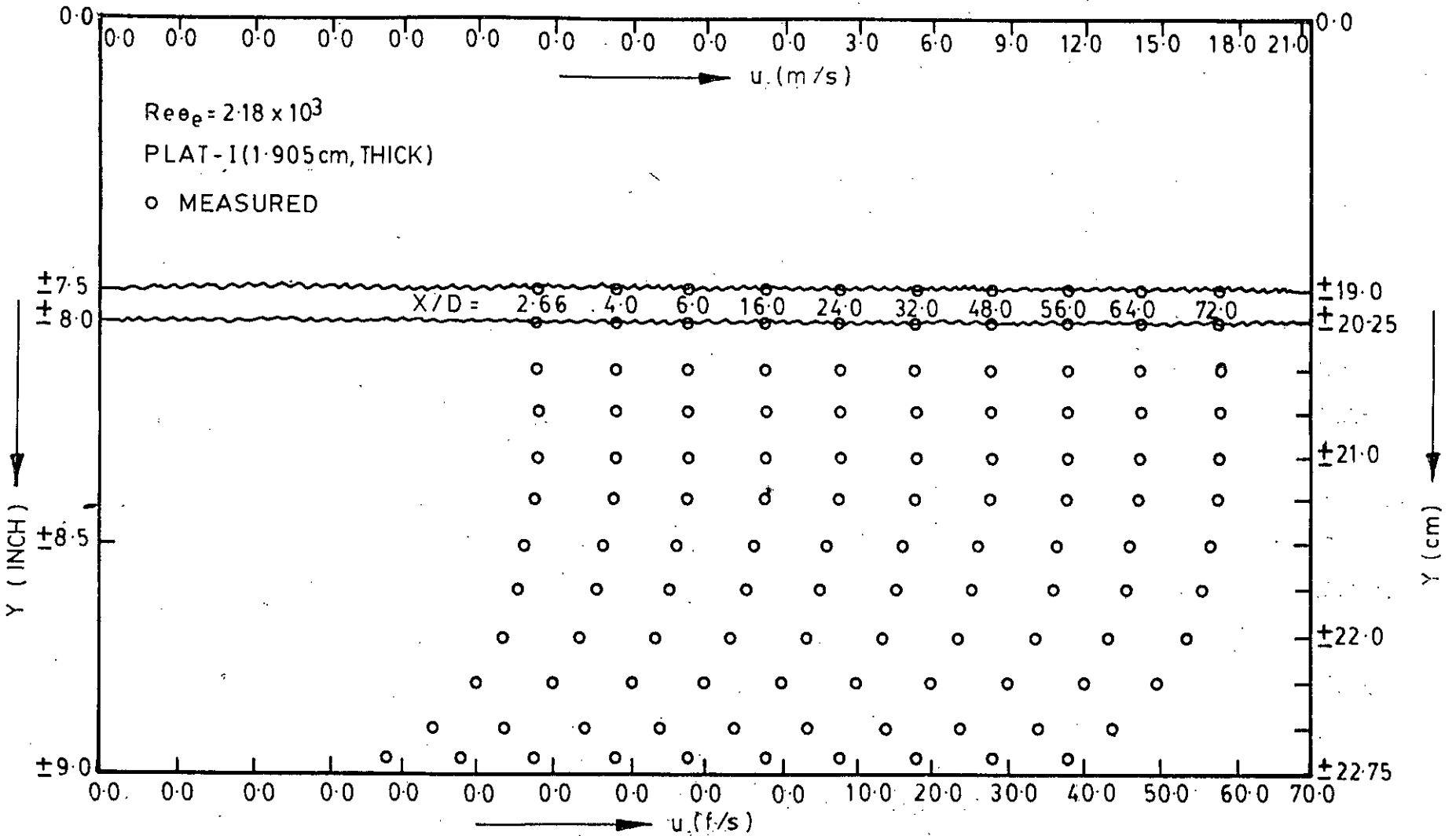

FIG·5·4e MAGNIFIED BOUNDARY LAYER VELOCITY PROFILE AT THE WALL OF THE TEST SECTION

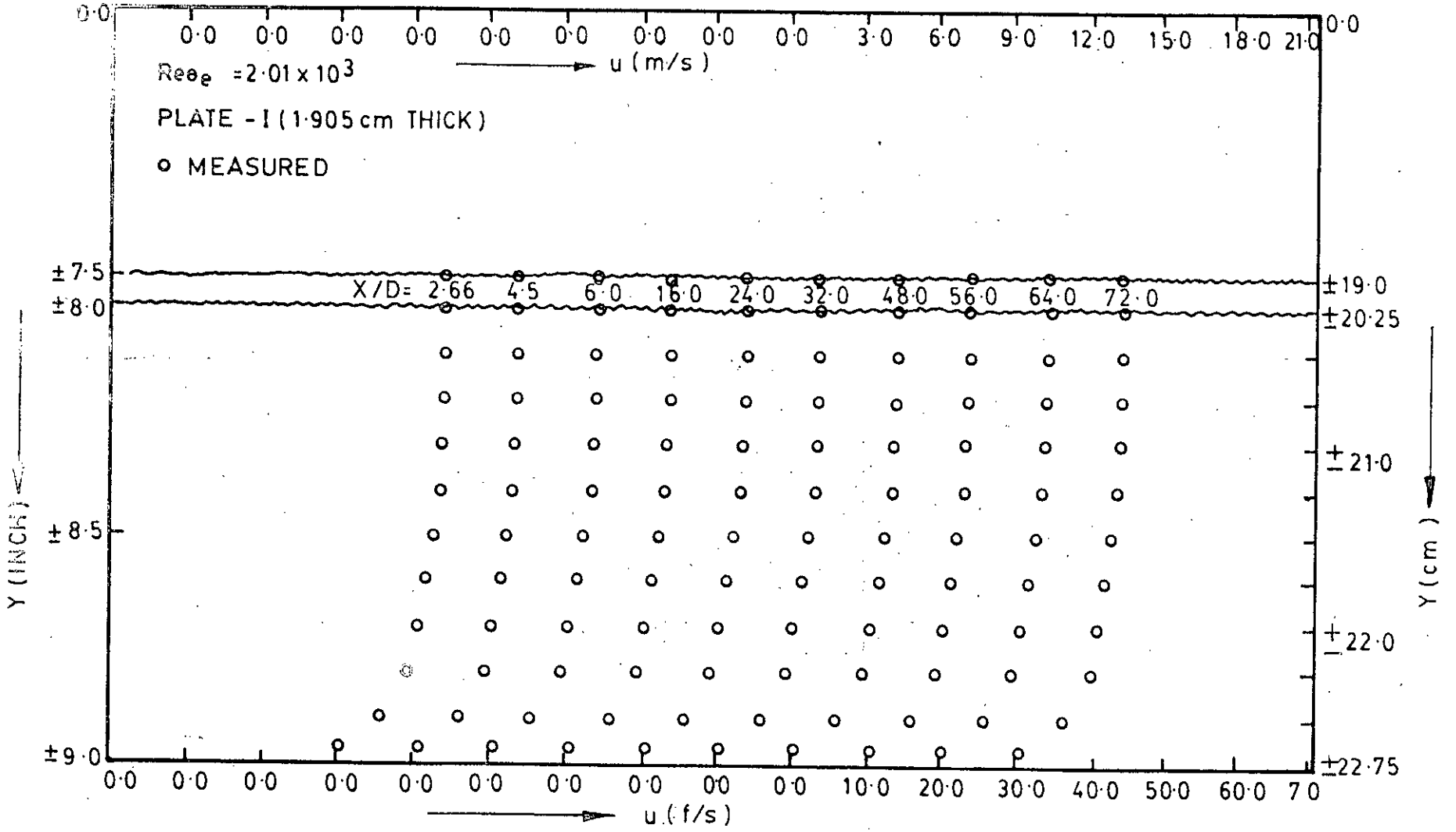

FIG. 5·4f MAGNIFIED BOUNDARY LAYER VELOCITY PROFILE AT THE WALL OF THE TEST SECTION

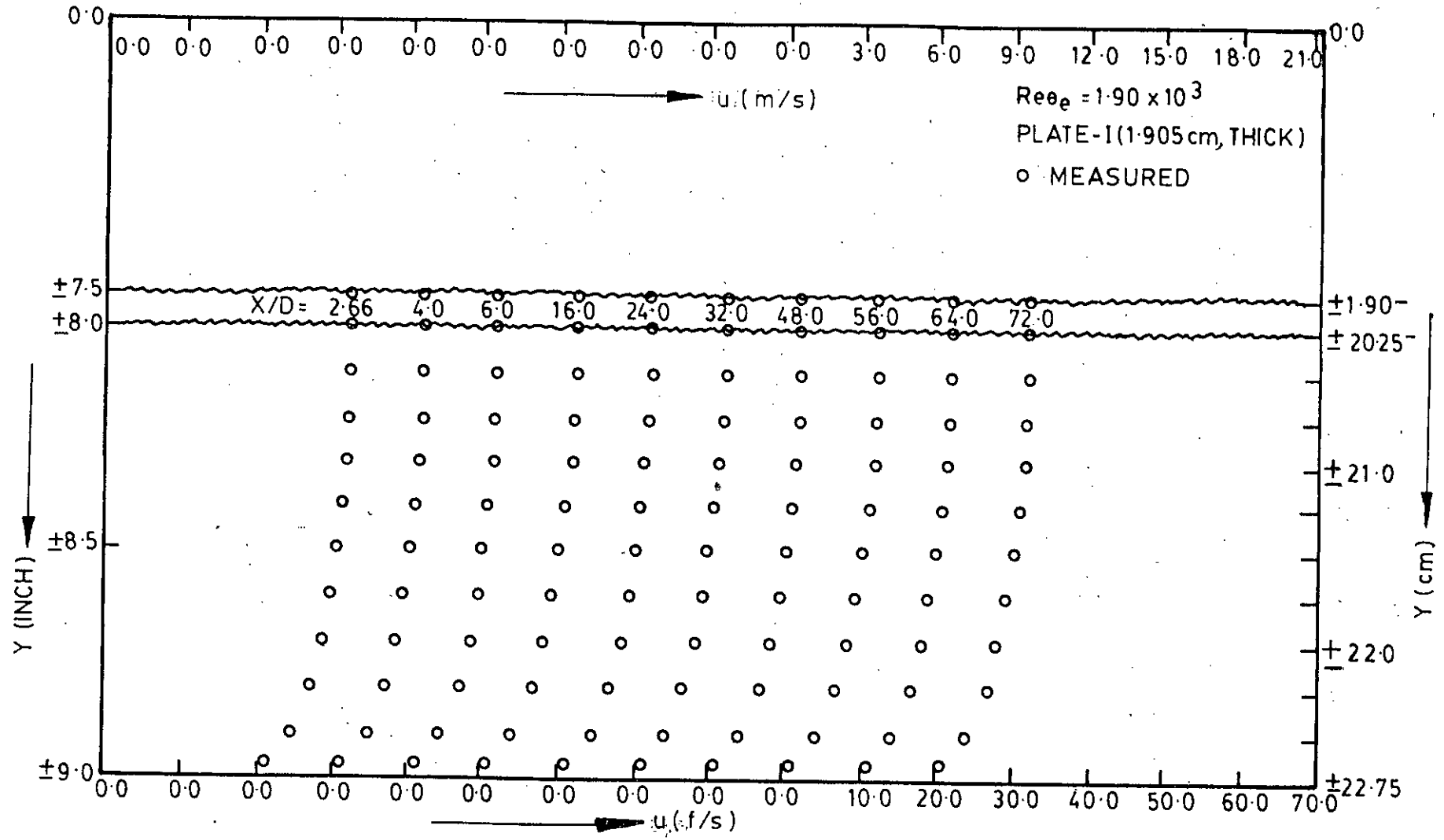

FIG. 5·4g MAGNIFIED BOUNDARY LAYER VELOCITY PROFILE AT THE WALL OF THE TEST SECTION

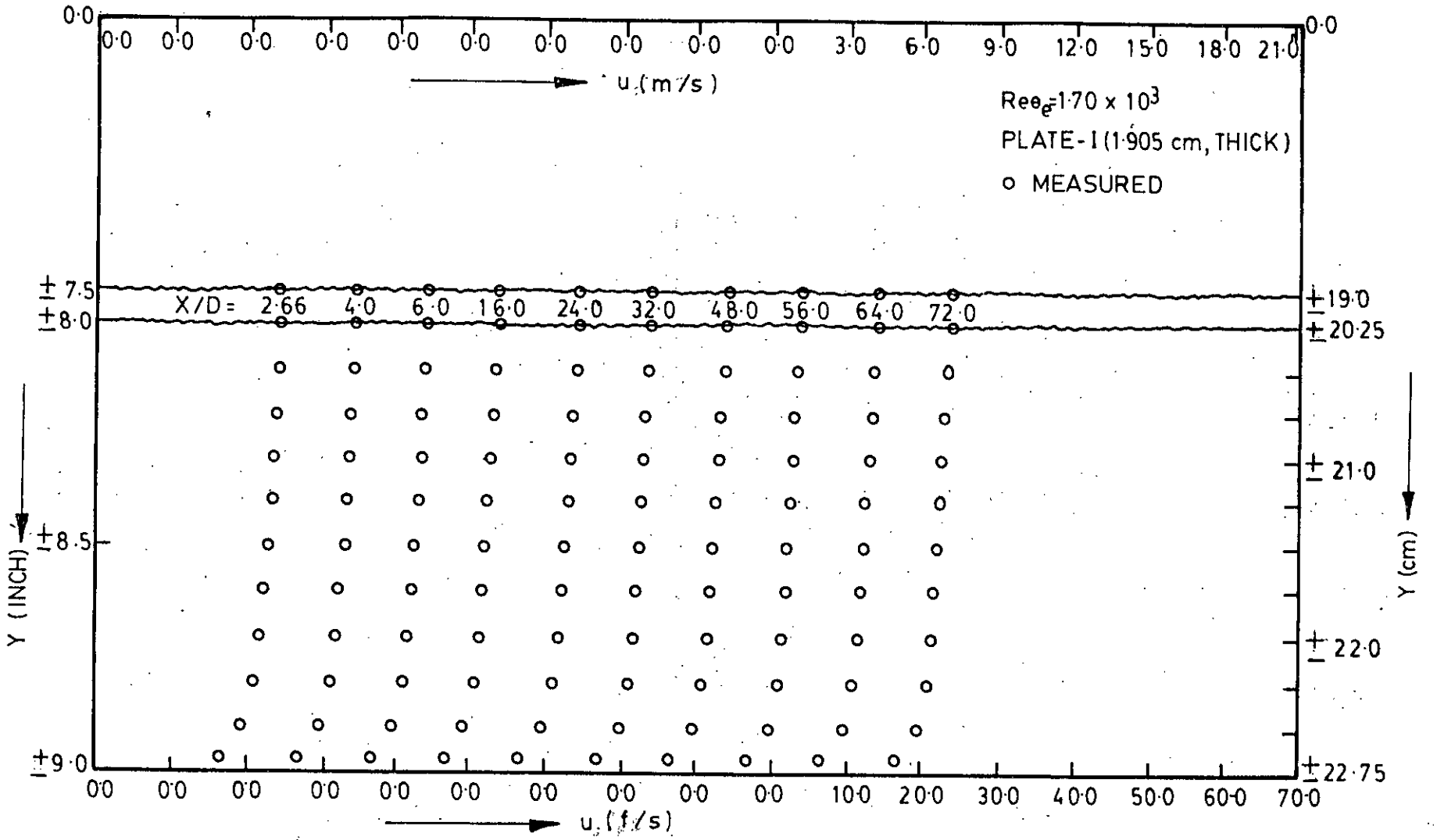

FIG. 5.4h MAGNIFIED BOUNDARY LAYER VELOCITY PROFILE AT THE WALL OF THE TEST SECTION

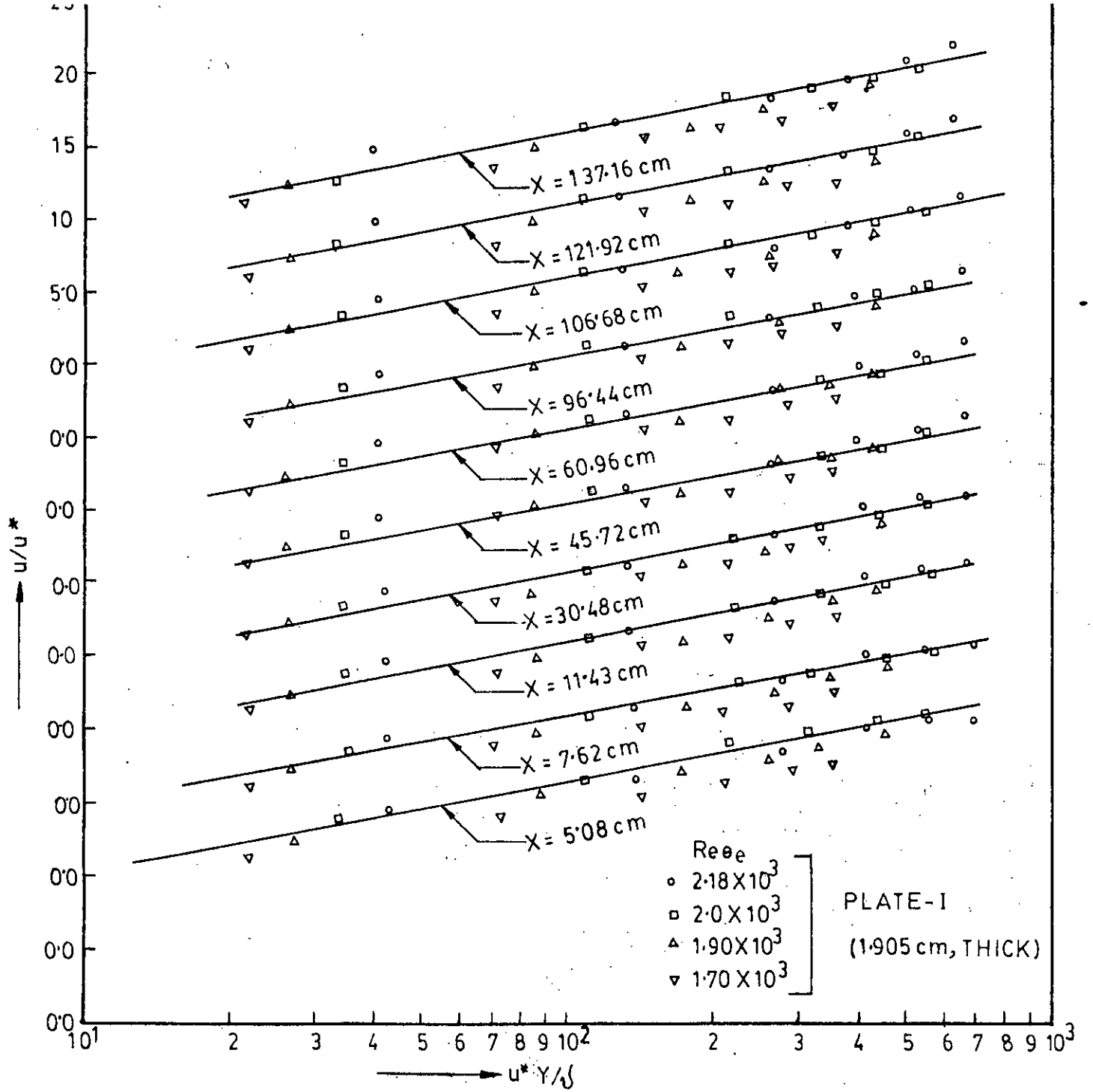

FIG.5.5 UNIVERSAL VELOCITY PROFILE AT THE WALL

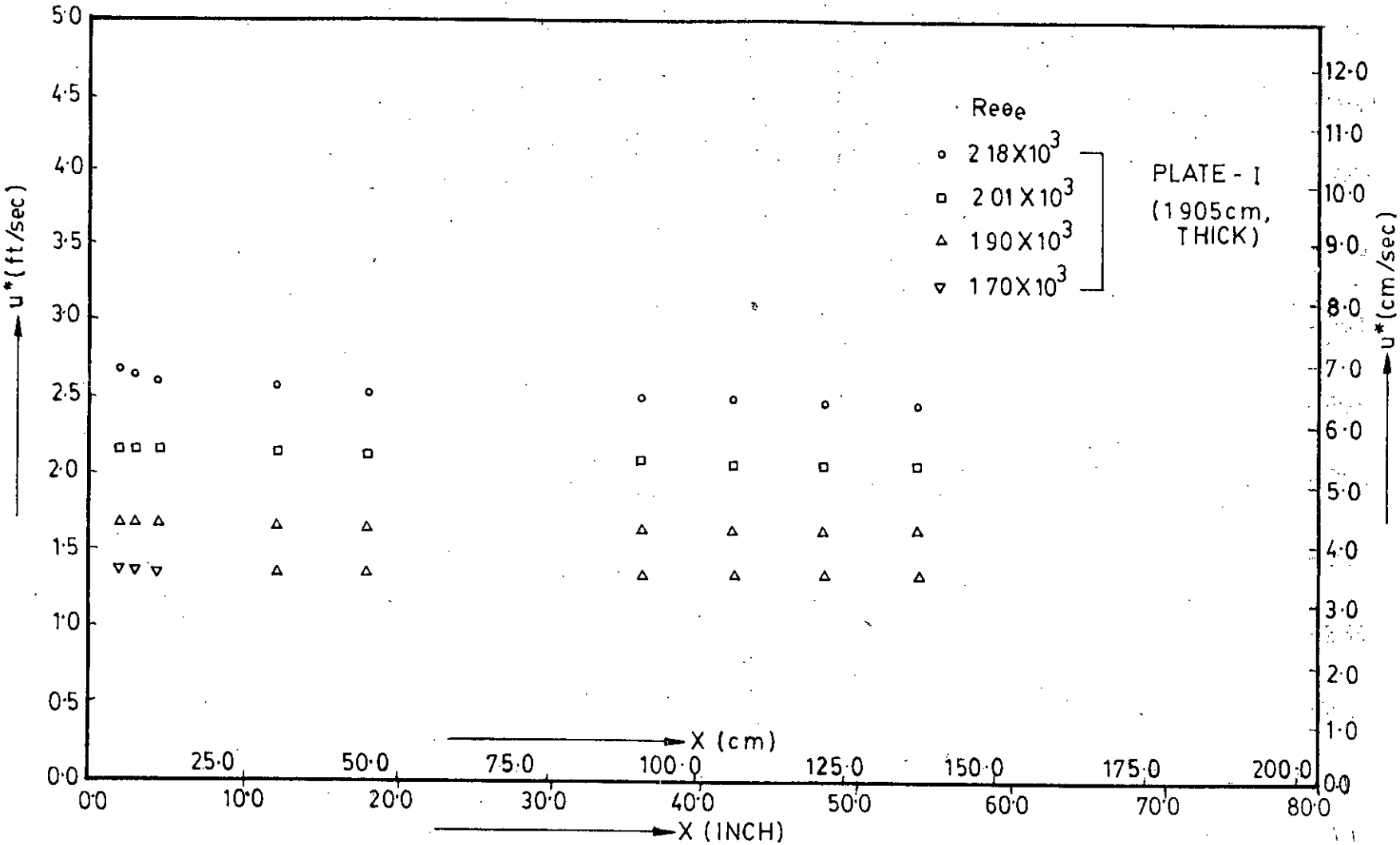

FIG. 5.6 VARIATION OF FRICTION VELOCITY (AT WALL) WITH DISTANCES

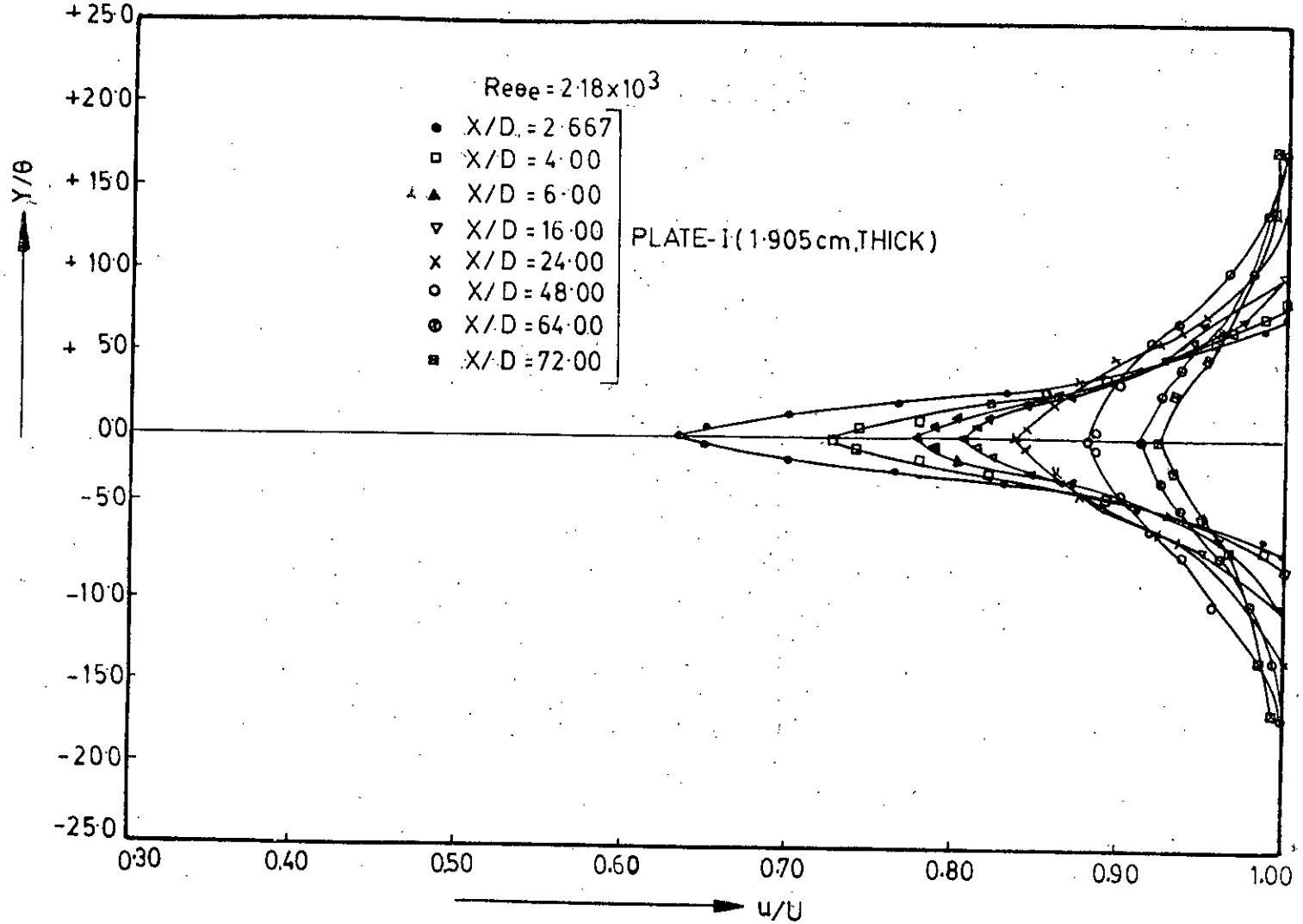

FIG. 5.7a MEAN VELOCITY DISTRIBUTION IN WAKE

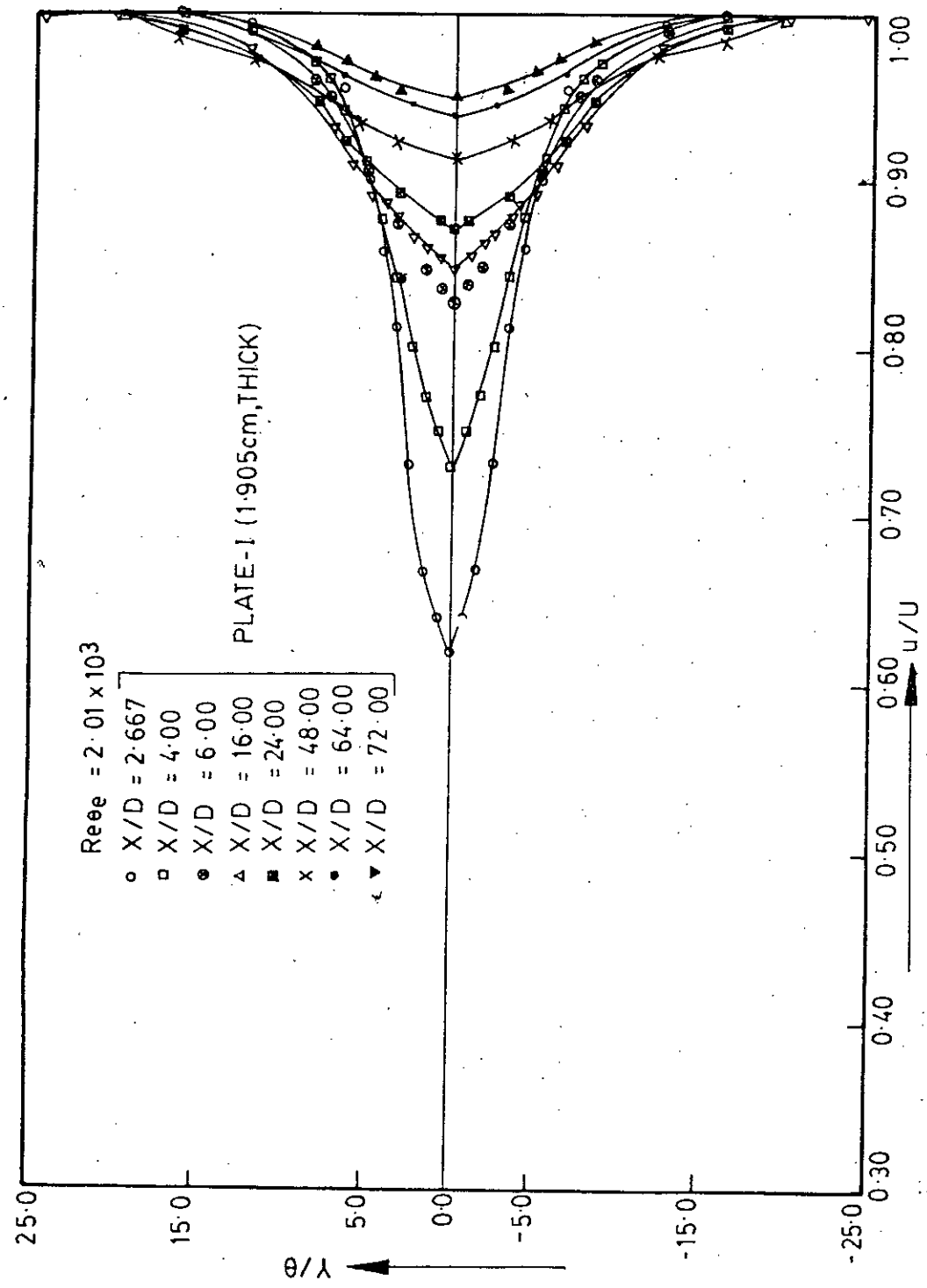

FIG.5.7b MEAN VELOCITY DISTRIBUTION IN WAKE

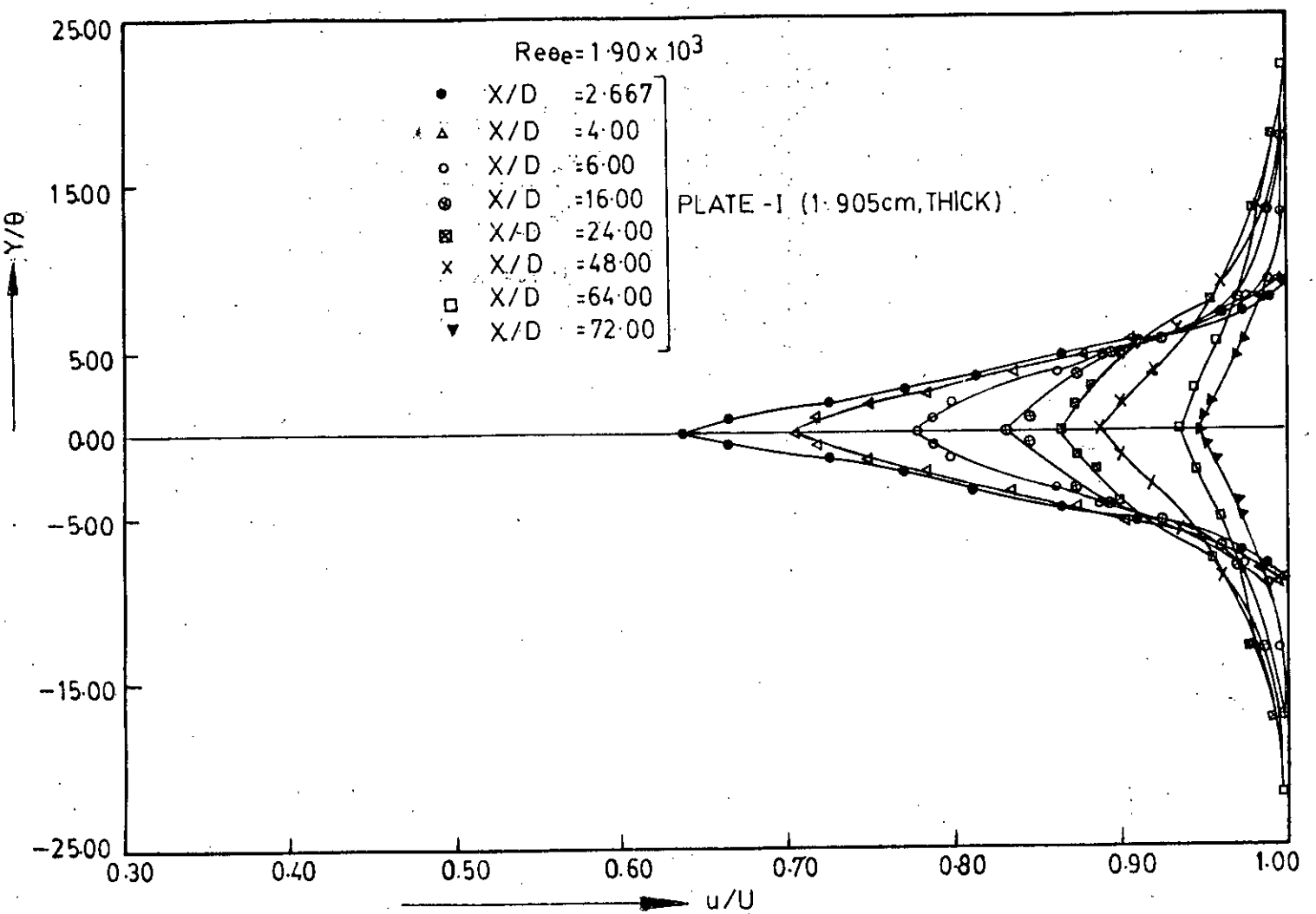

FIG. 5.7c MEAN VELOCITY DISTRIBUTION IN WAKE

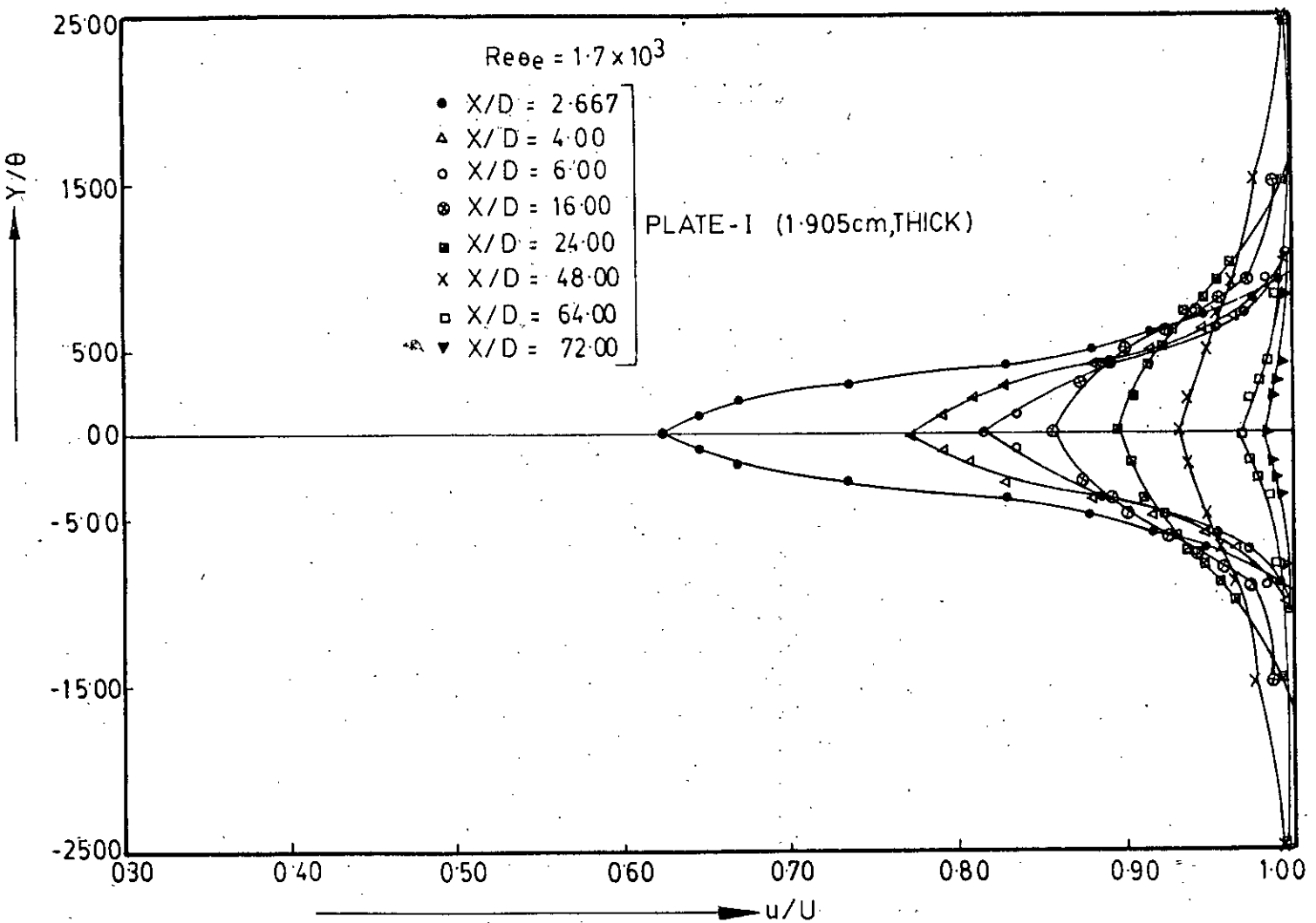

FIG. 5·7d MEAN VELOCITY DISTRIBUTION IN WAKE

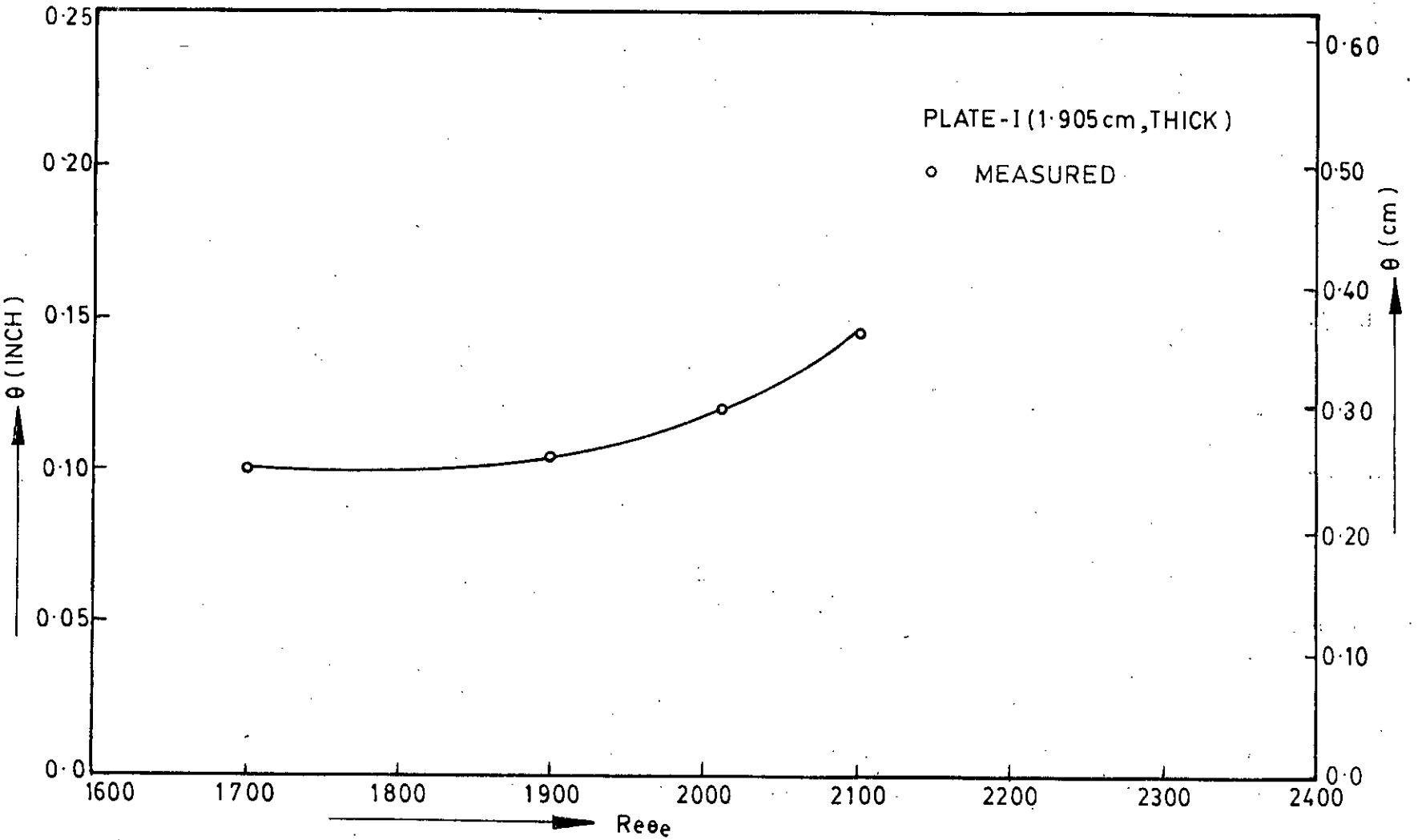

FIG.5.8 VARIATION OF WAKE MOMENTUM THICKNESS WITH REYNOLDS NUMBERS

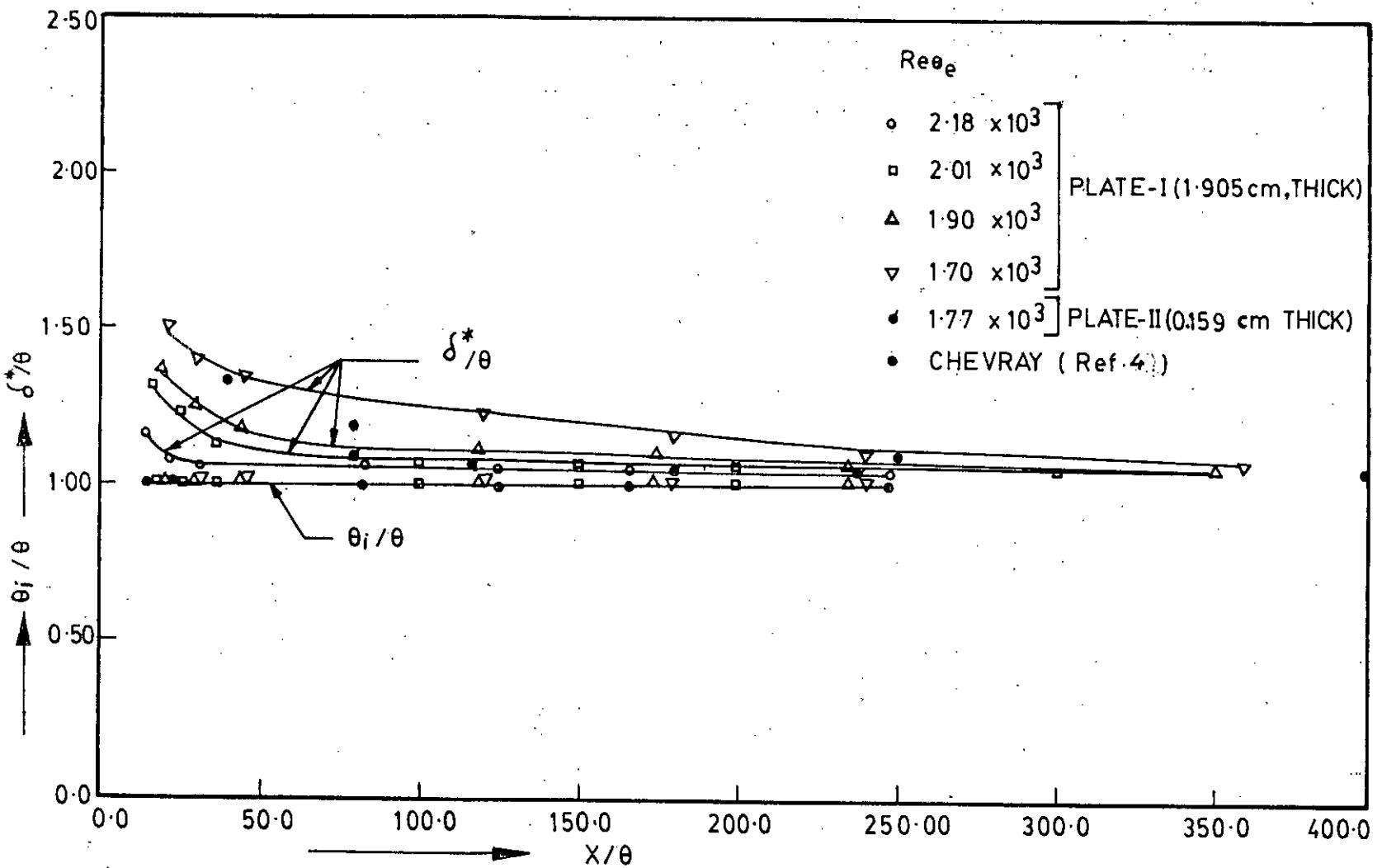

FIG.5.9 VARIATION OF SHAPE PARAMETERS WITH AXIAL DISTANCES

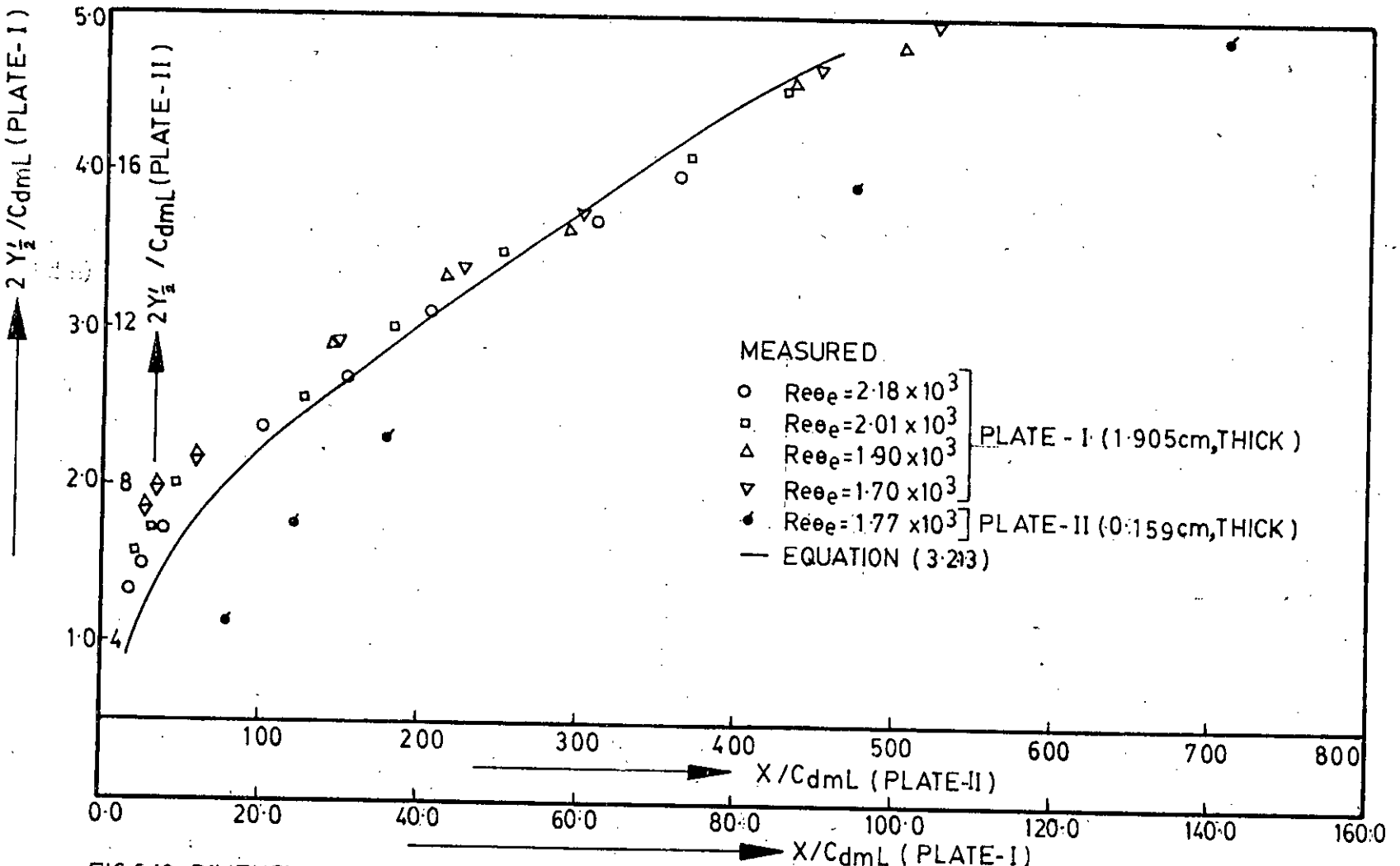

FIG. 5·10a DIMENSIONLESS HALF VELOCITY LINE AT VARIOUS DISTANCES FROM THE PLATE

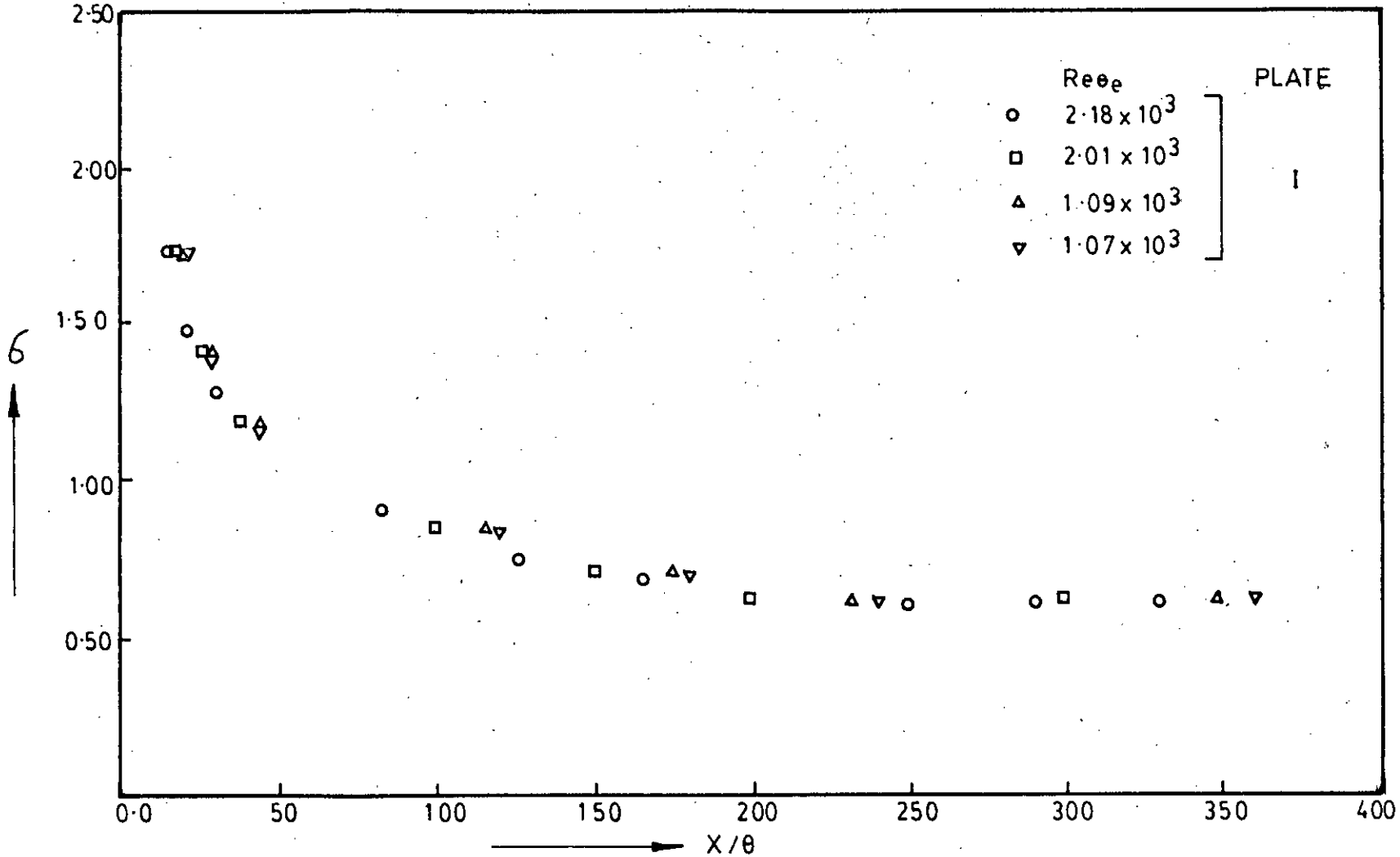

FIG 10·b VARIATION OF SPREAD PARAMETER WITH AXIAL DISTANCES

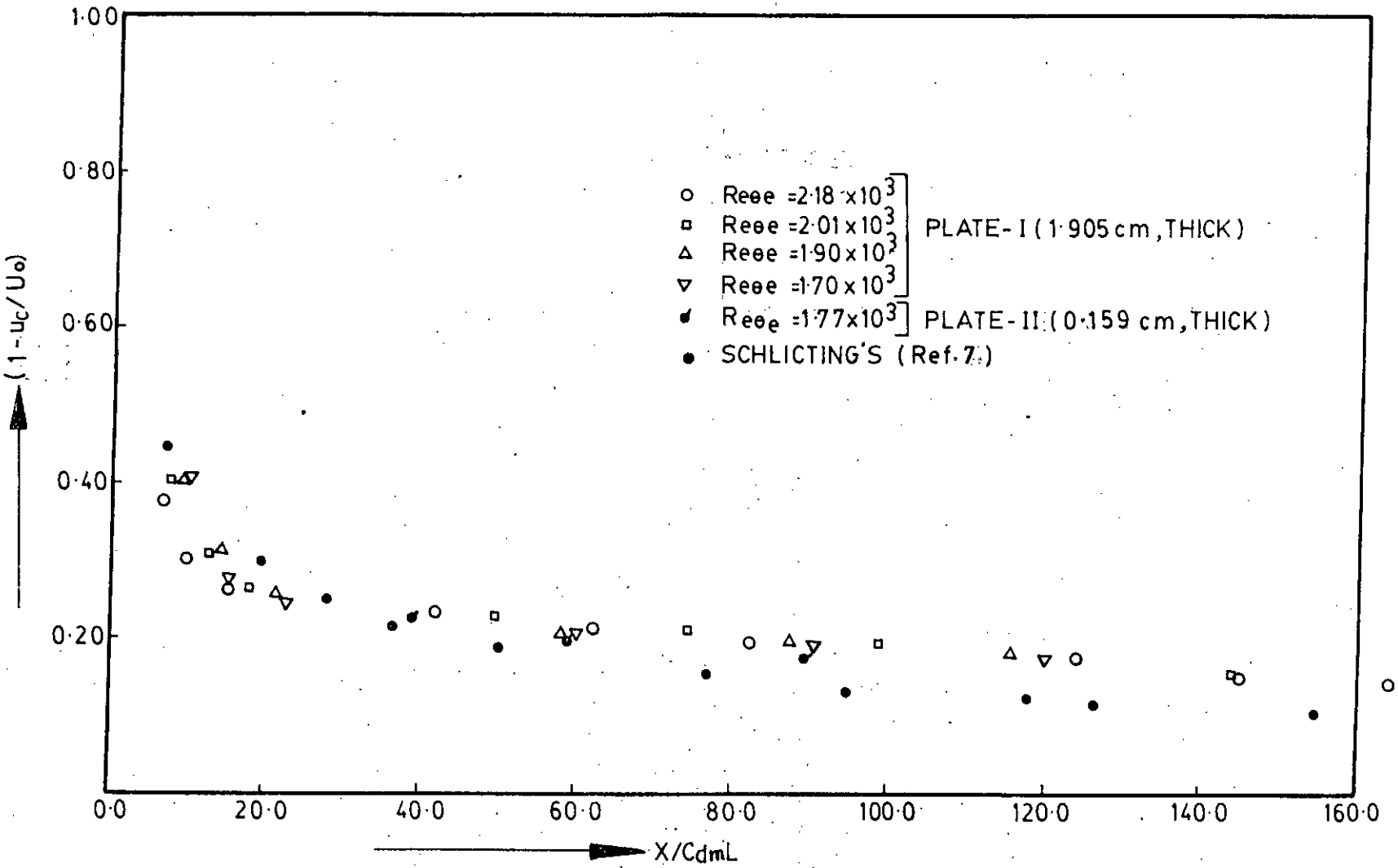

FIG.5.11 COMPARISON OF THE VARIATION OF RELATIVE VELOCITY DEFECT ON THE AXIS ALONG THE WAKE

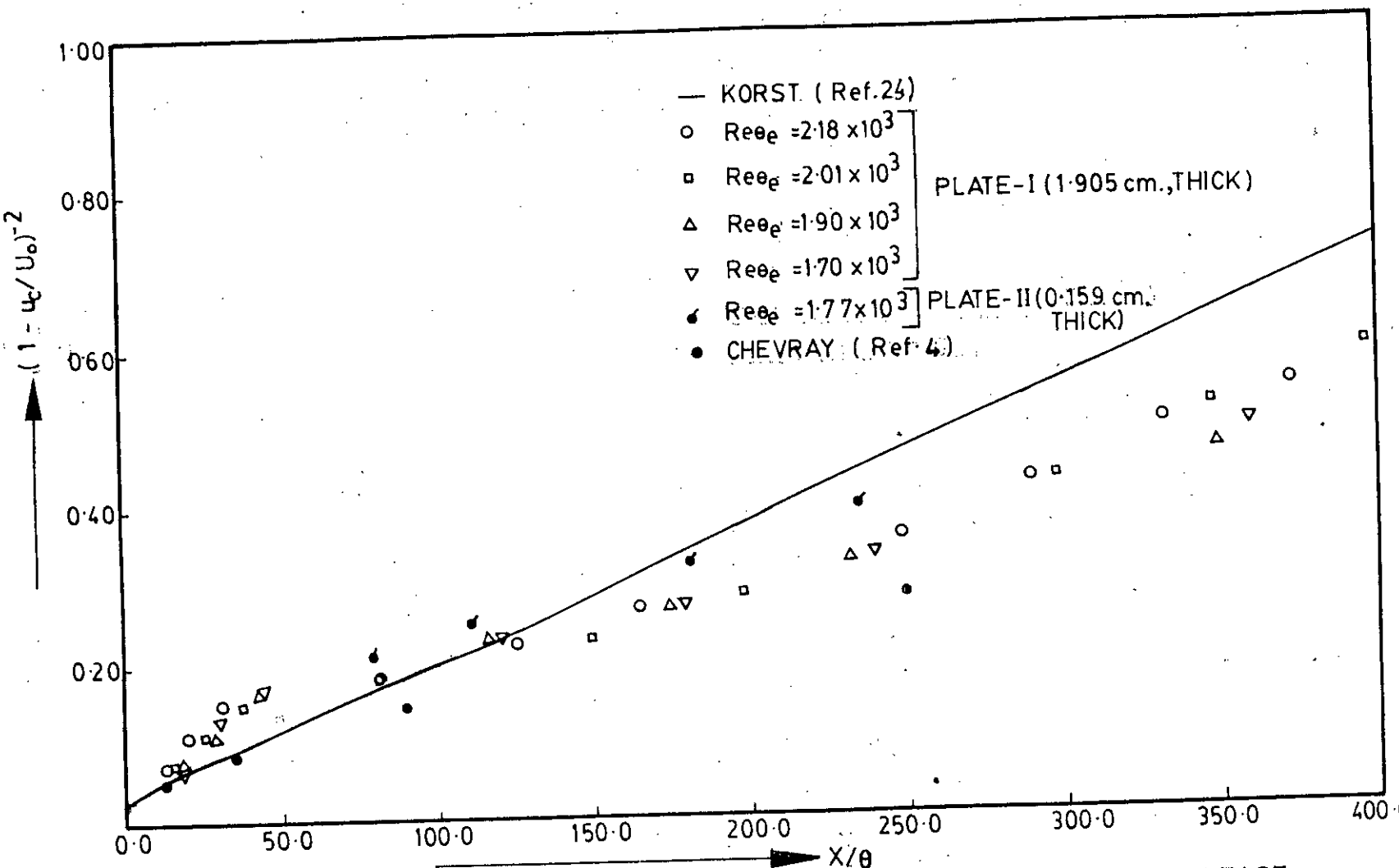

FIG. 5.12 COMPARISON OF EXPERIMENTAL CENTER-LINE VELOCITY INCREASE

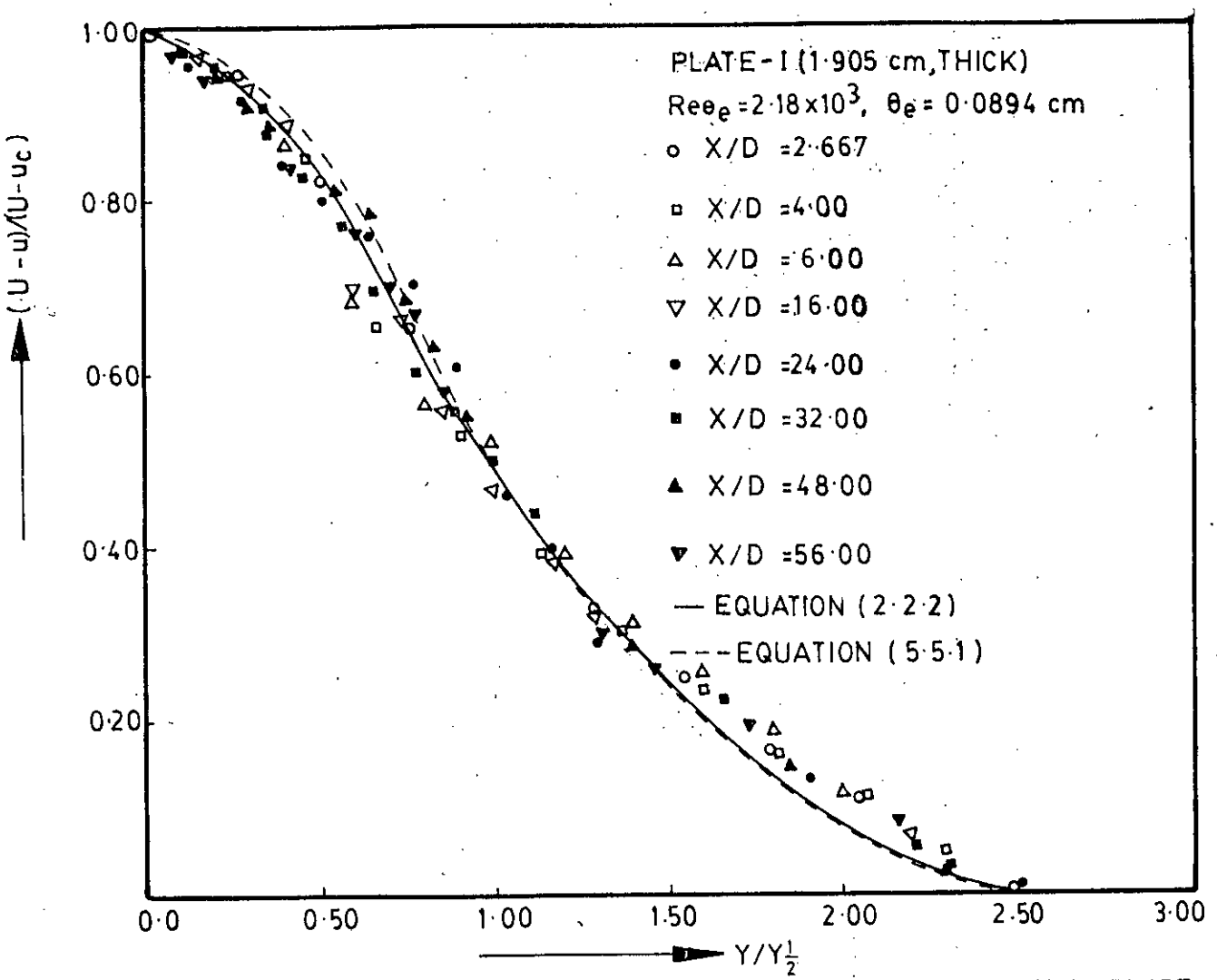

FIG.5.13a. DIMENSIONLESS VELOCITY PROFILE IN THE WAKE OF A FLAT PLATE

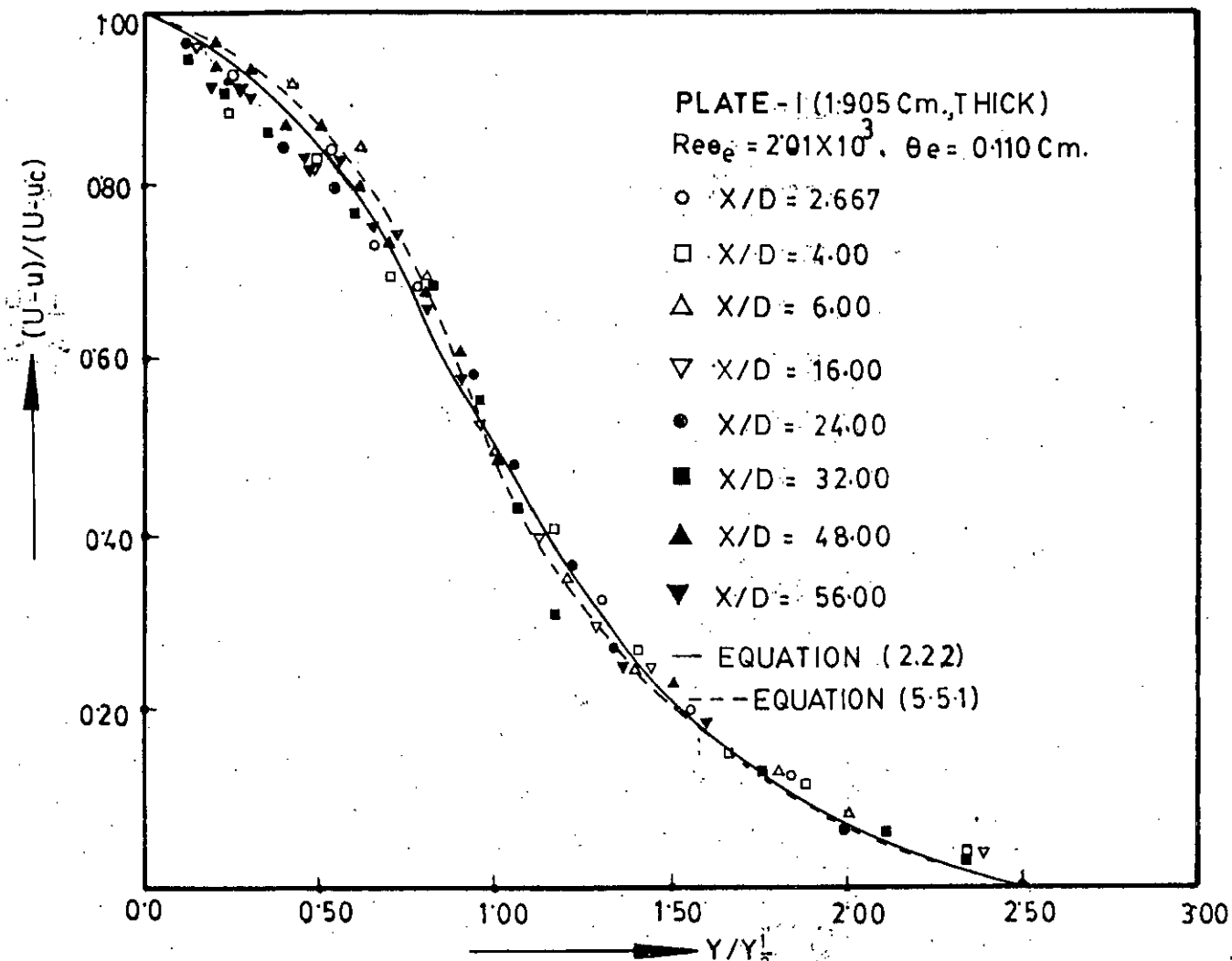

FIG·5.13b DIMENSIONLESS VELOCITY PROFILE IN THE WAKE OF A FLAT PLATE

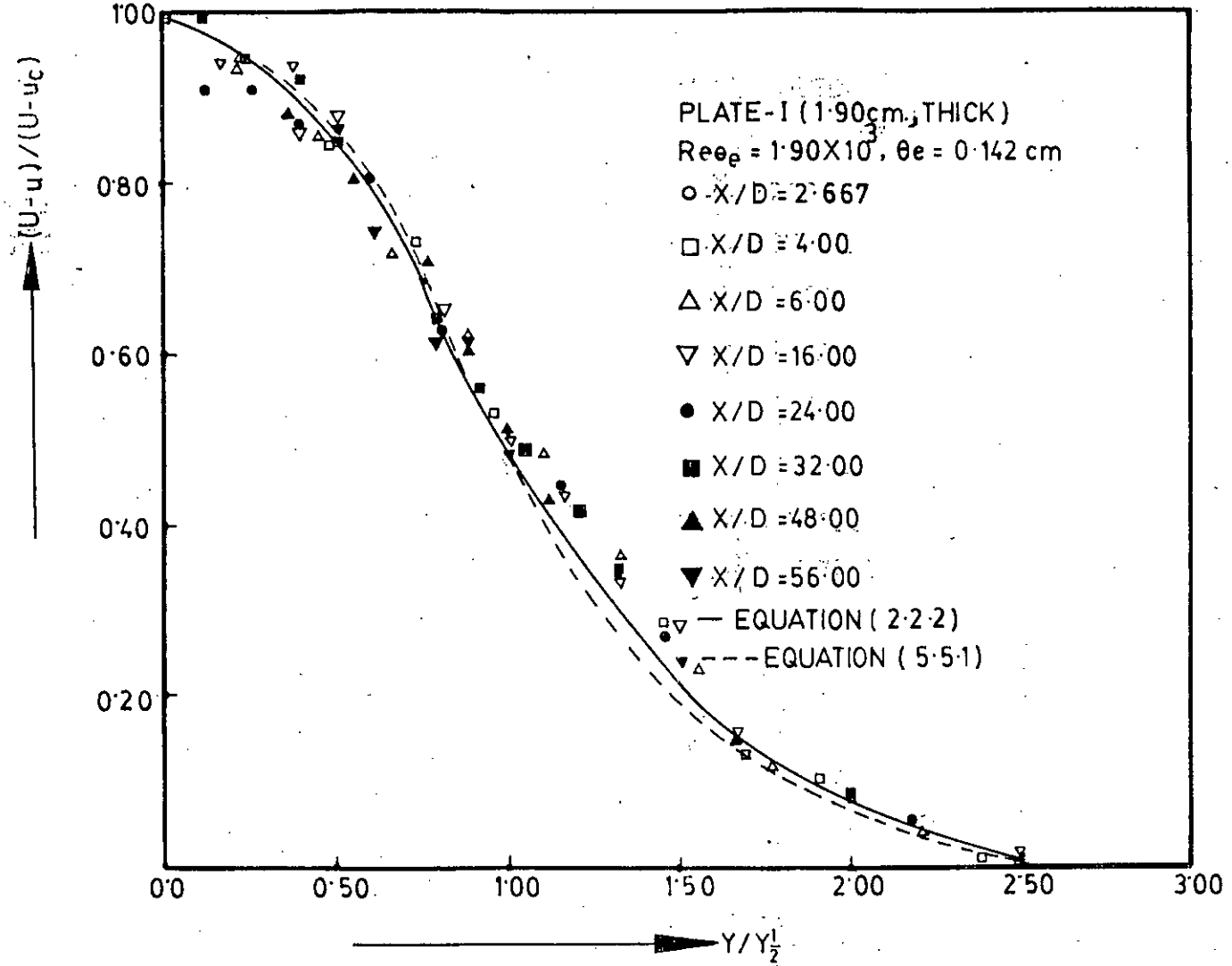

FIG·5·13c· DIMENSIONLESS VELOCITY PROFILE IN THE WAKE OF A FLAT PLATE

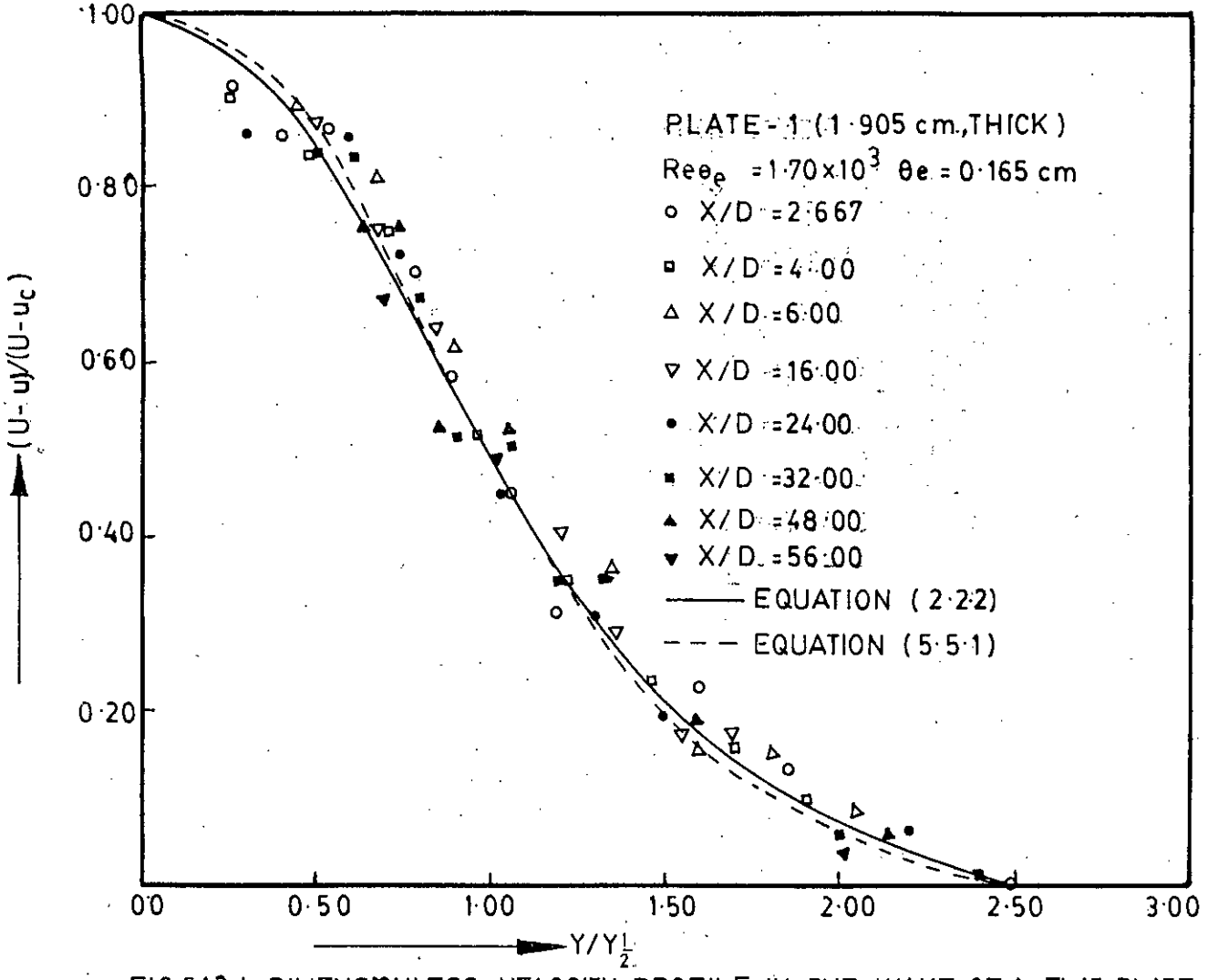

FIG.513d. DIMENSIONLESS VELOCITY PROFILE IN THE WAKE OF A FLAT PLATE

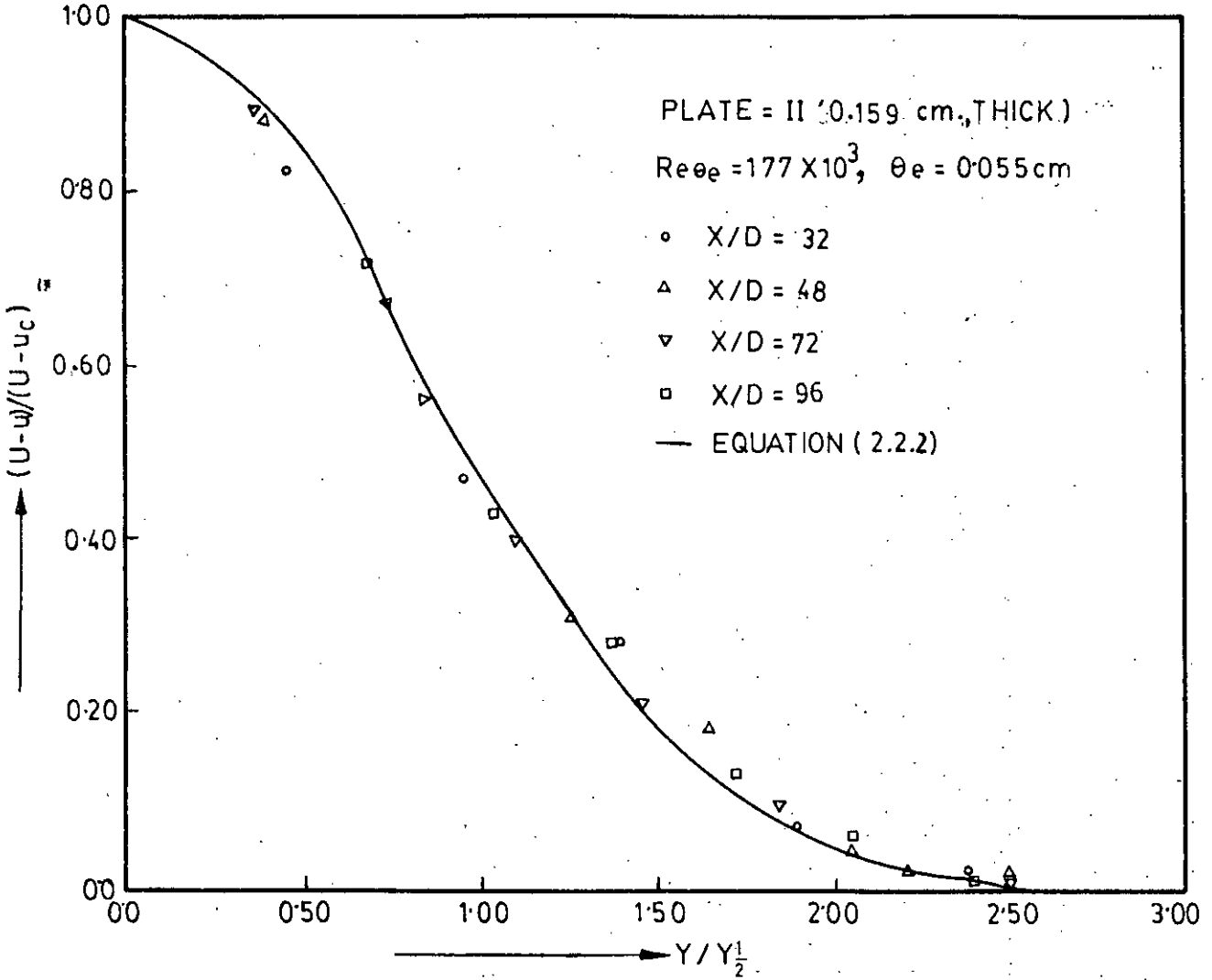

FIG.5.13e. DIMENSIONLESS VELOCITY PROFILE IN THE WAKE OF A FLAT PLATE-II.

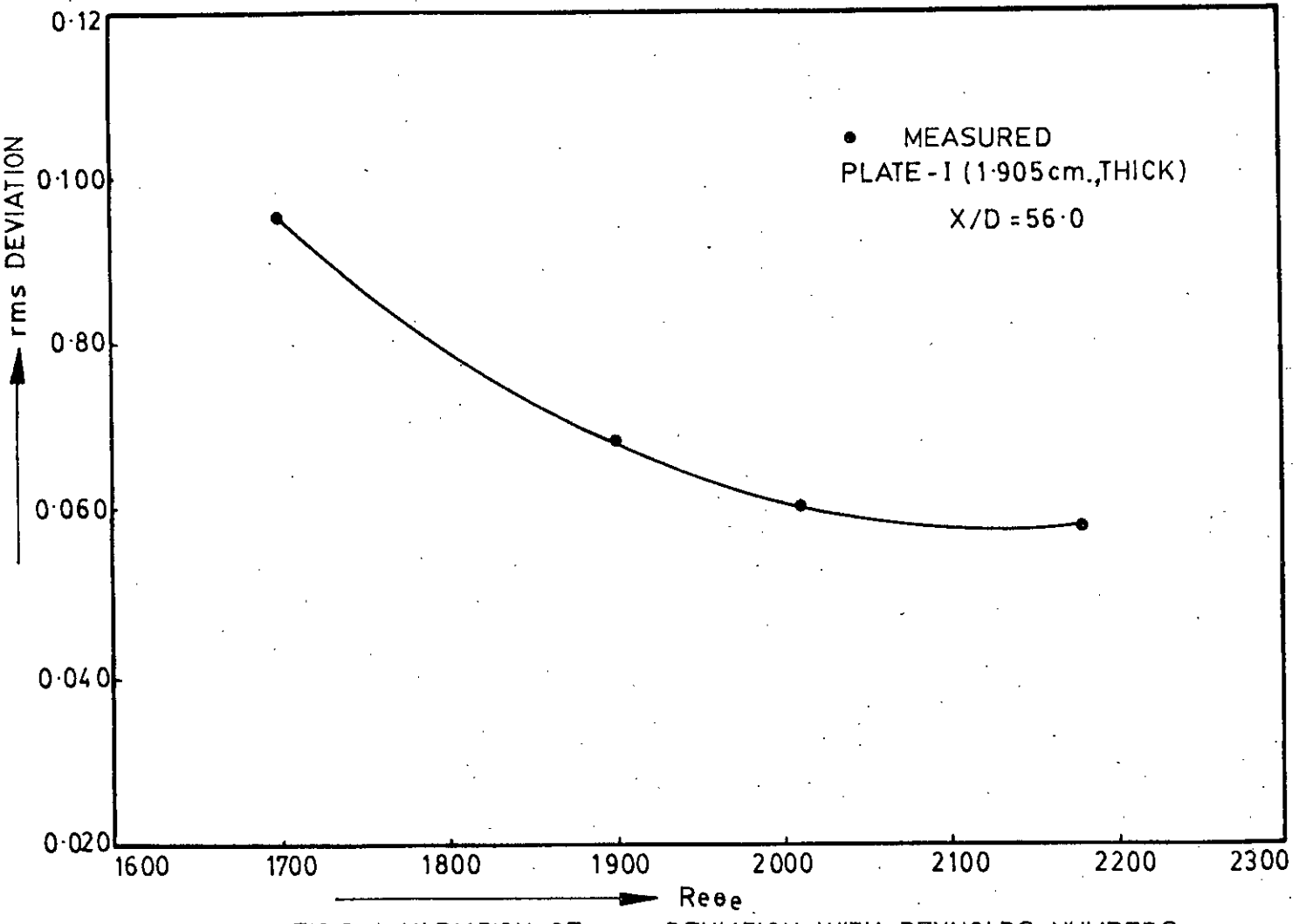

FIG.5.14 VARIATION OF rms DEVIATION WITH REYNOLDS NUMBERS

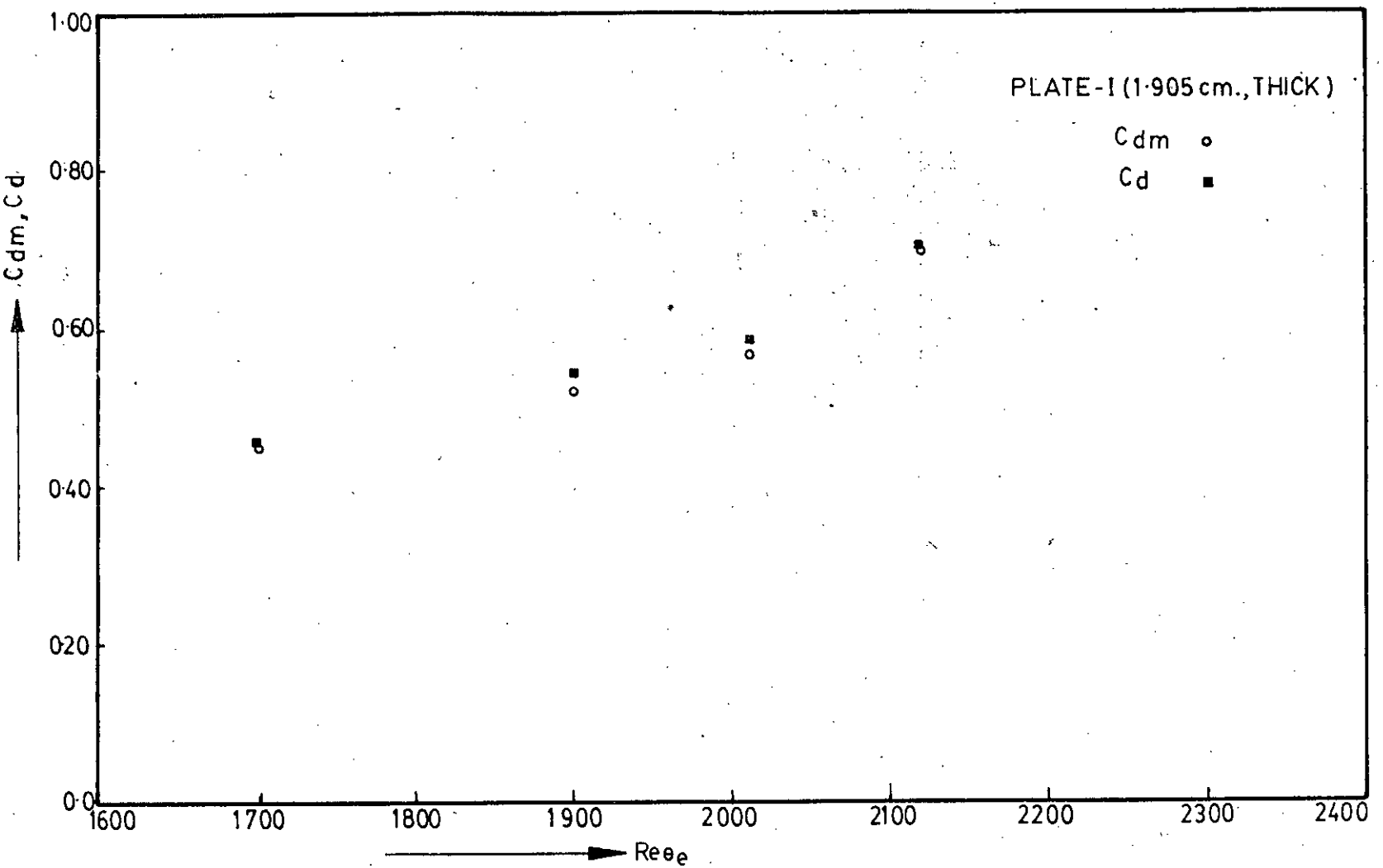

FIG. 5·15 VARIATION OF DRAG-COEFFICIENT WITH REYNOLDS NUMBERS

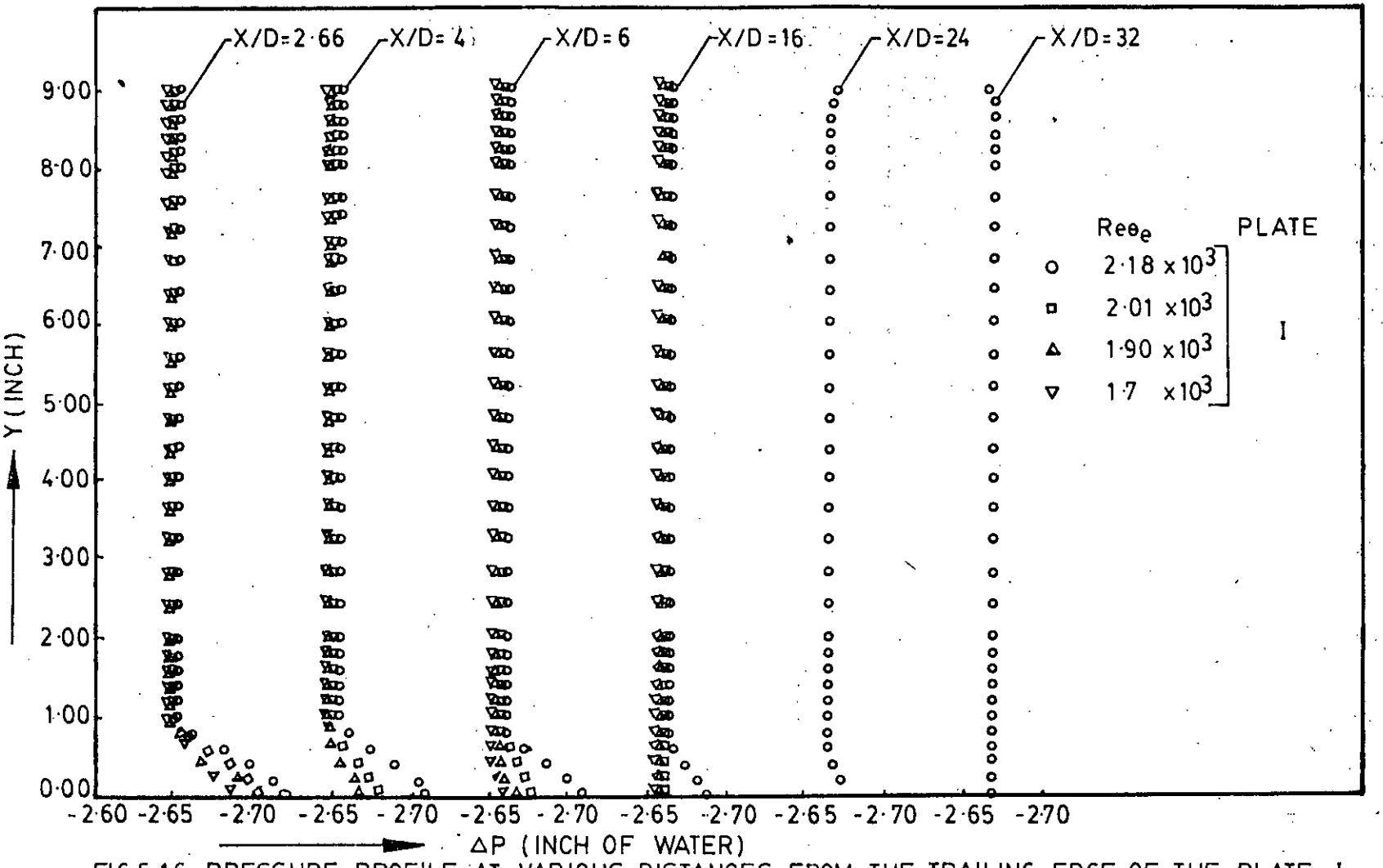

FIG 5·16 PRESSURE PROFILE AT VARIOUS DISTANCES FROM THE TRAILING EDGE OF THE PLATE - I

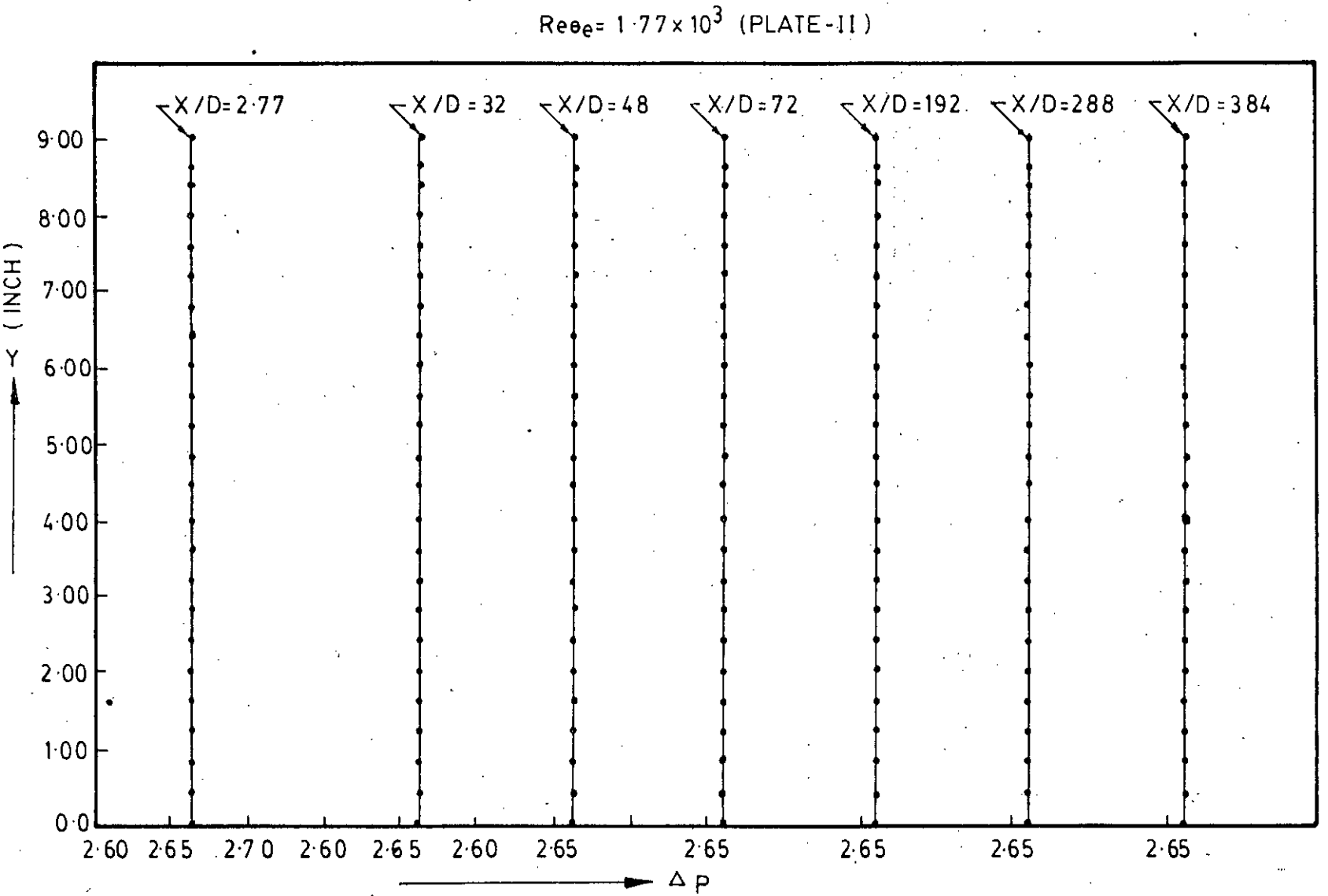

FIG. 5·17 PRESSURE PROFILE AT VARIOUS DISTANCES FROM THE TRAILING EDGE OF THE PLATE - II

APPENDICES

APPENDIX - I

UNCERTAINTY ANALYSIS

A- 1 Uncertainty for velocity measurements.

Air stream of density, ρ_{air}(slug/ft^3) flows with a velocity U(ft/sec). If a pitot-static tube is placed parallel to the air-stream, then the velocity head h'(inch) is measured from a draft gauge. If the density of monometric fluid is ρ_e(slug/ft^3), then

$$\tfrac{1}{2}\rho_a u^2 = h'\rho_\ell g \qquad (A-1.1)$$

$$\therefore \quad u^2 = 2(\rho_\ell/\rho_a)h'g$$

$$\text{or,} \quad u = \sqrt{2g(\rho_\ell/\rho_a)h'}$$

$$\text{or,} \quad u = \sqrt{2g(\rho_\ell g/\rho_a g)h'} \qquad (A-1.2)$$

If the sensing point of the pitot-static tube is deviated by an angle ϕ from the direction of flow due to wrong adjustment, then the measured velocity will be given by

$$u = \sqrt{2g(\rho_\ell/\rho_a)h}\ \cos\theta \qquad (A-1.3)$$

But we know,

$$p_a = \rho_a g T R \qquad (A-1.4)$$

$$\text{or,} \quad \rho_a = p_a/gTR$$

where p_a, R and T are the pressure the gas constant and the absolute temperature of the air respectively.

From equation(A 1.3) and (A 1.4)

$$u = \sqrt{\frac{2g(p_1 g\ RT\ h')}{p_a}} \cos \phi \qquad (A-1.5)$$

we know,

$$p_1 g = 62.4 \times s \qquad (A-1.6)$$

where s is the specific gravity of the liquid.

From equations(A 1.5) and (A 1.6)

$$u = \sqrt{2g \times 62.4 \times s \times RTh'/p_a} \cos \phi$$

or $$u = \sqrt{2g \times 62.4 \times R\ sh'T/p_a} \cos \phi$$

or $$u = \sqrt{2gR \times 62.4}\sqrt{\frac{sh'T}{p_a}} \cos \phi$$

if h' is in inches.

$$\therefore \quad u = q\sqrt{\frac{sh'T}{p_a}} \cos \phi \qquad (A-1.7)$$

where $$q = \sqrt{\frac{2gR \times 62.4}{12}} \qquad (A-1.8)$$

Now differentiate both sides of the equation(A 1.7) with respect to s, p_a T, h' and ϕ respectively.

$$\frac{\delta u}{\delta s} = q.\tfrac{1}{2}\left(\frac{sh'T}{p_a}\right)^{-\frac{1}{2}} \frac{h'T}{p_a} \cos \phi = \frac{q}{2}\sqrt{\frac{h'T}{Sp_a}} \cos \phi \qquad (A-1.9)$$

$$\frac{\delta u}{\delta p_a} = q.\tfrac{1}{2}\left(\frac{sh'T}{p_a}\right)^{-\frac{1}{2}} sh'T\left(-\frac{1}{p_a{}^2}\right) \cos \phi$$

or, $$\frac{\delta u}{\delta p_a} = \frac{q}{2}\sqrt{\frac{sh'T}{p_a{}^3}} \cos \phi \qquad (A-1.10)$$

$$\frac{\delta u}{\delta T} = \frac{q}{2}\left(\frac{sh'T}{pa}\right)^{-\frac{1}{2}} \frac{sh'}{p_a} \cos \phi = \frac{q}{2}\sqrt{\frac{sh'}{Tp_a}} \cos \phi \qquad (A-1.11)$$

$$\frac{\delta u}{\delta h'} = \frac{q}{2}\left(\frac{sh'T}{p_a}\right)^{-\frac{1}{2}} \frac{sT}{p_a} \cos\phi = \frac{q}{2}\sqrt{\frac{sT}{h'p_a}}\cos\phi \qquad \text{(A-1.12)}$$

$$\frac{\delta u}{\delta \beta} = q\sqrt{\frac{sh'T}{p_a}}\,(-\sin\phi) = -q\sqrt{\frac{sh'T}{p_a}}\sin\phi \qquad \text{(A-1.13)}$$

Let u_u be the uncertainty for velocity and s_u p_{au} T_u h'_u and ϕ_u be the uncertainties in the specific gravity, pressure, temperature, monometer reading and angle of deviation respectively.

Therefore,

$$u_u = \left[\left(\frac{\delta u}{\delta s}\, s_u\right)^2 + \left(\frac{\delta u}{\delta p_a}\, p_{a,u}\right)^2 + \left(\frac{\delta u}{\delta T}\, T_u\right)^2 + \left(\frac{\delta u}{\delta h'}, h'_u\right)^2 + \left(\frac{\delta u}{\delta \phi}\, \phi_u\right)^2\right]^{\frac{1}{2}} \qquad \text{(A-1.14)}$$

substituting the values of $\frac{\delta u}{\delta s}$, $\frac{\delta u}{\delta p_a}$, $\frac{u}{p_a}$, $\frac{\delta u}{\delta T}$, $\frac{\delta u}{\delta h'}$, and $\frac{\delta u}{\delta \phi}$ in the above equation(A-1.14).

We have,

$$u_u = \left[\frac{q^2}{4}\,\frac{h'T}{sp_a}\cos^2\phi\, s^2_u + \frac{q^2}{4}\,\frac{sh'T}{p_a{}^3}\cos^2\phi\, p^2_{au} + \frac{q^2}{4}\,\frac{sh}{Tp_a} \times \cos^2\phi T_u{}^2 + \frac{q^2}{4}\,\frac{ST}{h'p_a}\cos^2\phi\, h'_u + \frac{q^2}{4}\,\frac{sh'T}{p_a}\sin^2\phi.\phi_u\right]^{\frac{1}{2}}$$

$$\text{or } u_u = \frac{q.\cos\phi}{2}\left[\frac{h'T}{sp_a}\, s_u{}^2 + \frac{sh'T}{p_a{}^3}\, p_{a,u} + \frac{sh'}{Tp_a}\, T_u{}^2 + \frac{sT}{h'p_a}\, h'^2_u + 4\,\frac{sh'T}{p_a}\tan^2\phi.\,\phi_u{}^2\right]^{\frac{1}{2}} \qquad \text{(A-1.15)}$$

Diving equation(A-1.15) by equation (A-1.7)

We have,

$$\frac{u_u}{u} = \frac{1}{2}\left[\frac{s^2_u}{s^2} + \frac{p_{a,}{}^2_u}{p_a} + \frac{T^2_u}{T2} + \frac{h'_u{}^2}{h^2} + 4\phi_u{}^2\tan^2\phi\right]^{\frac{1}{2}} \qquad \text{(A-1.16)}$$

Let us assume the following values for the above equation (A-1.16).

$$s = 0.81 \pm 0.005$$

$$h' = 1.06 \pm 0.005$$

$$p_a = 29.90 \pm 0.050$$

$$T = 67^{\circ}F \pm 1.5^{\circ}F$$

$$\phi = 0^{\circ} \pm 5^{\circ}$$

Hence from equation (A-1.16) we get

$$\frac{u_u}{u} = 0.013927 = 1.3927\%$$

A-2 Uncertainty for pressure measurements

If the sensing point of the pitot-static tube is deviated by an angle ϕ from the direction of the flow due to wrong adjustment, then the measured relative static pressure will be given by-

$$p_{re} = \rho_l g h' - \frac{\rho_a u^2}{2} \cos^2(90^{\circ} - \phi)$$

$$\text{or, } p_{re} = \rho_l g h' - \frac{\rho_a u^2}{2} \sin^2\phi$$

$$\text{or, } p_{re} = 62.4 s h' - \frac{p_a u^2}{2RTg} \sin^2\phi$$

$$\text{or, } p_{re} = \frac{62.4 s h'}{12} - \frac{p_a u^2}{2RTg} \sin^2\phi \quad \text{if } h' \text{ is in inches}$$

$$\text{or, } p_{re} = R_1 s h' - R_2 \frac{p_a u^2}{T} \sin^2\phi \qquad (A\text{-}2.1)$$

where, $R_1 = \frac{62.4}{12} = 5.2$

$$R_2 = \frac{1}{2Rg} = \frac{1}{2 \times 53.3 \times 32.2} = 2.913 \times 10^{4}$$

Let $p_{re} = p - p_1$ (A-2.2)

$\therefore$ $p = R_1 sh'$ (A-2.3)

$= 5.2 \times 0.81 \times 3.36 = 14.15232$

and $p_1 = R_2 \frac{p_a u^2}{T} \sin^2\phi = 2.1606215 \times 10^{-4}$ (A-2.4)

Let p_u and p_{1u} be the uncertainties in p and p_1 respectively.

Then, $p_u = \left[\left(\frac{\delta p}{\delta s} s_u\right)^2 + \left(\frac{\delta p}{\delta h'} h'_u\right)^2 \right]^{\frac{1}{2}}$

or, $p_u = \left[(R_1 h' s_u)^2 + (R_1 s h'_u)^2 \right]^{\frac{1}{2}}$

or, $p_u = R_1 h' s \left[\left(\frac{s_u}{s}\right)^2 + \left(\frac{h'_u}{h'}\right)^2 \right]^{\frac{1}{2}}$

$\therefore$ $\frac{p_u}{p} = \left[\left(\frac{s_u}{s}\right)^2 + \left(\frac{h'_u}{h'}\right)^2 \right]^{\frac{1}{2}}$ (A-2.5)

and $p_{1u} = \left[\left(\frac{\delta p_1}{\delta p_a} p_{au}\right)^2 + \left(\frac{\delta p_1}{\delta u} u_u\right)^2 + \left(\frac{\delta p_1}{\delta T} Tu\right)^2 + \left(\frac{\delta p_1}{\delta \phi} \phi_u\right)^2 \right]^{\frac{1}{2}}$

or, $p_{1u} = \left[\left(\frac{R_2 u^2 \sin^2\phi}{T} p_{au}\right)^2 + \left(\frac{R_2 p_a 2 \sin^2\phi}{T} u_u\right)^2 \right.$

$\left. + \left(\frac{-R_2 p_a u^2 \sin^2\phi Tu}{T2}\right)^2 + \left(\frac{R_2 p_a u^2}{T} 2 \sin\phi \cos\phi \phi_u\right)^2 \right]^{\frac{1}{2}}$

or, $p_{1u} = \frac{R_2 p_a u^2 \sin^2\phi}{T} \left[\left(\frac{p_{au}}{p_a}\right)^2 + \left(\frac{2u_u}{u}\right)^2 + \left(\frac{Tu}{T}\right)^2 \right.$

$\left. \left(\frac{2\phi_u}{\tan\phi}\right)^2 \right]^{\frac{1}{2}}$

$$\therefore \quad p_{1u}/p_1 = \left[\left(\frac{p_a u}{p_a} \right)^2 + \left(\frac{2u_u}{u} \right)^2 + \left(\frac{T_u}{T} \right)^2 + \left(\frac{2\phi_u}{\tan\phi} \right)^2 \right]^{\frac{1}{2}}$$

$$= 1.4131529 \qquad \text{(A-2.6)}$$

$$\therefore \quad p_{re} = p - p_1$$

$$= 14.15232 - 2.160215\times10^{-4} = 14.1521$$

$$\therefore \quad p_{reu} = \left[\left(\frac{\delta p}{\delta p} p_u \right)^2 + \left(\frac{\delta p_1}{\delta p_1} p_{1u} \right)^2 \right]^{\frac{1}{2}}$$

$$\text{or,} \quad p_{reu} = \left[\left(\frac{\delta p}{\delta p} p_u \right)^2 + \left(\frac{\delta p_1}{\delta p_1} p_{1u} \right)^2 \right]^{\frac{1}{2}}$$

$$\text{or,} \quad p_{reu} = \left[\left(p_u \right)^2 + \left(p_{1u} \right)^2 \right]^{\frac{1}{2}} \qquad \text{(A-2.7)}$$

putting the following values in the above equation (A-2.5) and (A-2.6)

$$S = 0.81 \pm 0.005$$

$$h' = 3.36 \pm 0.005 \text{(inch)}$$

$$p_a = 29.9 \pm 0.05 \text{(inch of Hg)}$$

$$T = 67^{\circ}F \pm 1.5^{\circ}F$$

$$\phi = 0^{\circ} \pm 5^{\circ}$$

$$u = 59.169 \pm 0.82405 \text{(ft/sec)}$$

from equation (A-2.5) , we have

$$\frac{p_u}{p} = \left(3.81039\times10^{5} + 2.21442\times10^{6} \right)^{\frac{1}{2}}$$

$$= 6.34336\times 10^{-3}$$

$$p_u = 0.00898582$$

From equation (A-2.6), we have

$$p_{1u} = 1.4131529$$

$$\therefore \quad p_{iu} = 3.05241 \times 10^{-4}$$

From equation (A-2.7) , we get ,

$$p_{reu} = \left[8.07449 \times 10^{-3} + 9.3147 \times 10^{-8} \right]^{\frac{1}{2}}$$

$$= 0.0898581$$

$$p_{re} = p - p_1 = 14.1521$$

$$\frac{p_{reu}}{p_{re}} = \frac{0.0898581}{14.1521} = 6.34945 \times 10^{-3}$$

$$\text{or,} \frac{p_{reu}}{p_{re}} = 0.00634945 \quad \text{i.e. } \pm 0.634\%.$$

APPENDIX - II

METHODOLOGY FOR DETERMINING A, B AND u* IN UNIVERSAL VELOCITY PROFILE

The Universal velocity profile near the wall is ;

$$u^+ = B \log y^+ + A \qquad (A\text{-}2.1)$$

where , $u^+ = \frac{u}{u^*}$ and $y^+ = \frac{Yu^*}{\nu}$

Introducing the dimensionless co-efficient for local skin friction in the above equation (A-2.1);

$$C_f = \frac{\tau}{\frac{1}{2}U_o^2} \qquad (A\text{-}2.2)$$

$$\text{Shear stress, } u^* = \sqrt{\frac{\tau}{\rho}} = \sqrt{\frac{C_f}{2}}\, U_o \qquad (A\text{-}2.3)$$

Putting the volue of u* in the above equation (A-2.1)

$$\frac{u}{U_o\sqrt{C_{f/2}}} = B \log \frac{YU_o}{\nu}\sqrt{\frac{C_f}{2}} + A \qquad (A\text{-}2.4)$$

$$\frac{u}{U_o} = B\sqrt{\frac{C_f}{2}} \left\{ \log \frac{YU_o}{\nu} + \log\sqrt{\frac{C_f}{2}} \right\} + A\sqrt{\frac{C_f}{2}} \qquad (A\text{-}2.5)$$

$$\frac{u}{U_o} = B\sqrt{\frac{C_f}{2}} \log \frac{YU_o}{\nu} + \sqrt{\frac{C_f}{2}} \left\{ B \log\sqrt{\frac{C_f}{2}} + A \right\} \qquad (A\text{-}2.6)$$

The slope of the above equation is used to determine the shear stress velocity.

$$B\sqrt{\frac{C_f}{2}} = m \qquad (A\text{-}2.7)$$

$$u^* = \frac{mU_o}{E} \qquad (A\text{-}2.8)$$

$$\frac{u}{u^*} = B \log \frac{u^* Y}{\nu} + A \qquad \text{(A-2.9)}$$

u/u^* vs. $\frac{u^* Y}{\nu}$ curve is plotted to determine the constant A, and the slope B.

```
C
C
C
C
C
C
C
C
C                  APPENDIX  III
C
C
C
C
C     **DETERMINATION  OF  SHEAR  VELOCITY BY WALL SLOPE METHOD**
C
C      ************************************************************
C      *A=CONSTANT OF THE CLAUSER MODEL   B=SLOPE OF THE  CLAUSER*
C      *MODEL    N=NUMBER OF POINTS    PNEUE=KINEMATIC  VISCOSITY  *
C      *RE=REYNOLDS NUMBER    UC=FREE-STREAM VELOCITY   U(I)=AXIAL*
C      *VELOCITY   USTAR=SHEAR VELOCITY  YV(I)=TRANSVERSE DISTANCE*
C      ************************************************************
      DIMENSION X(20),Y(20),U(20),YV(20),XX(20),YY(20),UU(20),D(20),UNS
     ATAR(20),QM(20),QU(20),G(20)
      DO 999 III=1,4
      WRITE (3,199) III
  199 FORMAT (10X,'*********','EXPT. NO.',I3,'*********')
      PNEUE=0.00016
      N=6
      DO 1000 II=1,11
      WRITE(3,68)II
   68 FORMAT(10X,'********','STATION NO.',I3,'********')
      READ(1,6)UCON,RE
    6 FORMAT(2F10.5)
      READ(1,10)(U(I),I=1,N)
      READ(1,10)(YV(I),I=1,N)
   10 FORMAT(6F10.5)
      DO 12 I=1,N
      UU(I)=U(I)
   12 CONTINUE
      UC=UCON
      DO 15 I=1,N
      X(I)=ALOG10((U(I)*YV(I))/(12*PNEUE))
      Y(I)=U(I)/UC
   15 CONTINUE
      K=0
   40 K=K+1
      SUMX=0.0
      SUMY=0.0
      PDX2=0.0
      SUXY=0.0
      DO 16 I=1,N
      SUMX=SUMX+X(I)
      SUMY=SUMY+Y(I)
      PRXX=X(I)*X(I)
      PDX2=PDX2+PRXX
      PRXY=X(I)*Y(I)
      SUXY=SUXY+PRXY
   16 CONTINUE
      SUX2=SUMX**2
```

```
C
C
C
C
C
C       ********************************************************************
C       *CALCULATION OF THE CONSTANT A AND B OF THE CLAUSER MODEL*
C       ********************************************************************
0038            E=(N*SUXY-SUMX*SUMY)/(N*PDX2-SUX2)
0039            A=(PDX2*SUMY-SUMX*SUXY)/(N*PDX2-SUX2)
0040            IF(K.EQ.2)GO TO 100
C       ********************************************************************
C       *CALCULATION OF THE SHEAR STRESS VELOCITY*
C       ********************************************************************
0041            USTAR=((B*UCON)/5.75)
0042            UNSTAR(1)=USTAR
```

DOS FORTRAN IV 360N-FO-479 3-8 MAINPGM DATE 29/08/83 TIME 17.14.49

```
0043            DO 66 J=2,15
0044            UNSTAR(J)=UNSTAR(J-1)+0.02
0045         66 CONTINUE
0046        100 DIFF=0.0
0047            DO 55 I=1,N
0048            D(I)=Y(I)-(A+B*X(I))
0049         55 DIFF=DIFF+D(I)**2
0050            RMS=SQRT(DIFF)
0051            IF(K.EQ.2)GO TO 200
0052            WRITE(3,21)RE
0053         21 FORMAT(5X,'REYNOLDS NUMBER IS',2X,'RE=',G14.7)
0054            WRITE(3,22)UCON,PNEUE,N
0055         22 FORMAT(5X,'UCON=',G14.7,5X,'PNEUE=',G14.7,3X,'N=',I3)
0056            DO 65 J=1,15
0057            DO 77 I=1,N
0058            YY(I)=U(I)/UNSTAR(J)
0059            Y(I)=YY(I)
0060            XX(I)=ALOG10((UNSTAR(J)*YY(I))/(12*PNEUE))
0061            X(I)=XX(I)
0062         77 CONTINUE
0063            SUMNX=0.0
0064            SUMNY=0.0
0065            PDX2=0.0
0066            SUNXY=0.0
0067            DO 222 I=1,N
0068            SUMNX=SUMNX+X(I)
0069            SUMNY=SUMNY+Y(I)
0070            PRNXX=X(I)*X(I)
0071            PDNX2=PDNX2+PRNXX
0072            PRNXY=X(I)*Y(I)
0073            SUNXY=SUNXY+PRNXY
0074        222 CONTINUE
0075            SUNX2=SUMNX**2
C
```

```
C
C
C
C
C
C
C
      B=(N*SUMXY-SUMNX*SUMNY)/(N*PDNX2-SUNX2)
      A=(PDNX2*SUMNY-SUMNX*SUMXY)/(N*PDNX2-SUNX2)
      GM(J)=B-5.75
      GQ(J)=B
      G(J)=A
      EM=QQ(1)
      C=ABS(GM(1))
      AM=Q(1)
      USTAR=UNSTAR(1)
      IF(J.EQ.1)GO TO 65
      IF(C.GT.ABS(GQ(J)))AM=G(J)
      IF(C.GT.ABS(GM(J)))EM=GQ(J)
      IF(C.GT.ABS(GM(J)))USTAR=UNSTAR(J)
      IF(C.GT.ABS(GM(J)))C=ABS(GM(J))
   55 CONTINUE
      WRITE(3,225)USTAR
  225 FORMAT(//5X,'USTAR=',G14.7)
      WRITE(3,223)EM,AM
  223 FORMAT(5X,'U/UNSTAR=',G14.7,'*LOG(YY/NU)',,'+',G14.7)
      IF(K.LT.2)GO TO 40
  200 CONTINUE
      WRITE(3,33)
   33 FORMAT(///9X,'YY(I)',8X,'U(I)',7X,'UU(I)/USTAR',2X,'LOG(YU*/NU)',2
     AX,'DIFF')
      DO 89 I=1,N
      WRITE(3,26)YY(I),U(I),YY(I),XX(I),D(I)
   26 FORMAT(5X,5G14.7)
   89 CONTINUE
      WRITE(3,29)RMS
   29 FORMAT(//5X,'RMS DEVIATION=',G14.7)
      WRITE(3,79)
   79 FORMAT(//5X,'*********************************************************')
  100 CONTINUE
  995 CONTINUE
      STOP
      END
```